2024

PORCUPINE'S ROLE IN THE ENHANCEMENT OF ENZALUTAMIDE EFFICACY IN DRUG RESISTANT PROSTATE CANCER

Katelyn Jones
University of Kentucky, kate.jones1324@gmail.com
Author ORCID Identifier:
https://orcid.org/0000-0002-6613-4509
Digital Object Identifier: https://doi.org/10.13023/etd.2024.260

STUDENT AGREEMENT:

I represent that my thesis or dissertation and abstract are my original work. Proper attribution has been given to all outside sources. I understand that I am solely responsible for obtaining any needed copyright permissions. I have obtained needed written permission statement(s) from the owner(s) of each third-party copyrighted matter to be included in my work, allowing electronic distribution (if such use is not permitted by the fair use doctrine) which will be submitted to UKnowledge as Additional File.

I hereby grant to The University of Kentucky and its agents the irrevocable, non-exclusive, and royalty-free license to archive and make accessible my work in whole or in part in all forms of media, now or hereafter known. I agree that the document mentioned above may be made available immediately for worldwide access unless an embargo applies.

I retain all other ownership rights to the copyright of my work. I also retain the right to use in future works (such as articles or books) all or part of my work. I understand that I am free to register the copyright to my work.

REVIEW, APPROVAL AND ACCEPTANCE

The document mentioned above has been reviewed and accepted by the student's advisor, on behalf of the advisory committee, and by the Director of Graduate Studies (DGS), on behalf of the program; we verify that this is the final, approved version of the student's thesis including all changes required by the advisory committee. The undersigned agree to abide by the statements above.

Katelyn Jones, Student

Xiaoqi Liu, Major Professor

Isabel Mellon, Director of Graduate Studies

PORCUPINE'S ROLE IN THE ENHANCEMENT OF ENZALUTAMIDE EFFICACY IN DRUG RESISTANT PROSTATE CANCER

DISSERTATION

A dissertation submitted in partial
fulfillment of the requirements for
the degree of Doctor of Philosophy
in the College of Medicine at the
University of Kentucky

By Katelyn Jones
Lexington, Kentucky
Director: Dr. Xiaoqi Liu, Professor of
Toxicology and Cancer Biology Lexington,
Kentucky
2024

https://orcid.org/
0000-0002-
6613-4509

ABSTRACT OF DISSERTATION
PORCUPINE'S ROLE IN THE ENHANCEMENT OF ENZALUTAMIDE EFFICACY
IN
DRUG RESISTANT PROSTATE CANCER

Androgen receptor (AR) signaling continues to participate as a vital component of castration-resistant prostate cancer (CRPC). Subsequently, this has led to the development of Androgen Signaling Inhibitors (ASI), specifically Enzalutamide (ENZ), which is a direct inhibitor of AR, to clinically manage CRPC. Inevitably, ENZ treatment only provides improvement for approximately two months before advancing to an incurable form, ENZ-resistant CRPC. With PCa ranking as the second leading cause of cancer-related deaths in USA males, there is an urgency and necessity for the discovery and development of novel therapeutic approaches for CRPC. Wnt signaling has been extensively documented in its involvement in PCa and the tumor microenvironment (TME), however the mechanism of how the Wnt signaling cascades contribute to ENZ resistance is still ambiguous. Recently we have published that the activation of the canonical Wnt pathway contributes to the progression of ENZ resistance in CRPC and using a combination of β-catenin inhibitor with ENZ resulted in the synergistic inhibition of patient derived xenograft (PDX) tumor growth. Regarding the non-canonical Wnt pathway, we confirmed its contribution to invasion and migration which leads to metastasis in ENZ-resistant CRPC, and when the downstream effector ROCK is depleted or depleted ROCK cells are treated with ENZ, there is a significant hindering of cell migration and invasion. Also, utilizing a combination therapy of ROCK inhibitor with ENZ synergistically inhibited the growth of PDX tumors. Hence the reasoning that by simultaneously inhibiting both the canonical and non-canonical Wnt signaling cascade will result in the inhibition of cell proliferation, migration, and invasion. The goal of this study was to define the mechanism of PORCN in ENZ-resistant CRPC and develop a therapeutic approach to combat this disease. My research has determined that Porcupine (PORCN) is associated with CRPC progression to ENZ-resistance, and that an inhibition or loss of PORCN has resulted in the regain of ENZ sensitivity in ENZ-resistant models. This model has also demonstrated that PORCN and Wnt signaling engage in a paramount role contributing to AR activation, promoting CRPC progression, and the development of ENZ resistance.
Key Words: Enz-resistance, Mitochondrial Biogenesis, Wnt Signaling, Prostate Cancer

PORCUPINE'S ROLE IN THE ENHANCEMENT OF ENZALUTAMIDE EFFICACY IN DRUG RESISTANT PROSTATE CANCER

By
Katelyn Jones

Xiaoqi Liu

Director of Dissertation

Isabel Mellon

Director of Graduate Studies

07/09/2024

Date

To Kallie, Nala, Sorcerer, Onyx, Pippi, Maggie, Marley, Agatha, Mango, and Merida, for giving me the motivation to give you a better life.

ACKNOWLEDGEMENTS

I want to dedicate this section of my dissertation to express my sincere gratitude to all of those who have contributed to the successful journey and completion of my degree. Firstly, I would like to thank my advisor, Dr. Xiaoqi Liu, for all his support and guidance throughout my years and training here at the University of Kentucky. His ability to provide invaluable guidance, insight, and support cultivated an inclusive and educational environment. He was instrumental in developing a feasible timeline for graduation and ensuring proper milestones were met. With his expertise and resources, we were able to act as a collaborative team that resulted in the progression of science, and for that I am grateful. Secondly, I would like to thank my committee members, Dr. Binhua Zhou, Dr. Yekaterina Zaytseva, and Dr. Jin-Ming Yang, for their continuous support and thoughtful suggestions to improve both my education and future career endeavors. Their involvement through my Ph.D. candidacy has been monumental in the completion of my degree.

I would like to give a special thank you to Dr. Qing-Bai She for providing his time and expertise during my final examination. His contribution and suggestions were extremely insightful and beneficial to increase the depth of my project and understanding. Thirdly, I would like to share my appreciation for my lab members for their unwavering support and collaboration that pushed my research to a deeper level. Their constant communication propelled my knowledge and understanding of various assays, mechanisms, pathway, and other cancer models.

Fourthly, I would like to extend a special thank you to Dr. Mellon, Dr. O'Connor, Dr. Spear, Dr. Rice, Dr. Gao, and Dr. Evers for their tremendous support and dedication to ensure that my career, education, and scientific goals were fulfilled and provided the resources to continue towards my future aspirations.

Lastly, I want to thank my family, specifically my mother and father. They were always there to give me the strength and motivation to continue and be extraordinary. And for that I am eternally in their debt.

TABLE OF CONTENTS

LIST OF FIGURES

LIST OF ABBREVIATIONS

ADT: Androgen Deprivation Therapy

APA: Apalutamide

APC: Adenomatous Polyposis Coli

AR-V7: Androgen Receptor Variant 7

BMP: Bone Morphogenetic Protein

β-TrCP: β-transducin repeat containing protein

CI: Combination Index

CRPC: Castration Resistant Prostate Cancer

CSPC: Castration-Sensitive Prostate Cancer

CTHRC1: Collagen Triple Helix Repeat Containing Protein 1

DARO: Darolutamide

DSH: Disheveled protein

ENZ: Enzalutamide

ENZ-R: Enzalutamide-Resistant

ENZ-S: Enzalutamide-Sensitive

FDA: Food and Drug Administration

Frz: Frizzled

GS: Gleason Score

GSEA: Gene Set Enrichment Analysis

GSK3: Glycogen Synthase Kinase 3

JNK: JUN N-Terminal Kinase

LEF: Lymphocyte Enhancer Factor

LRP5/6: Lipoprotein Receptor-Related Protein

Myc: Myelocytomatosis

NEPC: Neuroendocrine Prostate Cancer

OS: Oxidative Stress

PCa: Prostate Cancer

PCP: Planar Cell Polarity

PORCN: Porcupine

PSA: Prostate Specific Antigen

PET: Positron Emission Tomography

PKC: Protein Kinase C

PSMA: Prostate Specific Membrane Antigen

ROR 1/2: Tyrosine-Protein Kinase Transmembrane Receptor 1 or 2

ROS: Reactive Oxidative Stress

RYK: Receptor-Tyrosine Kinase

SCD: Stearoyl CoA Desaturase

SG-ARIs: Second-Generation Androgen Receptor Inhibitors

TCGA: The Cancer Genome Atlas

TCF: T-Cell Factor

WNT: Wingless- Related Integration Site

CHAPTER 1. REVIEW OF WNT SIGNALING AND ITS INVOLVEMENT IN CANCER

1.1 Introduction

Wnt signaling was first described in *Drosophila* due to its function in the wing formation. This was mediated via glycoprotein resultant of the *Wg* gene [1]. Afterward, it was categorized to be homologous in the mammalian gene *INT1[2]*. This led to the fusion of the two genes names creating *Wnt1[3]*. After the establishment of *Wnt1*, additional Wnt genes were identified and investigated.

Wnt signaling is instrumental in various biological processes and has been shown to play a pivotal role in the initiation and progression of countless diseases and cellular functions. This signaling cascade is evolutionarily conserved and participates in several cellular processes such as proliferation, cell division, migration, polarity, cell fate, neural symmetry and morphogenesis, and stem cell regeneration [4, 5]. Traditionally, this pathway is associated with its paramount role in embryonic tissue development and homeostasis maintenance in adult tissue.

The process of Wnt signaling begins with the secretion of Wnt proteins, also referred to as Wnts. Wnts comprise a family of 19 extracellular, glycol secreted human proteins, which activate various biological processes [6]. These proteins engage in several post-translational modifications, such as glycosylation and palmitoleic acid modifications, to maintain moderate water solubility and promote protein-protein interactions [7]. Due to these processes, these proteins can participate in either autocrine or paracrine signaling activation simultaneously. After the secretion process, Wnts bind to cell surface receptor,

referred to as Frizzled (Frz) receptors, and cause the activation of downstream signaling cascades. Frz receptors are composed of seven hydrophobic domains and a cysteine-rich ligand-binding domain and are found exclusively in the plasma membrane [8]. These receptors have a distinct function in the regulation and activation of pathways associated with Wnt signaling. Due to its various functional abilities, abnormal activation of these processes can lead to several different diseases highlighting Wnt signaling as a vital therapeutic target. Wnt signaling can be devised into two subsets, which are classically labeled canonical and noncanonical pathways. The canonical pathway is known for its involvement in the cell proliferation and conventionally depends on β-catenin, whereas the noncanonical pathways is composed of two sub-types, referred to as Planar Cell Polarity (PCP) and Calcium (Ca^{2+}) cascades, known for their involvement in cell migration and cytoskeleton rearrangement.

1.2 Wnt Signaling Pathways and Modulators

1.2.1 Canonical Wnt Signaling Pathway

The canonical Wnt Signaling pathway is traditionally categorized by its utilization and reliance on the protein β-catenin. β-catenin, encoded by the CTNNB1 gene, is an evolutionarily conserved, multifunctional protein that contributes to cell development, cell renewal, and stem regeneration under normal physiological conditions, and is a crucial co-regulator transcriptional factor [9]. After Wnts bind to the Frz receptor, a phosphorylation event occurs that allows Lipoprotein Receptor-Related Protein (LRP) 5/6 cell surface receptor to form a trimetric complex with Frz. This complex phosphorylates the protein Disheveled (Dvl), which then recruits the β-catenin "destruction/degradation complex" to the plasma membrane, inhibiting its function. β-catenin "destruction/degradation complex"

is composed of five major proteins. These proteins consist of glycogen synthase kinase 3 (GSK3), AXIN 2, adenomatous polyposis coli (APC), β-transducin repeat containing protein (β-TrCP), and casein kinase 1 (CK1) [9]. This complex can capture β-catenin through the phosphorylation of CK1 and GSK3 resulting in the activation of ubiquitination and proteasomal degradation of phosphorylated β-catenin. With the degradation of this protein, β-catenin no longer can translocate into the nuclear fraction causing various transcription factor activation. The binding of Wnts to Frz renders the "destruction/ degradation complex" non-functional, and non-phosphorylated β-catenin is free to accumulate within the cytoplasm area. It then will translocate into the nuclear fraction of the cell and interact with T-cell factor (TCF)/ lymphocyte enhancer factor (LEF) to regulate gene transcription [10]. The activation of these downstream transcription factors are essential for normal Wnt signaling, but dysregulation of these events can lead to various disease, including cancer.

1.2.2 Non-Canonical Wnt Signaling Pathway

The noncanonical Wnt signaling pathway is typically associated with β-catenin independence. The non-canonical Wnt signaling requires binding to the Frz receptor and includes three different co-receptors. These co-receptors are known as receptor- tyrosine kinase (Ryk), tyrosine-protein kinase transmembrane receptor 1 or 2 (ROR 1/2), and roof plate specific-spondins (R-spondins) [11]. Ryks belong to a family of unconventional tyrosine kinases and consist of an extracellular Wnt inhibitory factor (WIF), an intracellular kinase domain, and a PDZ binding motif [12]. Typically, Wnt1 and Wnt3 bind to the WIF domain of Ryk and activate TCF to generate the transcription of various target genes [12]. Ryk also forms a ternary complex with Wnts and Frz via the WIF extracellular domain.

Then Dvl binds to the intracellular domain, utilizing the PDZ motif to activate TCF [12]. Tyrosine-protein kinase transmembrane receptors (RORs) belong to the receptor tyrosine kinase (RTK) family and consists of two components, ROR1 and ROR2 [13]. Both members are single-pass transmembrane receptors that contain an intracellular tyrosine kinase domain and proline-rich domain [14]. The proline-rich domain is surrounded by serine-threonine domains [14]. Wnt5a maintains a high affinity for ROR receptors, especially ROR2 [15]. Wnt5a binding to ROR2 leads to a heterodimer formation with Frz, resulting in the activation of the PCP pathway and causes the inhibition of the canonical Wnt signaling pathway [15]. R-spondins are composed of four members that include thrombospondin type 1 repeats (TSR-1) [16]. These membrane-bound receptors possesses and N-terminal signal peptide, two furin-like domains (FU1 and FU2), and a positively charged C-terminal region [17]. These proteins tend to bind to leucine-rich repeat-containing G-protein coupled receptors (Lgr) via their FU2 domain [17]. They can also bind to the ZNRF3 and RNF43 using the FU1 domain [18]. This binding is important because ZNRF3 and RNF43 are known E3 ubiquitin ligases that function to target Wnt ligands for degradation [19]. This decreases or prevents Wnt signaling activation, but R-spondins can bridge this interaction and stop ZNRF3/RNF43 activity via membrane clearance [20]. Due to the various co-receptors that can result in different ligand and receptor combinations, this affects the signaling of downstream effector proteins.

The non-canonical pathway can be further divided into two separate subsets. These subsets are referred to as the Ca^{2+} and the PCP pathways. These signaling cascades have different downstream effectors and act in various ways, but both functions to promote cytoskeletal rearrangement.

1.2.2.1 Calcium Pathway

Activation of the calcium pathway is normally triggered through the release of Ca^{2+} ions via Wnts and phospholipase C (PLC) to increase intracellular calcium concentrations. PLC is normally stimulated by a G protein upon the docking of Wnt ligands [21, 22]. PLC belongs to a family that consists of 13 members, all of which participate in different processes within various structures and components of the cell. PLC consists of EF-hand domains, PH domains, and C2 domains, and contain a catalytic X and Y domains [23]. The PH domain's function is to control the recruitment of PLC to the plasma membrane via interactions with PIP2 [24]. The EF-hand domain participates as part of the catalytic core, in addition to X, Y, and C2, and completes a conformational change in PLC after Ca^{2+} binding [25]. This confirmational change uncovers potential binding sites for other ligands [25, 26]. The X domain, which contains the catalytic residues, and the Y domain, which determines whether PLC, PIP2, PIP, or PI binds, domain are known to form triosephosphate isomerase (TIM) structures, whereas the C2 domain moderates the binding of PLC to phospholipids after Ca^{2+} interaction [26, 27]. The C2 domain can then mediate the signaling and membrane trafficking and determine phospholipid activity [27]. PLC acts by cleaving Phosphatidylinositol triphosphate (PIP) 2 into inositol phosphate (IP) 3 which results in a calcium release [28]. Another product of this cleavage is diacylglycerol (DAG), which is well-known secondary messenger for the activation of protein kinase C (PKC) [29, 30]. After the release of calcium, PLC can modulate various cellular functions such as proliferation, motility, and several others. PKC is a protein kinase that phosphorylates Ser and Thr residues and is stimulated by DAG [31, 32]. PKC can also be activated through tumor promoters that mimics DAG mechanism of action, called phorbol esters [32]. Both

DAG and phorbol esters work by binding to the C1 domain of PKC, which then allows it to translocate to various locations [33]. Due to this ability, PKC correlates with many cellular aspects, such as cell mobility. Cell division control protein (Cdc) 42 is a protein associated with the Rho GTPase family and plays a vital role in cytoskeleton regulation and cell polarity, as well as cell cycle progression [34]. Cdc42 has a similar function to other Rho GTPases in that its activation is regulated by Guanine Nucleotide Exchange Factors (GEFs), but since cdc42 is a hydrolase, it can hydrolyze GTP to GDP when GTPases activating protein (GAP) is present [35, 36]. Cdc42 is currently under investigation to determine whether they are viable targets for cancer therapeutics, but few mutations and no drivers have been associated to tumor formation [34]. Another player within this pathway is calcium/calmodulin (CAM)-dependent kinase II (CAMKII), which is a Ser/Thr protein kinase and acts as a calcium dependent regulator [37, 38]. This protein kinase also plays a role in glucose production, cell cycle production, and cardiac functions, and its upregulation has been linked to damage to cardiac tissue and Chagas disease [39]. An additional downstream effector is TCG-β activated kinase (TAK 1), which belongs to the mitogen- activated protein kinase kinase (MAPKK) group and acts as a Ser/Thr kinase that mediates TCF-β and bone morphogenetic protein (BMP) signaling [40, 41]. This kinase can be activated via several cytokines which cause a phosphorylation of TAK1. This phosphorylation event results in the activation of many pathways such as JNK, ERK, p38, NF-kB, MAPKs, and T- and B- cell signaling [42, 43]. Due to is involvement in immune and inflammatory processes, TAK1 has been implicated in multiple cancers, including lymphoma, colon, pancreatic, and ovarian. The activation of this kinase requires three main proteins: TAK1-binding protein 1 (TAB1), TAB2, and TAB3 [43]. The overproduction of

TAB1 leads to TAK1 activity, and TAB2 and TAB3 are used mainly to the sustain expression [43]. The activation of TAK1 triggers Nemo- like kinase (NLK) to phosphorylate TCF4 to inhibit gene transcription by preventing the β-catenin/TCF complex from interacting with DNA [44]. NLK is identified as a Ser/Thr MAPK and, in addition to repressing canonical Wnt signaling, it can also interact with NLK-associated RING finger protein (NARF) [45]. NARF is a E3 ubiquitin ligase that is regulated via NLK and can tag TCF/LEF for proteasomal degradation [45]. Due to its function in Wnt signaling, NLK plays a pivotal role in cell proliferation, migration, and death.

1.2.2.2 Planar Cell Polarity Pathway

Initiation of this signaling cascade starts with a Wnt ligand binding to Frz, ROR, or RYK receptors, which then leads to an interaction with Dvl. Dvl proteins are known as an intracellular mediator of the noncanonical Wnt signaling pathway and are comprised of three distinct domains called DIX domain, PDZ domain, and DEP domain [46]. Within this structure, the DIX domain is documented to interact with AXIN and prevent the degradation of β-catenin [47]. The PDZ and DEP are known to activate the noncanonical cascade via binding to Frz and Dvl, respectively [47]. After interaction, Dvl proteins are typically modified post-transitionally via phosphorylation. This phosphorylation event causes the activation of small GTPases, referred to as RhoA and Rac1. RhoA and Rac1 are associated with the Rho family, which are involved in various cellular functions including cell mobility and migration [48]. Both GTPases contain GDP/GTP binding domains, and their interaction causes conformational changes that require the activation of further downstream effectors. The conformational change is due to an exchange of GDP to GTP, which is regulated by GEFs and GAPs [49]. The GEFs and

GAPs are responsible for activating Rac1 or RhoA, so that there can be a continuation of signaling. To prevent downstream activation, Guanosine dissociation inhibitors (GDIs) are used to keep Rac1 within the cytoplasm fraction [50, 51]. Dysregulation of these GTPases has been closely associated with cancer development. The stimulation of these various proteins produces several phenotypical outcomes. For example, the activation of Rac1 and RhoA activation fuels changes within cell polarity due to their intense involvement in the regulation of cytoskeleton rearrangements [51]. Rac1 has been found to influence oxidative stress through NADPH oxidases [51]. Once Rac1 and RhoA are pushed into an active state, further proteins are triggered. Rho-associated coiled kinase (ROCK) is a Ser/Thr kinase that is normally stimulated due to RhoA initiation [52]. This kinase presents in two isoforms, which are referred to as ROCK1 and ROCK2 [53]. Switching on this kinase can result in cytoskeleton rearrangement, which can contribute to cell migration patterns, and in cancer models, invasion [54]. Rac1 initiation can lead to the activation of JUN N- Terminal Kinase (JNK), which is a family of the MAPK [55]. The functions of JNK normally conclude stimulating a mitochondrial release of cytochrome C to cause apoptosis, and possess a regulation ability in cell proliferation, migration, and differentiation [55]. The activation of this signaling cascade results in various phenotypical responses that contribute to the cell's regular and abnormal functions.

1.2.3 Post-Translational Modifications and Modulators

1.2.3.1 Wnt Glycosylation

Glycosylation can be defined as the process of a carbohydrate covalently attached to a macromolecule such as proteins and lipids and is most common posttranslational modifications in protein biosynthesis [56]. This posttranslational modification can cause

differences in stability, solubility, and folding, and these alterations affect Wnts in various ways [57]. Reports illustrate that Wnts have N-linked glycosylation sites and these sites can directly affect their stability, folding, and solubility of the protein [58, 59]. The affect these sites have are unique to different Wnts. For example, Wnt3a and Wnt5a glycosylation is important for ligand secretion but not activity [60, 61]. Whereas Wnt1 has four N-linked glycosylation sites, none of which are required for secretion [60, 61]. It is suggested that glycosylation of Wnt ligands regulate the direction of secretion in polarized epithelial cells [62].

1.2.3.2 Wnt Acylation

A basic definition of acylation is a chemical reaction that leads to the addition of an acyl group to a substrate [63]. Acylation of a secreted protein is only documented to happen in three signaling pathways: hedgehog, Wnt, and Ghrelin [64]. This fatty acylation during biosynthesis is a main reason to why Wnts are extremely hydrophobic [65]. There are two types of acylation that occur within the cell, O-acylation and S-acylation [66]. S-acylation is present when there is an addition of a palmitate to a cysteine residue via a thioester linkage [67]. The O-acylation occurs when there is addition of a monosaturated fatty acid or palmitoleic acid via an oxyester linkage to a serine residue on the Wnt molecule [68]. O-acylation of Wnt ligands has been widely documented through the literature, but S-acylation is still controversial. In general, Wnt ligands undergo modifications that play an essential role to their secretion and biological activity.

1.2.3.3 Porcupine

Porcupine (PORCN) was first discovered in *Drosophilia* and described as a 7-transmembrane, o-acyltransferase located on the endoplasmic reticulum (ER), that is the crucial player in palmitoylating Wnt ligands [69]. PORCN is known to belong to a family of 16 evolutionarily conserved genes called membrane-bound O-acyltransferase (MBOAT) [70]. PORCN contains 11 transmembrane domains with a carboxyl-terminal tail and its catalytic site can be located within the third loop facing the ER lumen, where there is a conserved histidine that is essential for enzyme activity [71]. This protein has four documented human isoforms (A-D) which are products of alternative splicing on exon 7 and 8 [72, 73]. Each tissue, such as the heart, liver, testis, and lung, contains different isoforms of PORCN within its structure. Unfortunately, the functions of the individual isoforms have not been elucidated.

The *PORCN* gene is known to be X-linked and its depletion has been linked to a disease called focal dermal hypoplasia and angioma serpiginosum [74]. PORCN acts in combination with Notum and Stearoyl CoA Desaturase (SCD) to deacylate or acylate, respectively, the Wnt ligands. In the endoplasmic reticulum, SCD provides a monosaturated fatty acid which is then added to the Wnt ligand via PORCN [65]. This same fatty acid will then be removed via Notum in the extracellular matrix [75]. Regulation of these processes is critical for the binding of Wnts; without the correct modifications, these proteins lose their ability to bind to Frz and activate the downstream signaling cascades [75]. This concept highlights the attractiveness of PORCN as a target for various diseases, particularly cancer.

1.3 Wnt Signaling Involvement in Cancer Models

Wnt signaling dysregulation has been extensively documented throughout the years to be closely associated with the initiation and progression of human cancers. Both the noncanonical and canonical Wnt signaling cascades have been documented to have an upregulation in cancer models, which leads to uncontrolled cancer growth, proliferation, migration, and other malignant characteristics [76]. Though these signaling pathways are a major driver of cancer phenotypes, their function within different cancerous systems may vary.

1.3.1 Lung Cancer

Lung cancer is a prominent disease that effects the lives of millions of Americas each year [77]. Currently, this cancer is ranked as the second most common malignancy among United States (US) males and females and categorized as the number one cause of cancer-related deaths [77]. Lung cancer can be divided into two different types, small cell lung cancer and non-small cell lung cancer (NSCLC) [77]. Small cell lung cancer normally develops due to cigarette smoking and presents with a more aggressive phenotype, making chemotherapy the usual treatment option [78]. Non-small cell lung cancer is more commonly diagnosed and has a lower metastatic growth rate [79]. This subtype can be further categorized into three different types, known as adenocarcinoma, squamous cell carcinoma, and large cell carcinoma [79]. Recently, Wnt signaling has been increasingly implicated in lung cancer initiation and progression, specifically within the non-small lung cancer model [80]. Wnt signaling's role in small cell lung cancer has yet to be determined and investigated.

In NSCLC models, the canonical Wnt signaling pathway has a prominent role with overexpression of Wnts –1,-2,-3, and –5a [81]. There have also been reports of an increased

expression of Frz-8, Dvl, PORCN, and TCF-4, all of which have been linked to poor patient prognosis [82]. There is growing evidence illustrating the importance of Wnt signaling in the development of NSCLC, especially showing an upregulation of this signaling pathway when exposed to cigarette smoke components [82]. Interestingly, transgenic mice harboring the *Kras* mutation have an upregulation of Wnt signaling in harvested lung tissue. This increased activation in the mutant mice results in a significant elevation in tumorigenesis [83].

1.3.2 Breast Cancer

Breast cancer is the most commonly diagnosed cancer among US females and is the second leading cause of cancer-related deaths, following lung cancer [84]. Breast cancer related deaths have begun to decrease over the years due to early disease detection, but this has led to an increase in incident rates [84]. Though treatment options have increased the survival rates of many patients affected with this disease, metastatic properties still have a tremendous impact on therapeutic strategies and outcomes. There has been substantial evidence demonstrating Wnt signaling in breast cancer metastasis; this is the first cancer documented to have an association with the Wnt signaling cascade [85].

Breast cancer is divided into either invasive or preinvasive groups [86]. Invasive ductal carcinoma no-special-type (IND-NST) and invasive lobular carcinoma (ILC) are labeled as the two most common histological types of breast cancer that patients present [87]. Recently, many studies have shown that various components of Wnt signaling contain alternations within breast cancer models. These alternations have been determined to occur at both DNA levels, including amplifications, mutations, deletions, and methylations, and protein levels, including posttranslational modifications [88]. For example, studies have

illustrated the loss of noncanonical Wnt signaling activation, through the depleted expression of Wnt5a [85]. This loss shows a stabilization of β-catenin in the nuclear fraction, resulting in the expression of breast cancer target genes [85]. The mouse Wnt5a$^{-/-}$ model confirmed that the absence of Wnt5a showed a promotion of tumor growth and an increase in β-catenin accumulation within the cytoplasmic domain [88]. This model also illustrated that the loss of Wnt5a led to increased transcriptional level of Wnt/β-catenin target genes, such as c-MYC, AXIN2, and TFC4, indicating that depletion enhances canonical signaling [88]. This highlights the complexity of this pathway. Contrastingly, Wnt5a and Frz2 have been determined to have elevated expression within metastatic breast cancer cell lines and high-grade tumor samples [89]. Researchers also indicated an increase Epithelial-Mesenchymal Transition (EMT) marker expression and revealed that Frz2 was a major driver in EMT progression and cell migration via Stat3 and Fyn [89]. β-catenin expression levels have been documented to be significantly correlated with histological types, but further investigation is needed to determine the role of this signaling cascade and its potential as a viable target [90].

1.3.3 Colorectal Cancer

Colorectal cancer (CRC) is noted as the fourth most common cancer to occur and is ranked second in cancer related deaths worldwide [91]. This malignancy can be surgically resected and has a relatively high 5-year survival rate [91]. Unfortunately, patients that present with distant metastasis or experience postsurgical reoccurrence have little to no treatment options that optimize quality of life and survival [91]. This highlights the vital importance of understanding and developing novel therapeutic targets. Since many CRC patients harbor mutations in either the canonical or noncanonical Wnt signaling

cascades, these pathways have gained popularity in becoming a possible target for new adjuvant therapies [92].

CRC development normally takes 10 or more years to transition from normal epithelium into a cancerous phenotype [93]. The slow growth of these diseases is partly a reason to why numerous genetic changes can be found in the β-catenin pathway [93]. Specifically, there is a high mutation rate in the APC gene. Researchers has shown that in the absence of APC formation, β-catenin's cytoplasmic accumulation results in nuclear translocation and interaction with the TCF/LEF [94]. This interaction activated the transcription of various CRC progression genes. Wnt signaling has also been known to play a pivotal role in the CRC stem cell self-renewal within the intestinal crypts [93].

The activation of Wnt signaling results in the promotion of either differentiation or proliferation of cancer stem cells [95]. This mainly relies on which protein, p300 or CREB, is bound to β-catenin as a co-activator [95]. If CREB is bound to β-catenin, then the maintenance of potency for the cancer stem cells will be supported [96]. If, in contrast, the binding partner is p300, then cancer stem cell differentiation will be favored [95]. Additionally, the Wnt signaling gene, Lrg5, is widely utilized as a marker for cancer stem cell expression within the intestinal crypts [97]. Researchers have also shown that crypt homeostasis can be restored when APC function is re-established into mice models, even *in vivo* models that harbor *Tp53* and *Kras* mutations [98]. Interestingly, the correlation between the dysfunction of Wnt signaling and progression of CRC suggests that targeting Wnt signaling would be a promising therapy to prevent disease continuation.

1.3.4 Prostate Cancer

Prostate cancer is known as the most common malignancy diagnosed and has moved into the number one spot for cancer related deaths in US males [99]. Generally, prostate cancer is a slow growing disease, and it is typically detected in patients that are 65 years of age or older [99]. Due to this cancer affecting an older subset of the population, screening techniques typically begin around 60 years of age, or if there is a history of family occurrence, then monitoring begins around 45 years of age [100]. Procedurally, prostate cancer is screened for by measuring prostate specific antigen (PSA), which is a clinical biomarker for prostate cancer initiation and progression [101]. PSA normally is found primarily in semen, with sparse levels circulating in the bloodstream. When an abnormal amount of PSA is found in circulation, further testing is done to determine if there is a malignancy present [101]. The slow growth of prostate cancer allows patients that present with a localized tumor to have nearly a 99% 5-year survival rate [102]. In contrast, patients that have distant metastasis result in their 5-year survival dropping significantly to 39% [102]. Due to the lethality of this disease, novel targets are needed to provide patients with further treatment options. Recently, many studies have shown that Wnt signaling plays an essential role in the progression and metastatic capabilities of prostate cancer.

Research has shown that both the noncanonical and canonical Wnt signaling cascades play various roles in the progression, invasion, and migration during the progressing stages of prostate cancer [103]. Wnt5a has been documented to play a vital role in the cytoskeleton regulation via the activation of the Wnt/Ca^{2+} and Wnt/Planar Cell Polarity pathway [7]. Interestingly, researchers have shown that a loss of CaMK11 led to a significant reduction of cell motility and wound healing abilities in PCa cells [104]. Recent studies have also documented that Wnt5a has the most common activation and has

a high association with EMT progression [105]. In terms of drug resistant prostate cancer models, teams were able to show that the pharmacological inhibition of ROCK1/2, a GTPase downstream of the Wnt/PCP pathway, resulted in a decrease of invasion and migration abilities, and produced a loss of mesenchymal cell markers [106].

1.4 Wnt Signaling and Drug Resistance in Cancer

An increasing interest in Wnt signaling's involvement in chemotherapy resistance has been intensifying throughout the years [107]. Many studies have reported that elevated Wnt signaling expression has contributed to the development of drug resistance in cancer therapeutic approaches. These aberrant expression levels and common alternations are being identified to establish possible mechanisms of drug resistance occurrence and establishing novel targets for malignancies that are impervious to traditional therapeutic intervention.

APC is known to act as an intracellular negative regulator of Wnt Signaling and functions as a tumor suppressor [108]. Subsequently, the *APC* gene has shown a high mutation rate in sporadic and hereditary CRC [109, 110]. Studies have reported that loss of function mutations within the APC gene have resulted in an increase of β-catenin stabilization and target gene transcription via β-catenin/TCF complex [111-113]. Researchers also described a point mutation found in the phosphorylation sites of β-catenin that prevented its degradation, in a small subset of CRC that maintained a wild-type *APC* gene [113]. Active Wnt signaling, has also been linked to increase resistance against growth factor inhibitors. Specifically, there has been substantial evidence showing elevated levels of nuclear β-catenin associated with PI3K/AKT/mTOR inhibitor resistance [114].

This increase was also seen in CRC cells that were treated with a BRAF inhibitor. It should be noted that abnormal Wnt signaling expression is not limited to CRC models.

Prostate cancer is a hormone sensitive cancer, that can unfortunately progress into a lethal and therapeutic, non-responsive disease [115]. Research has shown that patients that were non-responders to abiraterone/prednisone, therapeutic strategy for castration-resistant prostate cancer patients, presented elevated Wnt/β-catenin signaling in a clinical study [116]. They also reported that these samples harbored an increase in alterations of Wnt signaling components and illustrated that the inhibition of Wnt signaling could re-sensitize resistant patients to a therapy course of abiraterone/prednisone [117]. These findings indicated that Wnt/β-catenin signaling could be activated after prostate cancer cells have been exposed to androgen deprivation. In addition to the discoveries regarding the canonical Wnt signaling's involvement, studies have shown that the noncanonical Wnt signaling pathways have been determined to be activated in circulating tumor cells [118]. The increased expression of Wnt5a and Wnt7b within those cells mediated resistance to androgen receptor inhibitors. Reports also suggested Wnt signaling as a driver of bone metastasis, which is a common occurrence in prostate cancer patients[119].

In EGFR-mutated lung cancer, Wnt/β-catenin signaling has been shown to drive resistance to the EGFR inhibitors, although reports did not claim that exposure to EGFR inhibitors upregulated the Wnt/β-catenin pathway in lung cancer clinical studies [120]. Bromodomain and extra terminal protein (BET) inhibitors entered the realm of clinical trial as a targeted therapeutic to combat acute myeloid leukemia [121]. This inhibitor works by disrupting the BRD4-chromatin interaction and acts to repress BRD4-regulated genes [122]. Research shows that Wnt/β-catenin signaling promotes primary and acquired

resistance to BET inhibitors within a leukemia model [123]. This happens by β-catenin binding to the promoter region of BRD4-dependent genes such as MYC, maintaining their expression [122]. This information taken together indicates that Wnt/β-catenin signaling is a major driver of resistance to BET inhibitors in leukemia cells.

Wnt signaling has shown to play a paramount role in the ability of cancer cells to gain resistance against traditional cancer interventions. This unique characteristic has highlighted Wnt signaling as an attractive potential therapeutic target and has resulted in various researchers to create and test Wnt signaling inhibitors in multiple cancer models.

1.5 Current Clinical Trials for Malignancies Dependent on Wnt Signaling

Interestingly, many studies have alluded to Wnt signaling's role in tumorigenesis, and that the induction of chemotherapy and radiation activate the signaling pathway to protect cancer cells from cell death [124]. This raises the idea that Wnt signaling could be a promising target to combat various malignancies. Unfortunately, the Wnt signaling cascade has proven to be a difficult target clinically and there are no current FDA-approved Wnt signaling inhibitors for cancer treatment. However, several new promising drug prospects are entering clinical trials.

1.5.1 Upstream Targets of Wnt Signaling

1.5.1.1 Porcupine Inhibitors

PORCN is a known member of the MBOAT which palmitoylates Wnt ligands. This enzyme's upregulation is generally associated with poorer prognosis in head and neck squamous cell carcinomas [125]. Recently, PORCN has become an attractive target because its inhibition would result in the suppress of all Wnt ligand secretion [126]. This action would lead to a loss of both Wnt signaling pathways, canonical and noncanonical

Wnt signaling pathways. This led to the development of the following oral inhibitors: WNT-974 (LGK-974), ETC-253 (ETC-1922159), and CGX1321.

LGK-974 is a small, potent competitive inhibitor that is mechanistically functions by blocking the catalytic ability of PORCN [127]. Specifically, LGK-974 blocks the imidazole nitrogen that acts as a hydrogen acceptor on PORCN which allows the interaction with Wnt ligands, preventing Wnt ligands secretion and binding to plasma membrane receptors [127]. In renal carcinoma cell lines, this inhibitor has been shown to halt cell proliferation and migration in a dose and time dependent manner [128, 129]. In murine models, MMTV-Wnt1 mammary tumor samples were subjected to LGK-974 and results indicated a reduction in tumor volume in the treated group [127]. A similar effect was presented in a mouse model harboring head and neck squamous cell carcinoma (HNSCC) and the outcomes of this study indicated that there was substantial tumor regression with the LGK-974 treated group compared to the control group [127]. Both murine studies also confirmed that the administration of LGK-974 did not affect the weight of the animals within the experiment, indicating that the inhibitor many possess low toxicity. LGK-974 is in phase I clinical trial for Wnt dependent malignances. This study is recruiting patients currently harboring cancers such as triple-negative breast cancer, pancreatic cancer, head and neck squamous cancer, and cervical squamous carcinoma (NCT01351103). LGK-974 is also being used in a combination therapy with BRAF inhibitors, LGX818 and cetuximab, for patients with metastatic CRC cancer that possess WNT and BRAF mutations [130].

ETC-153 is another porcupine oral inhibitor that has high bioavailability and has been shown to reduce tumor growth in a Wnt1 overexpression breast cancer murine model [131]. The reduction was documented to be between 52%- 78%, without significant weight loss of the animals used [132]. This inhibitor has also shown great efficacy against tumors harboring R-spondin 2 and 3 gene fusion in colon cancer human samples [131]. Recently, ETC-153 was evaluated for tolerability by conducting a dose-escalation in phase I clinical study (NCT02521844). The study concluded that patients tolerated the compound up to 30mg, with side effects occurring in less than 20% of patients [133]. This suggests that ETC-153 can be well tolerated in a patient population with solid tumors.

CGX1321 is another small molecule inhibitor that has shown specificity for PORCN. This inhibitor's main function is to disrupt Wnt ligand secretion and has been document to have high efficacy in tumors possessing R-spondin or RNF43 mutations [134]. Currently, a dose-escalation (phase 1) and dose expansion (phase 1b) studies were conducted among 77 patients to test the safety of the compound [132]. Results demonstrated that the compound was well tolerated and recommended dosage was confirmed. Recently, CGX1321 has entered a clinical trial in combination with pembrolizumab for patients with advanced gastrointestinal tumors (NCT02675946, NCT03507998). Results have not been released regarding the conclusions of this combination approach.

1.5.1.2 Frizzled Receptor Antagonist

Vantictumab is a human IgG2 monoclonal antibody that has illustrated efficacy in inhibiting Frz receptors (NCT01345201, NCT01973309, NCT02005315). Specifically, this antibody has shown to be able to inhibit Frz1, Frz2, Frz5, Frz7, and Frz8 [135].

Vantictumab's mechanism of action is that it binds to the extracellular domain and sterically inhibits Wnt ligands from docking to the Frz receptor [135]. This entail leads to the loss of LRP6 phosphorylation and causes a blockage of the LRP6 co-receptor. This has been linked to a reduction in β-catenin expression, and Wnt signaling is seemingly halted. Previous studies have reported that Vantictumab has been able to inhibit tumor growth in various cancer types and prevent tumor reoccurrence [136]. In breast and pancreatic cancer murine models, it was documented that the antibody alone, or in combination with taxanes and gemcitabine, was able to reduce the number of tumor-initiating cells [136-139]. Currently, Vantictumab is in a phase 1b study for patients that harbor recurrent or metastatic HER2-negative breast cancer [139]. This study particularly looked at a combination therapy of Vantictumab and paclitaxel, and results showed that the combination was well tolerated [139]. Unfortunately, the study did not progress in the clinic due to increase fractures observed in patients [140].

1.5.1.3 LRP Co-Receptor Antagonist

Historically, LRP co-receptors were created as treatment for parasitic infections, but there has been increasing evidence showing their involvement in cancer therapy [132] [141]. Niclosamide is an anthelmintic drug that has been documented to have antiproliferative effects on cancers such as CRC, PCa, lung, ovary, and breast [141]. This is due to its ability to hinder Wnt signaling via promoting LRP6 co-receptor degradation [141]. This drug has also been observed to degrade Frz1 receptors, Dvl, and β-catenin. The mechanism of action for how Niclosamide decreases Wnt signaling is still undetermined, but many studies speculate that it is due to mediated autophagy [142]. This is because LC3, an autophagy marker, was found to be co-localized with Wnt signaling makers after being

exposed to Niclosamide [143]. Though the mechanism is unknown, Niclosamide has had great success in preventing cancer progression. In ovarian cancer, the drug was able to reduce the number of tumor stem cells and that it was able to halt cell proliferation in chemotherapy-resistant ovarian cancer cells [144]. Currently, this drug is in phase 1b of clinical trial with prostate cancer patients, but unfortunately the maximum dosage does not seem to yield therapeutic effect in other cancer types and will not be pursued further (NCT 03123973).

1.5.2 Targeting Downstream Wnt Signaling Pathway

Targeting the Wnt/ signaling pathway has been associated with prominent drug discovery. Historically, the compounds created to inhibit this cascade, were created to directly affect components of the pathway [129]. These components included the β-catenin, β-catenin degradation complex, TNKS, Frz, PORCN, and many others. β-catenin/TCF4 interaction was also an interest but showed difficulty in targeting. The identification of these targets has led to several clinical trials openings, in hopes to provide patients with increased survival outcomes.

1.5.2.1 β-catenin Proteasomal Degradation Promoters

Another method that researchers have explored to combat aberrant expression of Wnt signaling, is to restore the component responsible for β-catenin degradation. This idea is what launched the repurposing of an FDA-approved, anthelmintic drug called pyrvinium [132]. Pyrvinium has been shown to successfully restore the activity of several different kinases that function to degrade β-catenin [145, 146]. Specifically, pyrvinium works by directly binding to CK1α as a coactivator and stabilizes the protein [146]. Since CK1α is the first step in the phosphorylation of β-catenin for degradation, the restoration of its

activity inhibits Wnt signaling [147]. Pyrvinium has also been documented to inhibiting AKT and this results in a restraint for Wnt signaling, further suppressing the pathway [147]. In colon cancer cell lines, this inhibitor showed a reduction in cancer cell proliferation and was able to deplete cancer cells harboring APC mutations [148]. Currently, this drug is in phase 1 clinical trial for the treatment of pancreatic cancer (NCT05055323).

1.5.2.2 β-catenin and CBP Complex Inhibitors

There are many coactivators that form complexes with β-catenin. Some of those coactivators are TCF, LEF, CBP, and p300 [149]. The CREB binding protein (CBP) is labeled as an attractive target for preventing target gene transcription [132]. This led to the development of PRI-724, which is a small molecular inhibitor of the CBP/β-catenin interaction [132]. This inhibitor works by competitively binding to CBP, and preclinical studies have shown that this inhibitor functions to make cancer cells more sensitive to chemotherapy and prevent proliferation [132]. In the phase 1 clinical trial study, PRI-724 was widely tolerated by patients with solid tumors and a maximum dose of 905 mg was confirmed [132]. This led to a progression into phase 2 of clinical trial, but results have not been reported. PRI-724 was also used in combination with gemcitabine in metastatic pancreatic cancer. Results showed that the inhibitor stabilized the disease in 40% of patients, and seven of the patients presented with grade 3 and 4 side effects (NCT 01302405, NCT 001764477) [132].

1.5.3 Clinical Side Effects Using Wnt Signaling Inhibitors

Though the clinical trials for targeting Wnt signaling to combat various cancer types has shown great promise, side effects that present with the administration of these compounds still occur and need to be taken into account when implementing them into

clinical settings. Since Wnt signaling has a strong involvement in normal cell function to maintain homeostasis, as well as ensures cellular differentiation for the regeneration of many tissues, the inhibition of this pathway can cause serious side effects. The most common side effects documented have been gastrointestinal problems, hair loss, immunosuppression, fatigue, anemia, neutropenia, bone fractures, and neurodegeneration [150]. Though the delivery of Wnt signaling inhibitors has shown serve side effects, the presented symptoms do not outweigh the therapeutic benefits [132]. To overcome some of these symptoms caused by inhibition of Wnt signaling, strategies have been discussed in implementing nanoparticles and liposomes to directly target the tumor cells [151].

1.6 Discussion

In conclusion, it has been documented and presented in various preclinical and clinical studies that Wnt signaling plays a paramount role in the homeostasis, disease onset, cancer initiation, and cancer progression. Multiple researchers have linked Wnt signaling overexpression and upregulation to poor patient outcome and prognosis, and resistance to traditional chemotherapies. There has also been a growing development of pharmacological inhibitors that show great promise in preventing the survival of cancer cells. With these continuing efforts in understanding the mechanistic workings of Wnt signaling, and all its components within the cancer cell, and the progression of creating novel targets, it is hopeful that these methods will be translated into a clinically setting, in order to present patients with more effective therapies.

Though we have seen that both Wnt signaling cascades play an intrinsic role in cancer initiation and progression, and alluded to possible therapeutic targets, this study will primarily focus on PORCN and its role in Enz-resistant prostate cancer. This project will

work to determine if the inhibition of PORCN can silence both Wnt signaling pathways and enhance the efficacy of Enz treatment in drug resistant PCa. Also, there will be a determination of PORCN's role in the metabolic switch that drug resistant PCa harbors. In the completion of this study, our team hopes to identify a novel target for this lethal disease.

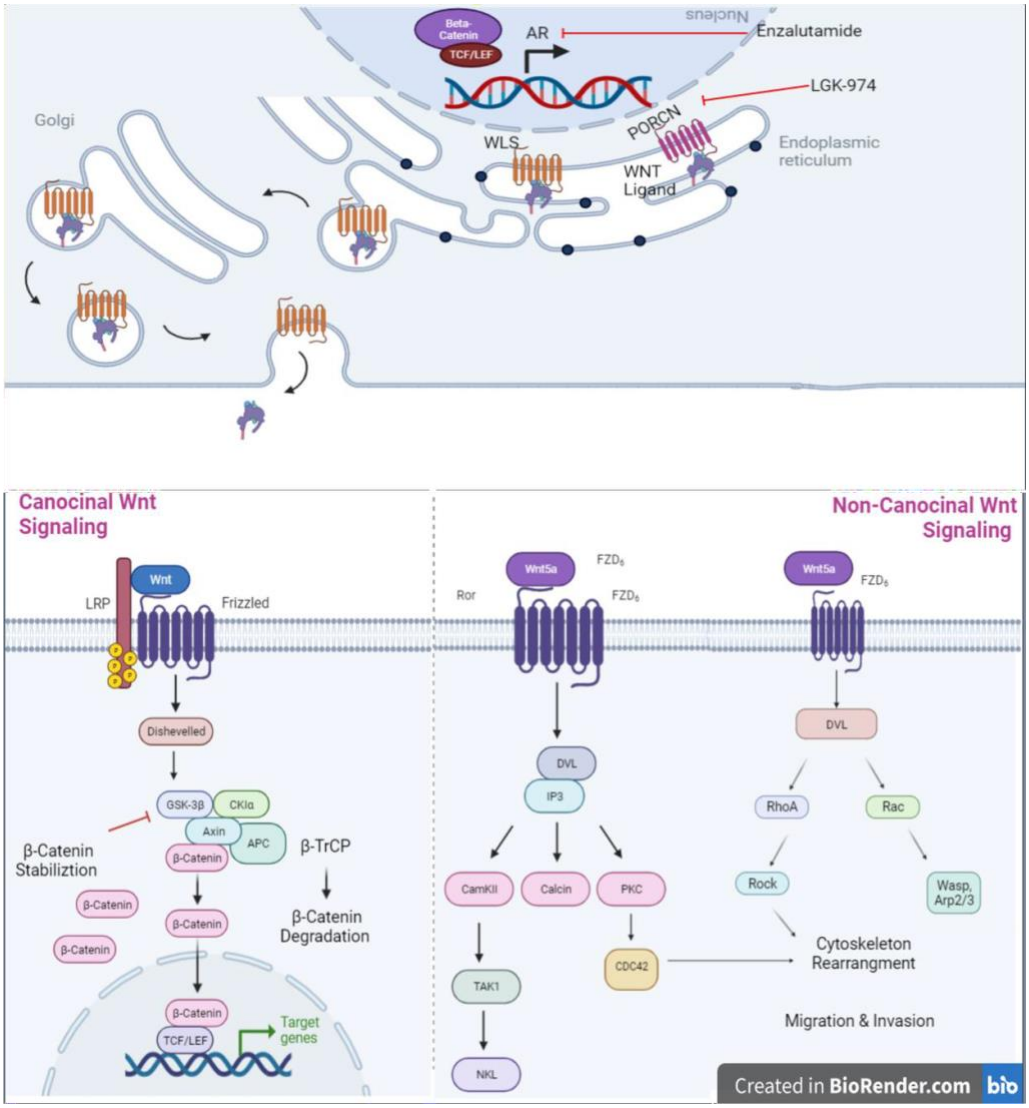
Nucleus
Beta-Catenin
TCF/LEF
AR
Enzalutamide
LGK-974
Golgi
PORCN
WLS
Endoplasmic reticulum
WNT Ligand
Canocinal Wnt Signaling
Non-Canocinal Wnt Signaling
Wnt
LRP
Frizzled
Dishevelled
GSK-3β
CKIα
Axin
APC
β-Catenin
β-TrCP
β-Catenin Stabiliztion
β-Catenin Degradation
TCF/LEF
Target genes
Wnt5a
FZD6
Ror
DVL
IP3
CamKII
Calcin
PKC
CDC42
TAK1
NKL
RhoA
Rac
Rock
Wasp, Arp2/3
Cytoskeleton Rearrangment
Migration & Invasion
Created in BioRender.com

Figure 1

Figure 1. Wnt Signaling Cascade.

This scheme is to further illustrate the Wnt Signaling cascade and our current working model for the duration of this project. In this picture, it is depicting the various downstream effectors and what their activation leads to within cellular function. It also depicts the process in which Wnt ligands are palmitoylated and secreted for plasma membrane receptor interaction.

COMPOUND NAME	TARGET	CANCER	CLINICAL PHASE
LGK-974	PORCN	Pancreatic Cancer CRC with BRAF mutations Melanoma Triple-negative breast cancer Squamous cell carcinomas	Phase 1 NCT 01351103
ECT-159	PORCN	Solid Tumors	Phase 1 NCT 02521844
CGX1321	PORCN	Solid Tumors GI Tumors with pembrolizumab CRC adenocarcinoma Gastric adenocarcinoma Pancreatic adenocarcinoma Bile Duct Cancer Hepatocellular carcinoma GI Cancer	Phase 1 NCT 02675946 Phase 1 NCT 03507998
VANTICTUMAB (OMP-18R5)	Frz Receptor Antagonist	Solid Tumor Metastatic breast cancer with paclitaxel Metastatic pancreatic carcinoma	Phase 1 NCT 01345201 Phase1 NCT 01973309 Phase 1 NCT 02005315
NICLOSAMIDE	LRP6 co-receptor Antagonist	Colon Cancer Metastatic Prostate Cancer	Phase 1 (terminated) NCT 02687009 Phase1 NCT03123978
PYRVINIUM	β-catenin Degradation-CK1α activator	Pancreatic Cancer	Phase 1 NCT 05055323

Table 1. A list of inhibitors that are currently in clinical trial for cancers that are Wnt-dependent malignancies.

COMPOUND NAME	TARGET	CANCER	CLINICAL PHASE
PRI-724	CBP/β-catenin complex	Advanced pancreatic cancer Metastatic pancreatic cancer Pancreatic Adenocarcinoma Advanced solid tumors	Phase 1 NCT 01764477 Phase 1 NCT 01302405

Table 1 (*continued*). A list of inhibitors that are currently in clinical trial for cancers that are Wnt-dependent malignancies.

CHAPTER 2. METHODOLOGY

2.1 Cell Culture

All prostate cancer cell lines (LNCaP, MR49F, C4-2, C4-2R, and 22Rv1) were cultured at 37°C in RPMI 1640 medium with 10% Fetal Bovine Serum (FBS) and 5% penicillin-streptomycin in 5% CO2. LNCaP and 22Rv1 lines were purchased from ATCC, whereas C4-2 and C4-2R were obtained from Dr. Allen Gao. To maintain ENZ resistance, 20μM of ENZ was added to the media of C4-2R and 10μM of ENZ was added to the media of MR49F. To removal any residual effects of ENZ, cells were cultured in media without ENZ for 48 hrs.

2.2 RNA Isolation and RT-qPCR

Total RNA was isolated using Qiagen RNeasy Mini Kit (Qiagen, 74104) and then concentration of RNA was collect using the ThermoFisher™NanoDrop One Microvolume UV-Vis Spectrophotometer (Thermo, 13400519). RNA was then converted into cDNA using the kit QuantiTect Rev. Transcription Kit (Qiagen, 205311) via manufacture's instruction. Real-time qPCR was performed using ABI 7900HT thermal cycler and SYBUR Green Master Mix (Thermo, 4309155). Data was normalized to GAPDH transcript.

2.3 Immunoblotting

Cells were harvested and washed with ice-cold 1x PBS and then a lysis buffer containing 1x RIPA, 25x protease inhibitor cocktail, 0.1% SDS, and 25x phosphatase inhibitor were added into the dish. Samples were then collected and placed into the heating block for 10 mins at 95°F. Protein concentration was verified via Pierce BCA Protein Assay Kit (Thermo, 23225) and a total of 15μg of samples were loaded onto the SDS-Page gel

for electrophoresis. Next protein was transferred onto nitrocellulose membranes and blocked with 5% skim milk. Primary antibody was placed in 5%BSA in 1xTBST and placed on a shaker in the 4°C fridge overnight. The next day, the primary antibody was collected, and the membrane was washed 3 times for 15 mins with 1x TBST. HRP-linked secondary antibody in TBST were placed on the membrane for 1 hr room temperature. Secondary antibody was then discarded, membrane was washed 3 times at 15 mins. And protein bands were probed using SuperSignal West Dura Extended Duration Substrate (Thermo, 34076) and imaged using ChemiDoc Imaging Sysytem. Immunoblots were repeated three times and one blots was used as representation.

2.4 Clonogenic Assay

22Rv1 cells were plated in 6-well assay plated at 500 cells per well. Cells were given 24 hrs. to adhere to the plate and then media was replenished with the addition of the chemical compounds. Media and compounds were replaced every 2 days, for a duration of 14 days. On the 14th day, the media and chemicals compounds were removed and washed with 1x PBS 3 times. The cells were fixed with 10% formalin for 30mins and then stained with crystal violet reagent for 15 mins. After staining, cells were washed 3 times with water and imaged using the ChemiDoc Imaging System. All experiments were performed in triplicate, and one was used as a representative image.

2.5 Cell Viability and Cell Proliferation

Cells were seeded into 96-well plates (C4-2R: 2,000 cells per well, MR49F: 4,000 cells per well) and allowed 24hrs to adhere to the plate before addition of treatment. After 24 hrs, the media was refreshed with indicated concentration of chemical on day 0 and day 3. On the day 3, AquaBluer (MultiTarget Pharmaceuticals LLC, 6015) reagent was added

to the media and the incubated at 37°C for 4hrs. Fluorescent intensity was read at 540ex/590em by GloMax Discover plate reader from Promega. All experiments were performed in triplicate, but one was used as representation.

2.6 Xenograft

All animals, cell lines, and inhibitors utilized in this study were approved by the University of Kentucky's Institutional Animal Care & Use Committee (IUCAC). 22Rv1 (2×10^6 cells per mouse) were mixed with Corning™ Matrigel and inoculated on the left side of each pre -castrated, nude mouse (The Jackson Laboratory) subcutaneously. Mice were then randomized into four treatment group: Control, LGK-974, Enzalutamide, and Combination. There where n=5 per each group. All treatments were mixed into corn oil and give via oral gavage for a treatment scheme of 5 days on and 2 days off. Tumor volumes were calculated via the following formula, V= L x W2/2 (V= volume in cubic millimeters, L= Length in millimeters, and W=Width in millimeters). Treatment lasted for 4 weeks and then animals were humanely euthanized, and tumors collected for further experiments.

2.7 Wound Healing

Cells were plated in 6-well plates ($3x10^6$) and allowed 24hrs to adhere to the plate. After 24hrs, a scratch assay was performed by taking a 1mL pipette tip and scratching down the middle of the plate creating a gap within the cell. Wells were then imaged and measured to determine day 0 of migration ability. Media was then replenished, and chemicals were added to each well. Everyday cells were imaged and measured to determine the rate of migration. The experiment was completed in a replicate of three and qualified accordingly. One representative image was used.

2.8 Flow Cytometry

Cells ($1x10^5$) were plated in a 12-well plate and allowed 24hrs to adhere to the plate. After 24hrs incubation, cells were subjected to chemical addition and kept for a time point of 12hrs. Cells were then collected or stained based on the following assays: *2.8.1 JC-1:* Cells were stained with JC-1 Dye (Mitochondrial Membrane Potential) (ThermoFisher, T3168) 1hr at 37°C within the cell culture incubator. All gating and channels were done via the manufacturer's instruction. FCCP was used for control. This experiment was done in triplicate and quantification with one replication is shown. *2.8.2 MitoTracker Green:* C4-2 and C4-2R cells were stained with MitoTracker ™Green FM Dye (ThermoFisher, M46750) for 1 hr at 37°C in the cell culture incubator. Cells were then washed with 1x PBS, trypsin was added to collect the cell, and the cell pellet was re-suspended in 1X PBS. Cells were non-fixed per the guidelines of the manufacture's instruction. Channels and gating were done according to the manufacturer's instruction. FCCP was used as control. This experiment was done in triplicate and quantification shown. *2.8.3 DAPI Cell Cycle:* Collected cells were spun at 500g for 5min in a 4 °C centrifuge, and then washed twice with cold 1x PBS. After washing, the cells were spun at 5oog for 5 mins in the 4°C centrifuge and resuspended in 1x PBS to ensure single cell suspension. Once in single cell suspension, 4.5L of ice-cold 70% ethanol is added and incubated for at least 2hrs for fixation. Cells are then centrifuged for 5 mins at 1000g and the supernatant is removed. Pellet was resuspended in 1x PBS and allowed to sit at room temperature for 15 mins. Cells were then spun at 1000g for 5 mins and cell pellet was resuspended in DAPI/TritonX-100 for a light-protected incubation of 30 minutes. The DAPI signal was

then determined using the 405-450/50 lineal mode and data was quantified. The experiment was performed in triplicate and FCCP was used as a control.

2.9 Seahorse Analysis: MitoStress Test

C4-2 and C4-2R cells were seeded at 20,000 cells/well in Agilent XFe 96 well cell culture plates in RPMI 1640 medium with 10% FBS and 1% antibiotics. Cells were allowed 24 hrs to adhere to the plate and then checked the morning of experiment to ensure attachment. Before analysis, 12hrs, cartridges were hydrated in calibrant buffer non-CO2 incubator at 37C̊Æ†Before exposed to seahorse analysis, cells were washed multiple times with corresponding medium and then placed in with medium into non-CO2 incubator for 1 hour. Next, the GST medium was prepared by utilizing XF base medium and adding 2mM glutamate, ensuring a temperature of 37°C and a pH of 7.4. The reagents glucose, oligomycin, and 2-DG were provided via the XF Glycolysis Stress Test Kit and diluted to reach the desired concentrations (Glucose: 80mM, Oligomycin: 9μM, 2-DG: 500mM). Then these reagents were added to the appropriate areas of the cartridge. The cartridge was calibrated via manufacture's instruction, cells were subjected to GST. After the addition of those reagents, the MST medium was prepared by using the XF base medium in congruence with 2mM glutamine, 1mMpyruvate, and 10mM glucose, which was then warmed until 37°C and adjust for a pH of 7.4. The remaining regents were provided via the Glycolysis Stress Test Kit and were diluted to the following concentrations: Oligomycin: 8μM, Carbonyl cyanide-4-(trifluoromethoxy) phenylhydrazone (FCCP): 9μM, Retenone/antimycin A: 5μM. These reagents were then added to the correct portions of the calibrated cartridge and then cells were subjected to MST. Please reference the following publication: Chen L, Ahmad N, Liu X. Combining p53 stabilizers with

metformin induces synergistic apoptosis through regulation of energy metabolism in castration-resistant prostate cancer. Cell Cycle. 2016;15(6):840-9. doi: 10.1080/15384101.2016.1151582. PMID: 26900800; PMCID: PMC4845973.

2.10 Glycolytic Stress Test

C4-2 and C4-2R cells were seeded at 20,000 cells/well in the Agilent XFe 96 well cell culture plates in RPMI 1640 medium with 10% FBS and 1% antibiotic. Cells were placed in incubator overnight and were checked the morning of the experiment to ensure adherence. To prepare for the following experiment, the following steps needed to be completed the day before the analysis. The day prior, the sensor cartridge was rehydrated with the Seahorse XF calibrant in a 37°C, non-CO2 incubator overnight. The next the following reagents were prepared for the experiment to commence. Assay medium was prepared utilizing the Seahorse XF Base medium with the addition of 2mM of glutamine and warmed to 37°C with an adjust pH of 7.4. The assay medium was kept in 37°C until used, and stock compounds were prepared. Oligomycin, glucose, and 2-DG were provided via the Glycolysis Stress Test Kit and diluted to the recommended concentrations. These reagents were then added to the hydrated cartridge in the appropriate ports provided at a final concentration as followed: Oligomycin: 1.0μM, Glucose: 10mM, 2-DG: 50mM). Using a multichannel pipette, the cell culture growth medium was replaced with the warmed assay medium described above, and placed into a 37°C, non-co2 incubator for a duration of 45 minutes to 1 hour before the execution of the assay. Using the appropriate software, place the sensor cartridge into the utility plate of the instrument and calibrate. After completion of the calibration, replace the sensor cartridge with the cell culture assay plate and run the analysis. Seahorse XF Glycolysis Stress Test Report Generator will

automatically calculate the parameters from the Wave data software and export it into an excel file.

2.11 Immunohistochemistry

22Rv1tumor samples were harvested from the mouse host, placed in 10% formalin, and rocked on the shaker for 24hr. After the 24hr incubation, the tumors were placed in 70% ethanol, and taken to our Biospecimen Procumbent and Translational Pathology Shared Resource Facility to create a parafilm-embedded slides. These slides were then stained with the Ki-67 antibodies and H&E staining. To quantity the staining, the AI Halo software was used to determine the intensity of each stain. Three slides were used, and each slide had four random sections analyzed and quantified via the software.

2.12 Lactate and Glucose Measurement Analysis

2.12.1 LactateGlo: The LactateGlo was purchased from Promega (J5021) and all reagents were prepared based on the recommendations of the manufacture. To determine the extracellular lactate levels, C4-2 and C4-2R cells (4,000 cells/well) were plated in 96-well cell culture plated and allowed 24hrs to adhere. Control wells were included that only harbored medium. 5μL of sample medium was collected and added to 95μL of PBS. Then 50μL of the mixture was transferred to the 96-well assay plate, then 50μL of the Lactate Detection Reagent, previously prepared, was to each sample well. The plate was then shaken for 60 secs to allow for mixing and incubated for 60 minutes at room temperature. Luminescence was then recorded via GloMax Discover plate reader from Promega. For the drug treatment portion, all steps listed above were replicated but the drug treatment was added for 12hrs before collections. All experiments were performed three times and statically quantified.

2.12.2 GlucoseGlo: GlucoseGlo kit was purchased from Promega (J6021) and all reagents were prepared based on the recommendations of the manufacture. To determine the intracellular glucose levels, C4-2 and C4-2R cells (4,000 cells/well) were plated in 96-well cell culture plated and allowed 24hrs to adhere. Media was removed from the cells, washed with PBS, and then fresh PBS was added to the plate. The Inactivation Solution (provided in kit) was then added to the cells and the plate was placed on the shaker to mix for 5 minutes. After the 5-minute rock, the Neutralization Solution (provided in kit) was added, and the plate was shook for 60 seconds. At this point the Glucose Detection Reagent (provided in kit) was added and allowed to mix with other compounds for 60 seconds. The plate was then incubated at room temperature for 60 minutes and then the Promega's GloMax Discover plate reader was used to record luminescence. For the drug treatment portion, all steps listed above were replicated but the drug treatment was added for 12hrs before collections. All experiments were performed three times and statically quantified.

2.13 Statistical Analysis

Statistical analyzes were performed utilizing the statistical functions found in GraphPad Prism 8. Unless referenced, an unpaired two-sided t test was used as a default method and normality and variance of results were checked to confirm requirements were met. The mice weights, a one-way ANOVA was used to determine significance. Statistical significance was set at $p < 0.5$, unless indicated otherwise.

CHAPTER 3. ENHANCING ENZALUTAMIDE EFFICACY IN DRUG RESISTANT PROSTATE CANCER

3.1 Introduction

Therapeutic intervention for prostate cancer varies based on the tumor staging/grading, location, and previous treatments that have been administrated. Localized tumors are normally combated surgically with a radical prostatectomy, or patients can receive radiation therapy [152]. Both approaches are intended for a curative result, with the desired outcome of abolishing cancer cells from the patient's body and increasing survival. Though many patients have a positive reaction to this treatment course, several individuals will still have a recurrence that will lead to clinicians modifying the treatment plan. This modification could lead to Androgen Derivation Therapy (ADT), which is to deplete the patient's body of androgen through medical or chemical castration [153]. The reasoning for this approach is due to prostate cancer's reliance on the Androgen Receptor (AR) activation.

Prostate cancer's main driver is AR, and this gene plays a pivotal role in the initiation and progression of this cancer type. AR is a member of a nuclear receptor family and contains five main regions, such as the N-terminal, NH2 terminal transactivation domain, a ligand binding domain DNA-binding domain, and a hinge region [154]. According to various reports, the NH2 terminal transactivation domain contains glutamine repeats, and these repeats vary among the male population [155, 156]. These repeats have also been correlated to the risk of prostate cancer occurrence. For example, shorter glutamine repeats have been associated with higher transcriptional activity of AR, which has resulted in a high risk of prostate cancer [156]. Whereas longer repeats of glutamine

have been linked to lower transcriptional activity of AR and has caused issues such as erectile dysfunction, testicular atrophy, etc [156].

Androgens are a male sex hormone that are synthesized in the testis and the adrenal gland. In the adrenal gland, androgens are converted to testosterone by 17-beta-hydroysteriods dehydrogenase in prostate cells [157]. Testosterone normally binds to a sex hormone globulin and about 1-2% remains unbound [158]. This unbound testosterone is then converted into dihydrotestosterone (DHT), which contains a high binding affinity for AR, via 5-alpha-reductase in prostate cells [157]. Testosterone and DHT bind to the ligand binding domain of AR and cause a conformational change that allows AR to translocate to the nucleus [159]. Within this fraction of the cell, AR dimerizes and binds to the androgen response elements (ARE) [159]. AR also interacts with the enhancer of various target genes via the zinc-finger of the DNA-binding domain [159]. The AR dimer can form a complex with coactivator and coregulatory proteins, such as activation function-1 (AF1) and activation function 2 (AF-2) and regulate the gene expression of various downstream effectors [160]. Some of the genes regulated via AR are fusion genes (TMPRSS2), growth stimulators (IGF1R, APP), transcription factors (NKX3.1), metabolic enzymes (CAMKK2), secreted proteins (KLK3), etc [154]. In prostate cancer, the major features of AR are the synthesis of PSA (KLK3), the regulation of lipid metabolism, and cell proliferation.

Due to the importance of AR in the progression and activation of prostate cancer, it is understandable why it has become the main treatment focus. In ADT therapy, once the body has been depleted of androgens, theoretically AR should have little to no activation. Unfortunately, AR can be activated through various other pathways and maintain cancer

cell growth and invasive properties. This was the reasoning for scientists to create a second-generation AR inhibitor called Enzalutamide, also referred to as Xtandi [161].

Enzalutamide (Enz) contains a threefold therapeutic approach. Firstly, it acts as a potent and competitive binder of androgen [161]. This prevents androgens from effectively binding to AR's binding domain. Secondly, it works to inhibit the translocation of AR to the nucleus to prevent interaction with AREs [161]. Thirdly, once in the nucleus, Enz inhibits AR from binding to the chromosomal DNA and sequentially preventing further transcription of tumor genes [161]. Clinically, this inhibitor has shown great efficacy in impeding or decelerating cancer cell growth, providing patients with improved outcomes [161]. Though Enz has been a life changing intervention, patients still report side effects such as induced or worsening of hypertension, increase fall risk, fatigue, rash, diarrhea, weight loss, and seizures [162]. Due to the severity of these side effects, researchers developed derivatives of Enz, Apalutamide (Apa) and Darolutamide (Daro). Apa and Daro have similar mechanisms of action to Enz, but differ in their binding efficacy to AR, dosage, and presentation of side effects [163]. Also, Enz is the only androgen signaling inhibitor (ASI) that is Food and Drug Administration (FDA) approved for metastatic castration-resistant prostate cancer (mCRPC), but Apa and Daro are still used widely in the clinic to treat mCRPC [163]. Though it is not FDA approved, Daro is used widely due to its decrease in side effect occurrence, its increase in efficacy for AR binding, and its ability to account for an AR splice variant that results from a truncated binding domain, AR-variant 7 (AR-v7) [163].

Unfortunately, after this line of treatment, there are little to no options for patients. Thus, patients are placed into a palliative care plan and must rely on clinical studies.

Currently, approved for mCRPC are PARP inhibitors such as Olaparib, Rucaparib, Talazoparib, and Niraparib [164]. For Olaparib and Rucaparib, this is given to patients after the tumor cells have stopped responding to Enz or Abiraterone [165]. Whereas Talazoparib and Niraparib are to be given in combination with Enz [165]. These new targeted therapies were approved in 2023, but only show efficacy towards patients with specific gene mutations such as BRCA1/2 or HPR [164]. There also has been an emergence in the immunotherapy sector with the utilization of sipuleucel-T (Provenge) [164]. Before treatment, blood is collected from the patient and immune cells are separated, modified, and then infused back into the patient [164]. This is to train the immune system into recognizing and destroy prostate cancer cells. Alas, the effectiveness of this treatment arm is difficult to document because it does not decrease PSA serum levels, shrink the tumor, or prevent worsening of the disease [164]. Though recent reports suggest that this treatment option can provide mCRPC patients with up to 4 months increased survival and less aggressive side effects [166]. Common side effects are skin reactions, flu-like symptoms, diarrhea, and weight changes [166]. Another avenue that patients can take is radiation therapy via infusion. Actively, there are two ongoing methods for administration. One is Radium-223 (Xofigo), which is intended for mCRPC that has metastasized to the bone and functions via mimicking calcium and targeting areas of the bone where cancer has caused disruptions [167]. Though this course limits damage to healthy tissues, a combination of abiraterone and prednisone, along with radiation, is given due to an increased risk of bone fracture. The second option for radiation would be Lutetium Lu 177 vipivotide tetraxetan (Pluvicto), which targets the prostate specific membrane antigen (PSMA) and is directly delivered to the PCa cells [168]. This treatment is for patients that have already received

ASIs or taxane chemotherapy and requires a positron-emission tomography (PET) scan to confirm the presence of PSMA expression of the cancer cell [169]. Though there are various paths a patient can take to manage their prostate cancer after administering ASIs, all listed options are palliative care [170]. Based off the Surveillance Epidemiology and End Result (SEER) Database, only 35% of patients with distant malignancies will have a 5-year relative survival rate [171]. This highlights the need for novel targets and therapeutic design, to enhance the 5-year survival rate of drug resistant CRPC.

Recent publications from our lab have identified various major pathways that may contribute to drug resistance within a prostate cancer model. During our RNA-seq screening, it was shown that both Wnt signaling cascades, non-canonical and canonical, ranked first and sixth, respectively, when comparing non-treatment patient samples and cell lines to Enz-treatment patient samples and cell lines [106, 172]. This discovery led to the idea that Wnt signaling played a paramount role in the emergence of drug resistance and aided in cancer cell survival. To further elucidate Wnt signaling's role in prostate cancer, each pathway was investigated separately. Utilizing a β-catenin inhibitor in combination with Enz, results showed that there was a loss of cell proliferation and survival in a synergetic manner both *in vitro* and *in vivo* [172]. The inhibition of β-catenin also alluded to the idea that loss of canonical signaling could lead to increased efficacy of Enz [172]. When understanding the mechanism of the non-canonical Wnt signaling pathway, researchers saw that inhibition of a downstream GTPase, Rock1/2, in combination with Enz resulted in loss of cell proliferation and survival, but also migration and invasion abilities [106]. This finding lead to the idea that co-inhibition of both the non-canonical

and canonical Wnt signaling could possibly halt cancer cell proliferation, survival, migration, and invasion.

3.2 Results

3.2.1 Porcupine Upregulated in Enzalutamide-Resistant PCa Cells

Previously, our team has reported the paramount involvement of Wnt signaling within drug resistant PCa. Within those publications it was documented through RNA-seq that Wnt/β-catenin and the Non-canonical Wnt Signaling pathways were ranked within the top 6 genes highly enriched within Enz-resistant PCa cell lines and tumor samples. Preceding this finding, our team produced two publications highlighting the role of Wnt Signaling within drug resistance and defining this pathway as a novel therapeutic approach.

To identify the importance of PORCN and its role in the development of ASI resistance, we determined the levels within PCa cell lines. Enz -sensitive and -resistant PCa cells were analyzed by protein and mRNA level to determine PORCN expression. Cells were plated for 24hrs and then harvested utilizing lysis buffer and loading dye to create western blot sample. After blotting protein expression for PORCN between LNCaP and MR49F, and C4-2 and C4-2R there was a clear elevation within the resistant cell lines (Figures 3.1 A,C). The protein expression levels were then quantified to show a significant upregulation of PORCN expression within the Enz-resistant cell lines, C4-2R and MR49F (Figure 3.1 B, D). To further validate our findings, mRNA levels were investigated. Seeded cells were harvested, RNA was extracted, and cDNA was purified of LNCaP, MR49F, C4-2, and C4-2R. These cell lines were then compared in groups of Enz-sensitive and –resistant respectively, LNCaP vs. MR49F and C4-2 vs. C4-2R. After the RT-qPCR data

collected was analyzed, results showed that the mRNA levels of MR49F showed increased PORCN expression levels when compared to LNCaP (Figure 3.1 F). To maintain scientific rigor, C4-2 and C4-2R were also tested and results yielded a higher level of PORCN expression within C4-2R when compared to C4-2 (Figure 3.1 E). These findings indicated that PORCN has an upregulation in drug resistant samples, which is congruent to our previous discoveries. Though we have a higher expression of this protein, our next steps were to determine if this target was appropriate for therapeutic use. As shown, Porcupine had a clear elevation of expression within C4-2R and MR49F when compared to C4-2 and LNCaP respectively (Figure 3.1 A-F).

3.2.2 LGK-974 and Enzalutamide Combination Treatment Synergistically Yields Loss of Cell Proliferation

Already, our team has published two papers that showed that loss of β-catenin and ROCK1/2, via pharmacological inhibitors, lead to a decrease in cell proliferation and showed a synergistic effect when used in combination with Enz. These findings lead us to develop a strategy to co-inhibit both signaling pathways to enhance the efficacy of Enz and provide clinical options for drug resistant patients. Hence the utilization of LGK-974, a potent and specific PORCN inhibitor, in combination with Enz. Enz-resistant cell lines, MR49F and C4-2R, were subjected to monotherapies of LGK-974 and Enz, to determine individual IC_{50} (Figure 3.2 A, B). Once this data was gathered, cells were exposed to a 1:1 ratio of both LGK-974 and Enz in a combination approach (Figure 3.2 A, B). All plates were plated in a 96-well cell culture plates, allowed 24hrs to adhere to the plate, treated for a duration of 72hrs, and analyzed using AquaBluer to determine cell survival. Results

showed that for C4-2R, the IC_{50} LGK-974 was 6.8µM and Enz was 80µM (Figure 3.2 A, B, C).

Once the individual IC_{50} were determined, the following equation was used to calculate the combination index:

$$CI50\%\ (ENZ) = (IC50\ ^{*}/IC50) + 0.500$$

The CI was used to determine if LGK-974 and Enz were able to work in a synergistic manner with a value being less than 1. The calculation was able to show that C4-2R has a CI of 0.609 (Figure 3.2 C) and MR49F yielding a CI of 0.571 (Figure 3.2 C), indicating a value that is lower than 1 and confirming a synergistic approach. Also to further validate the importance of utilizing the combination approach in comparison to single monotherapies, the IC_{50}s were quantified and graphed to show a significant decrease in cell viability in the combination therapy when compared to LGK-974 and Enz in both C4-2R and MR49F (Figure 3.2 A, B). This data shows that the combination therapy is synergistic, enhances Enz in Enz-resistant cell lines, and significantly decreases cell survival indicating that this combination treatment is an appropriate approach and could potentially decrease patient cancer burden. To further determine the effect of this inhibitor combination on cell proliferation, a clonogenic assay was performed to show a decrease in ability to for a single cell to growth into a colony. Enz-resistant cells, 22Rv1, were plated in a 6-well cell culture plate and then subjected to LGK-974, Enz, and a combination of LGK-974 and Enz. After treatment for 14 days, cells were stained and quantified. Results showed that though the monotherapy of LGK-974 had a decrease in colony recruitment, control and Enz seemed to have similar confluence (Figure 3.2 D). Though LGK-974 singular treatment decreased

in formation, the combination therapy yielded a reduced colony formation when compared to both monotherapies and control (Figure 3.2 D). These data points indicate that the combination therapy prevents cancer cell proliferation in an Enz-resistant model.

Next, we analyzed the effect that the combination treatment had on cell cycle. Since Wnt signaling plays a pivotal role in cell cycle, specifically in G1/S phase progression. With this information, a DAPI Cell Cycle flow experiment was performed on 22Rv1 cells with the four treatment groups of control, LGK-974, Enz, and combination. After 12hrs of treatment, cells were stained, and flow cytometry was used to determine the relative cell cycle phases of each sample within each treatment group. The control group showed a large number of cells in the G2/M phase when compared to S and G1 phase, where the monotherapies of LGK-974 and Enz had a larger number of cells within the G1 phase (Figure 3.2 E). Though when analyzing the combination treatment group, most cells within the population were in the G1 phase and this indicated G1 arrest of the cells (Figure 3.2 E). This assay was then quantified and found that the combination therapy had a significantly higher population of cells in G1 phase than the control and monotherapy sets (Figure 3.2 E). This data indicates that LGK-974 and Enz leads to cell cycle arrest in G1 phase and hints at the potential for cell death. Taken together this data suggests that combination therapy of LGK-974 and Enz leads to a loss of PCa ability to survive and proliferate, halting disease progression and growth.

3.2.3 Porcupine Inhibition and Enzalutamide Addition Results in Reduced Wnt and AR Signaling

Traditionally, Enz can bind directly to AR and block its translocation into the nucleus or its interaction with Androgen Receptor Elements (ARE) to decrease AR

signaling and disease progression. Similarly, LGK-974 has been shown to block the enzymatic activity of PORCN and hence blocking all secretion of Wnt ligands. This process indirectly results in a loss of Wnt signaling cascade protein expression. Hence the aim to ensure that the combination of LGK-974 and Enz will lead to a loss of both AR and Wnt signaling to prevent PCa progression and growth.

To determine whether the addition of inhibitors, LGK-974 and/or Enzalutamide, influence their desired targets and cause loss of downstream effectors that lead to the progression and metastasis of our disease state, Enz-resistant cells were treated and harvested for various experimental aspects. Firstly, Enz-resistant PCa cells, 22Rv1, were treated with the following scheme: Control, LGK-974, Enz, and a combination of both inhibitors. These cells were treated for 72hrs and harvested for western blot analysis to determine the status of Wnt Signaling downstream activation. Samples were blotted against ROCK2, Axin2, RhoA, and β-catenin. Results showed that a decrease in protein expression in LGK-974 and Enz in ROCK2 and Axin2, but there was no difference in expression for RhoA and β-catenin (Figure 3.3 A). When compared to control, LGK-974, and Enz, the combination treatment had a distinctive loss of protein expression in ROCK2 and β-catenin, and decreased expression of Axin2 and RhoA (Figure 3.3 A). These results indicate that the combination therapy is necessary to induce loss of both the noncanonical and canonical signaling cascade where the monotherapies were unable to produce the same phenotype. Since the combination treatment was able to halt Wnt signaling abilities, the next step was to ensure that there was also loss of AR activation. So, 22Rv1 and C4-2R cells were treated with the previously mentioned procedure and RNA was isolated to test mRNA levels of Wnt signaling and AR transcription factors. To validate our protein

findings, AXIN2 was also measured at mRNA and results were congruent with our western blot, showing a significant decrease when compared to control and Enz (Figure 3.3 B). Additionally, combination also had a significant decrease of mRNA expression of c-Myc when compared to control, LGK-974, and Enz (Figure 3.3 B). These results further confirm that the combination treatment decreases Wnt signaling transcription ability, alluding to the idea that tumor gene transcription may also be discontinued.

Next was to deduce whether the combination approach would also silence AR transcription factors. This was an important aspect to elucidate due to prostate cancer's strong reliance on AR for progression and metastatic capabilities. Transmembrane serine protease 2 (TRMPSS2), Prostate-Specific Antigen (PSA), AR-v7, and NKX3.1 were the transcription factors used to determine the activation of AR transcription. TMPRSS2, which is a prostate-specific androgen- response gene and has a strong function in prostate carcinogenesis, was found to have a significant decrease in combination treatment when compared to control, LGK-974, and Enz (Figure 3.3 C). NKX3.1, which has a strong correlation to the development and progression of PCa, and AR-v7, which is a variant of AR found solely in 22Rv1 cells that is constitutively active and lacks a ligand-binding domain, showed significantly lower mRNA expression in the combination treatment when compared with control, LGK-974, and Enz (Figure 3.3 C). Also, we determined that when cells are subjected to the combination regiment, mRNA expression of PSA, which is a clinical prognostic marker for prostate cancer progression, was found to be significantly decreased in the combination treatment when compared to its other sample counterparts (Figure 3.3 C). The decrease of these transcription factors indicates that there is a loss of AR transcription and possible activation, that would hint to the idea of the cancer cell

having suppression of its main driver. These data points taken as a whole show that the cancer cell has lost its ability to maintain both Wnt signaling and AR transcription at a protein and mRNA level with the addition of the combination therapy and suggests that the cancer cell may have lost its ability for survival. Due to the aggressive and invasion features of advanced prostate cancer, the next step was to determine whether the combination treatment could prevent or decelerate the migration and invasion properties that frequent Enz-resistant prostate cancer.

3.2.4 Porcupine and AR Combination Treatment Reverses EMT and Prevents Migration/Invasion Capabilities

Epithelial-mesenchymal transition (EMT) is a process in which the epithelial cancer cell gains characteristics of mesenchymal cells that have invasive properties, and these properties lead to the breach of other organs [173]. The metastasis of these cancer cells accounts for the majority of cancer deaths and poor prognosis for patients [173]. Previously, our lab established that the noncanonical Wnt signaling pathway had played a prominent role in the activation of small GTPases which led to the induction of cytoskeleton rearrangement resulting in EMT and migration of PCa cells [106]. We showed in this publication that the suppression of ROCK1/2 either via pharmacological inhibition or knockdown gene expression with the addition of Enz, resulted in a loss of migration and invasion within an Enz-resistant model [106]. To ensure the current working model is appropriate as a treatment for this cancer stage, we investigated the combination therapy to various assays to determine its efficacy in deterring metastasis.

To test our treatments efficacy, 22Rv1 cells were subjected to the four treatment categories: Control, LGK-974, Enz, combination. These samples were treated for 72hrs

before they were harvested for western blotting against the antibodies E-cadherin, N-cadherin, and Vimentin. As shown, the combination therapy increased the protein expression of E-cadherin, an epithelial cell marker, and indicated that the cell has higher epithelial cell characteristics suggesting less chance for metastatic capabilities (Figure 3.4 A). In contrast, the combination therapy shows a decrease of N-cadherin, which is associated with promotion of invasion and metastasis, and vimentin, which is a traditionally marker for EMT, when compared to the monotherapies and control (Figure 3.4 A). The loss of this protein expression suggests that the cancer cell when subjected to both LGK-974 and Enz results in the inability to gain metastatic abilities. This could be due to the lack of activation of the GTPases that are downstream of the noncanonical Wnt signaling pathway. To further validate the responsiveness of the combination treatment, C4-2R cells were plated, imaged, and distance measured in a wound healing assay to determine the migration ability between the different inhibitor groups. The cells were imaged for 96 days and results showed that the combination therapy had a significantly slower migration of cells compared to control (Figure 3.4 B, C). This indicates that both LGK-974 and Enz are necessary to suppress cell migration and suggests the loss of metastatic properties. These data points taken together suggest that with a loss of both Wnt and AR signaling, the cancer cell loses the ability of mobility and invading into distant organs.

3.2.5 LGK-974 and Enzalutamide Combination Therapy Leads to a Reduction of Tumor Proliferation

To ensure that our combination therapy approach remains clinically relevant, the two inhibitors were tested in an *in vivo* model to ensure efficacy and determine whether

there is a loss of tumor burden. Pre-castrated nude mice were purchased from Jackson Laboratory and inoculated subcutaneously with 22Rv1 cells. Approximately 2 $x10^6$ cells were injected and mice harboring tumor were randomly assigned into four separate treatment groups. All groups had a vehicle of corn oil which was administrated via oral gavage. The control group contained the corn vehicle corn oil and 0.1% Dimethyl sulfoxide (DMSO), LGK-974 was given at 5mg/kg, Enz was given at 20mg/kg, and the combination treatment contained 5mg/kg of LGK-974 and 20mg/kg of Enz. These treatment concentrations were determined based on previous published data and past experiments performed by our laboratory. The routine scheme that the inhibitors were administrated was five days on and two days off for four weeks. This schedule was determined via previously published data. We established a humane endpoint to be reached if one or more criteria was reach: 1) Body conditioning score (BSC) reaching and going below 2, indicating emaciation 2) Tumor burden reaching a total volume of $2000mm^3$ 3) Any adverse events appearing to cause unnecessary pain or discomfort outlined by our IACUC protocol and committee 4) Mice reached the end of the experimental time point of four weeks. Once the mice reached any of these points, they were humanly euthanized via CO_2 and the tumors were collected for further experiments. The mice's tumors were measured, weighed, and recorded every three days. As shown, the combination therapy, when compared to the control and monotherapies, significantly decreased the tumor burden and slowed tumor growth within an Enz-resistant model (Figure 3.5 A, C, D). This indicates that the combination therapy is needed to prevent further cancer progression, but we needed to ensure that this approach did not cause adverse effects such as weight loss. Documented mice's weights illustrated that there was not a significant difference between the treatment

groups, suggesting that the inhibitors did not cause loss of weight or other adverse effects (Figure 3.4 B). To further validate that the combination approach had an effect on tumor weigh, the harvested tissue was weighed before fixation. The weight of the tumors showed that there was a significant loss of mass in the combination treatment group when compared to control, LGK-974, and Enz (Figure 3.4 A). This result further highlights the need for combination treatment to reduce tumor growth as opposed to utilizing single agents. To further investigate mechanism, the tumor samples were also extracted for RNA and used for RT-qPCR to quantify the mRNA levels of TFAM within the samples. This experiment showed a significant decrease in TFAM mRNA expression within the combination treatment group when analyzed against the control and single agents (Figure 3.4 E). This data is congruent with our *in vitro* findings and further validates that the combination therapy leads to a possible decrease in mitochondrial biogenesis. These discoveries taken together suggest that the usage of the combination treatment is a necessary step in preventing tumor progression and growth *in vivo* and supports our current working model for combatting drug resistant prostate cancer.

3.3 Discussion

As presented above, there has been an array of data to conclude that the co-inhibition of both Wnt signaling cascades, via loss of PORCN, in conjunction with Enz, created a reliable and potential therapeutic approach for Enz-resistant prostate cancer. This project alluded to the idea that PORCN has an instrumental role in the development of drug resistance within prostate cancer and contributes to the aggressive phenotype. As shown, it was illustrated that PORCN had both an increase in protein and mRNA expression in Enz-resistant PCa cell lines. Due to this striking elevation, we implored to use a

combination therapy approach of a PORCN inhibitor, LGK-974, and the FDA approved AR inhibitor, Enz. The addition of these compounds to Enz-resistant PCa cells resulted in a decrease of cell survival in a synergistic manner. There was also a significant loss of colony formation ability within the clonogenic assay, suggesting that the combination treatment inhibited the cell's ability to colonize and proliferation. The next set of experiments illustrated that the combination therapy was able to show a loss of AR and Wnt signaling transcriptional targets and downstream effectors. The combination treatment was able to show the decrease of several downstream Wnt signaling effectors, indicating that the treatment scheme was able to effectively silence the signaling cascade. It was also depicted that the combination treatment was able to silence AR and Wnt signaling transcription factors, suggesting that the lack of β-catenin translocation causes a loss of tumor promoting transcription and that Enz can, once again, directly target AR expression. Due to the metastatic abilities of advanced prostate cancer and non-canonical Wnt signaling's involvement in migration and invasion, the combination treatment was tested to ensure its capacity in reversing EMT. As shown, the combination treatment was able to revert EMT and prevent migration abilities of the cancer cells at a significant rate. Though the *in vitro* data provides an attractive model for combating this disease, there remained a determination to whether this proposal would flourish in an *in vivo* setting. Utilizing 22Rv1 xenograft, results showed that the combination treatment was able to significantly decrease tumor burden while maintaining the weight of individual mice. This suggests that the combination treatment could prevent tumor growth, without detrimental effects to the host. Interestingly, the loss of TFAM within the combination treatment was a hint to the possible mechanism to the detailed proposal.

Currently, the data provided above is a solid foundation of results that illustrates a possible method to combating an aggressive cancer phenotype, but there are still limitations to the study that need to be addressed to further verify the clinical impact of this approach. It has been published by our lab that both Wnt signaling cascades have enriched expression in Enz-resistant cell lines and patient tumor samples, it would be beneficial to the study to show that PORCN has a similar correlation. Recently, I had search and analyzed the patient biobank of non-responder vs responder, but I have not found a significant or clear connection for PORCN. I also used the database to look at PORCN expression in terms of survival rate and disease-free state, and the expression level of PORCN made no difference in outcome. Objectively, during this search I only found 6 patients within the thousands of samples harboring PORCN expression. Due to the lower population, it is not feasible to draw conclusions from the current search. Another experiment that would be vital in determining the role of PORCN is utilizing shPORCN in an Enz-resistant cell lines. I have used shPORCN in C4-2R and MR49F, and then subjected these cells to Enz treatment. After the additional of Enz, the cells were used to perform a cell survival assay and results showed that the loss of PORCN lead to a significant increase in Enz efficacy (S. Figure 3.6, A). In a clinical setting, patients are not limited to Enz treatment. They also are prescribed Daro and Apa, with the parameters primarily being how well the patient tolerates the medication. In these terms, a test should be concluded to determine if prostate cancer cells resistant to Daro or Apa can also benefit from PORCN inhibition. This would increase the clinical relevance of the model. Another aspect to mention is whether the LGK-974 or the combination therapy can prevent the translocation of β-catenin. Previously, I performed an immunofluorescence (IF) experiment that showed both the

LGK-974 and combination treatment has loss of β-catenin translocation (Not shown). Though the confocal images are striking, they need to be further explored with a cell fractionation and immunoblotted for active β-catenin and whole β-catenin. This will further confirm the finding and hopefully show the combination treatment is more efficient than the monotherapies. Lastly, it would be appropriate to utilize NSG mice and inoculate them with a patient derived xenograft (PDX) and hopefully see the combination treatment produce similar results as the 22Rv1 xenograft. With these additional experiments, the findings above will have a stronger advocacy for clinical impact.

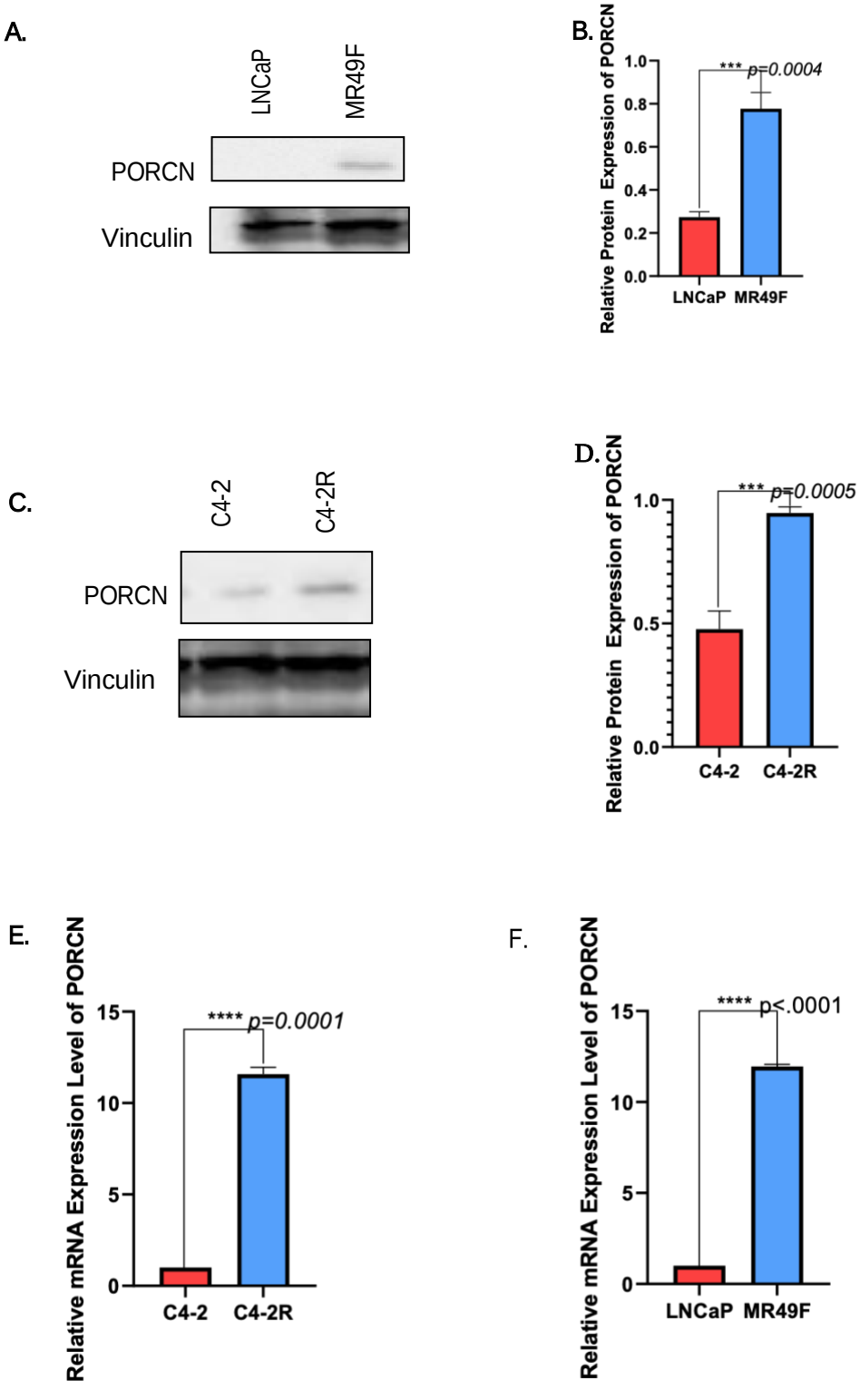
A.
LNCaP
MR49F
PORCN
Vinculin
B.
Relative Protein Expression of PORCN
*** p=0.0004
1.0
0.8
0.6
0.4
0.2
0.0
LNCaP MR49F
C.
C4-2
C4-2R
PORCN
Vinculin
D.
Relative Protein Expression of PORCN
*** p=0.0005
1.0
0.5
0.0
C4-2 C4-2R
E.
Relative mRNA Expression Level of PORCN
**** p=0.0001
15
10
5
0
C4-2 C4-2R
F.
Relative mRNA Expression Level of PORCN
**** p<.0001
15
10
5
0
LNCaP MR49F

Figure 3.1

Figure 3.1 Porcupine Upregulated in Enzalutamide-Resistant PCa Cells

A,C) Western blotting was performed to detect levels of PORCN protein expression in Enz-sensitive (C4-2 and LNCaP) and –resistant (C4-2R and MR49F) PCa cell lines. Results showed PORCN protein level increased in the Enz-resistant PCa cell lines, C4-2R and MR49F. (B,D) Western blotting was performed in triplicate (n=3) and then quantified to show that PORCN was significantly increased in the Enz-resistant cell lines, C4-2R and MR49F, when compared to the Enz-sensitive PCa cell lines, C4-2 and LNCaP. (E,F) mRNA levels were evaluated via RT-qPCR to determine the transcription levels of PORCN and within Enz-sensitive and –resistant PCa cell lines. Results revealed that PORCN had a significantly higher mRNA expression in E) C4-2 vs. C4-2R, F) and also in LNCaP and MR49F. All experiments were performed in triplicate (n=3), where $p>0.05$ for significant relevance.

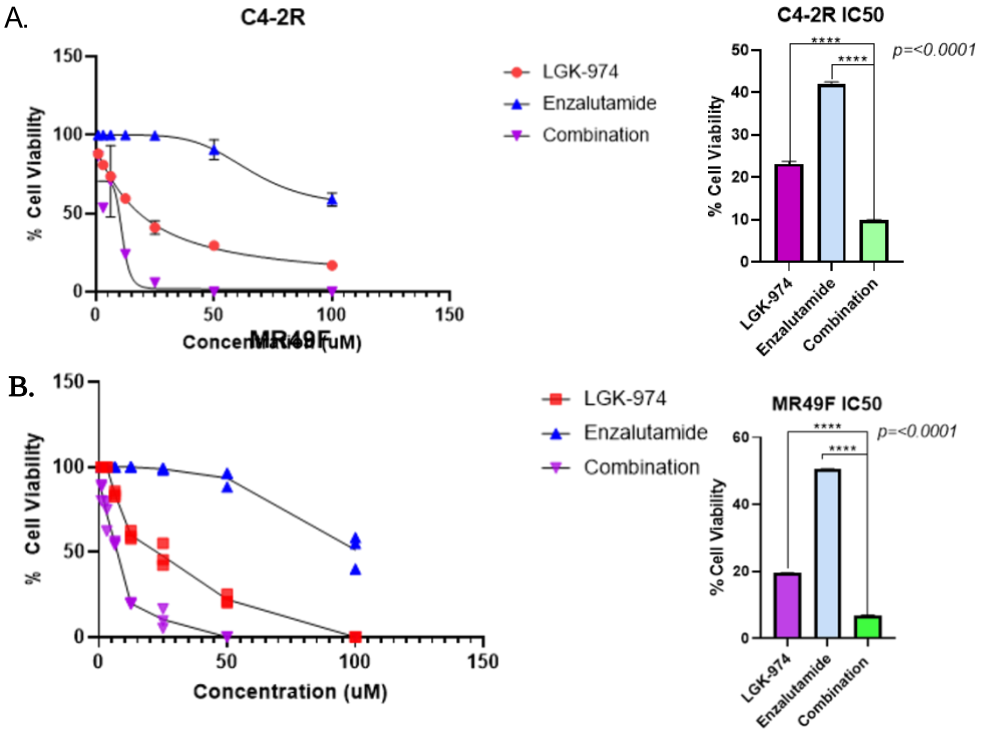

C.

	C4-2R	MR49F
IC_{50} ENZ	41.46	50.62
IC_{50} LGK-974	23.52	19.50
IC_{50} Combination	9.83	6.821
Combination Index (CI)	.566	.38522

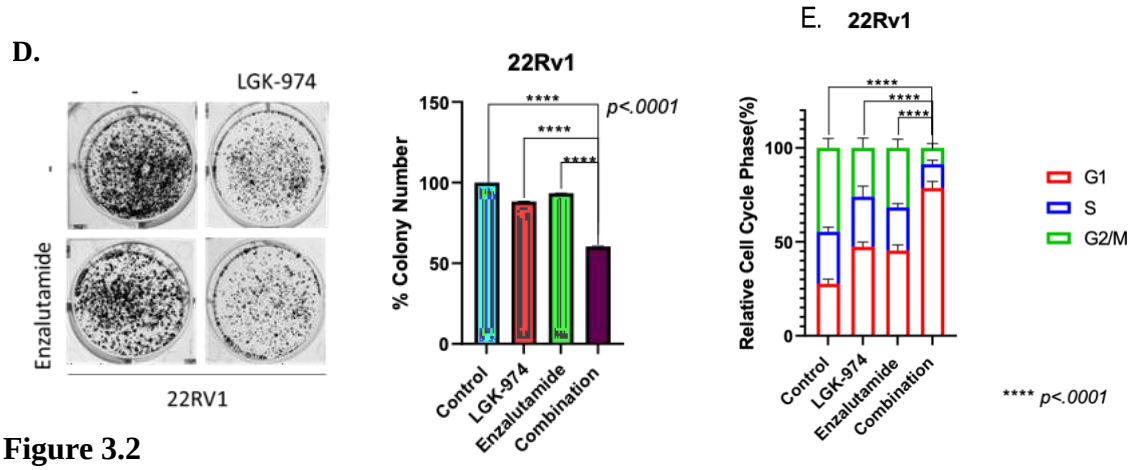

Figure 3.2

Figure 3.2 LGK-974 and Enzalutamide Combination Treatment Synergistically Yields Loss of Cell Proliferation.

A,B) Enz-resistant Pca cells, C4-2R and MR49F, were plated in 96-well plates at a cell density of 2,000 cells/well and 4,000 cells/well, respectively. Cells were treated with a serial dilution of LGK-974 and Enz, independently, to obtain the monotherapy IC50s. Cells were treated for 72hrs and cell survival was determined via AquaBluer. After the additional of AquaBluer, plates were read using a plate reader after a 4hrs incubation. The combination IC_{50} for LGK-974 and Enz was plated similarly to the above experiments and treated for 72 hrs. The combination treatment was administrated at a 1:1 ratio of LGK-974 and Enz, and AquaBluer was added for a 4hrs incubation and then read via a plate reader for absorbance rate. Experiments were completed in triplicate (n=3) and statistics were done to indicate a significant loss of cell survival in the combination therapy. C) Table of the IC_{50} for both cell lines as well as the combination index calculated for synergistic effect for the combination treatment. For combination index lower than 1, indicates synergistic effects. D) Enz-resistant PCa cells, 22Rv1, were plated at 500 cells/well and kept for 14 days before they were with formalin fixed and stained with crystal violet. Inhibitors were refreshed every two days. Using ImageJ software, results showed a significant decrease in colony formation in the combination treatment of 22Rv1. Experiment was completed in triplicate (n=3) and quantified and with a significance factor of $p< 0.05$ E.) C4-2R cells were plated 1×10^5 cells/well in 24-well and subjected to drug combination for 12hr. Cells were then collected via the DAPI cell cycle protocol and analyzed through flow cytometry showing that combination therapy resulted in G1 arrest. Experiments were completed in triplicate (n=3) and $p< 0.05$. Statistical analysis showed that the combination treatment had

a significant increase in G1 arrest compared to the other treatments. FCCP was used as control.

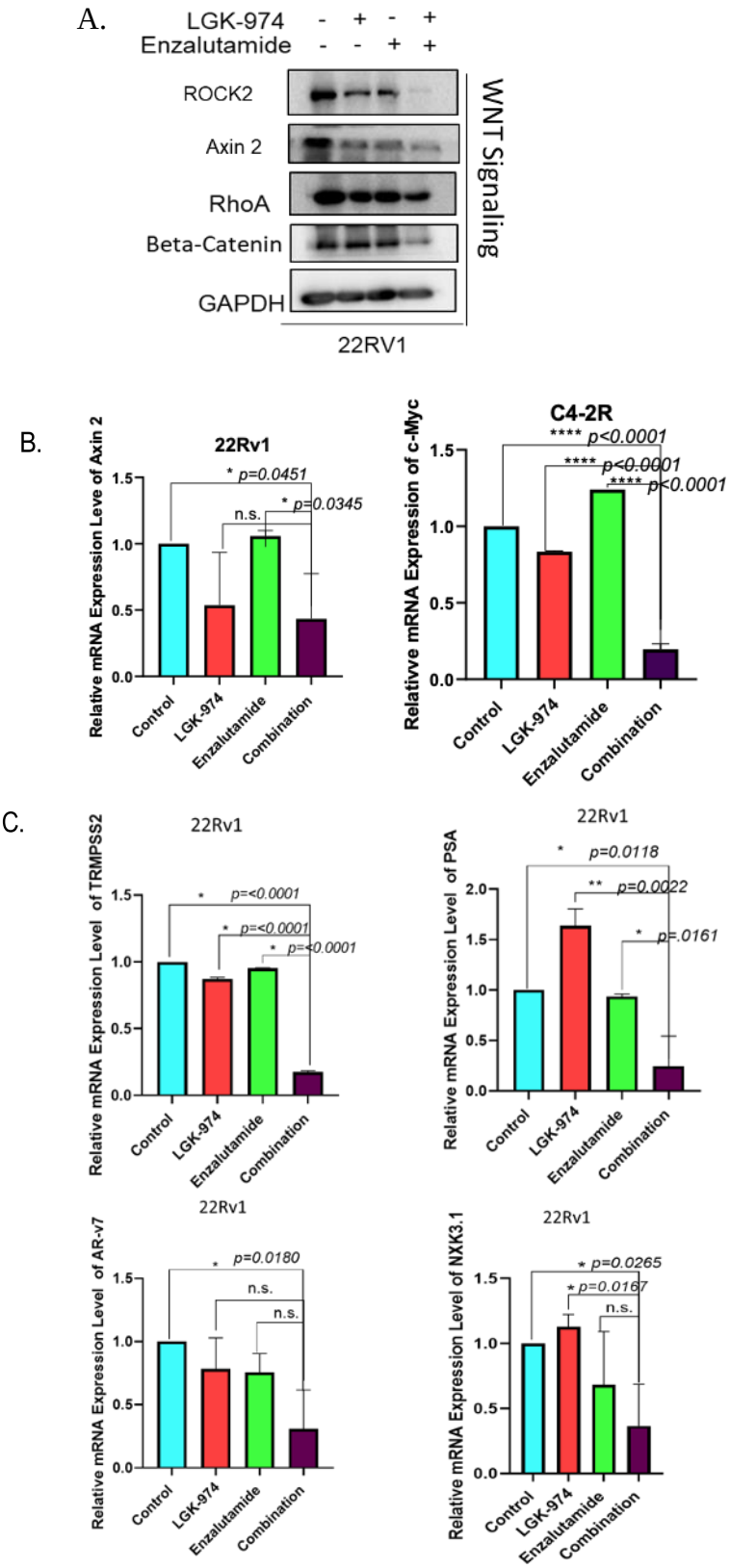
A.
LGK-974 - + - +
Enzalutamide - - + +
ROCK2
Axin 2
RhoA
Beta-Catenin
GAPDH
WNT Signaling
22RV1
B.
22Rv1
Relative mRNA Expression Leve of Axin 2
* p=0.0451
* p=0.0345
n.s.
C4-2R
Relativve mRNA Expression of c-Myc
**** p<0.0001
**** p<0.0001
**** p<0.0001
Control
LGK-974
Enzalutamide
Combination
C.
22Rv1
Relative mRNA Expression Level of TRMPSS2
* p=<0.0001
* p=<0.0001
* p=<0.0001
22Rv1
Relative mRNA Expression Level of PSA
* p=0.0118
** p=0.0022
* p=.0161
22Rv1
Relative mRNA Expression Level of AR-v7
* p=0.0180
n.s.
n.s.
22Rv1
Relative mRNA Expression Level of NXK3.1
* p=0.0265
* p=0.0167
n.s.

Figure 3.3

Figure 3.3 Porcupine Inhibition and Enzalutamide Addition Results in Reduced Wnt and AR Signaling

A) 22Rv1 were plated in 6cm dishes at 3 x10^5 and treatment as control, LGK-974, Enz, and combination of both inhibitors. The concentrations used were half of the IC50s indicated previously. Cells were treated for 72hrs before being harvested via lysis buffer. Western blot was then done to determine the protein levels of Wnt signaling downstream effectors, ROCK2, axin2, RhoA, and β-catenin. Results showed that the combination therapy had a reduction in Wnt signaling downstream effectors within the in the combination treatment group. B) Enz-resistant PCa cell lines, 22Rv1 and C4-2R, were treated with control, LGK-974, Enz, and combination treatment for 72hr and then the RNA was extracted and converted into cDNA for further experiments. The cDNA was used in RT-qPCR to indicate the mRNA levels of Wnt signaling targets such as Axin2 and c-MYC. Results showed that the combination treatment had a significantly lower mRNA level compared to the other treatment groups. Experiments were performed in triplicate (n=3) and statistical analysis was done with $p < 0.05$. C.) mRNA of 22Rv1 was measured to determine the levels of AR transcription targets such as, AR-v7, TRMPSSR2, PSA, and NXK3.1. Results showed that the combination treatment significantly decreased the mRNA level of all four AR transcription targets and statistics were done with $p < 0.05$.

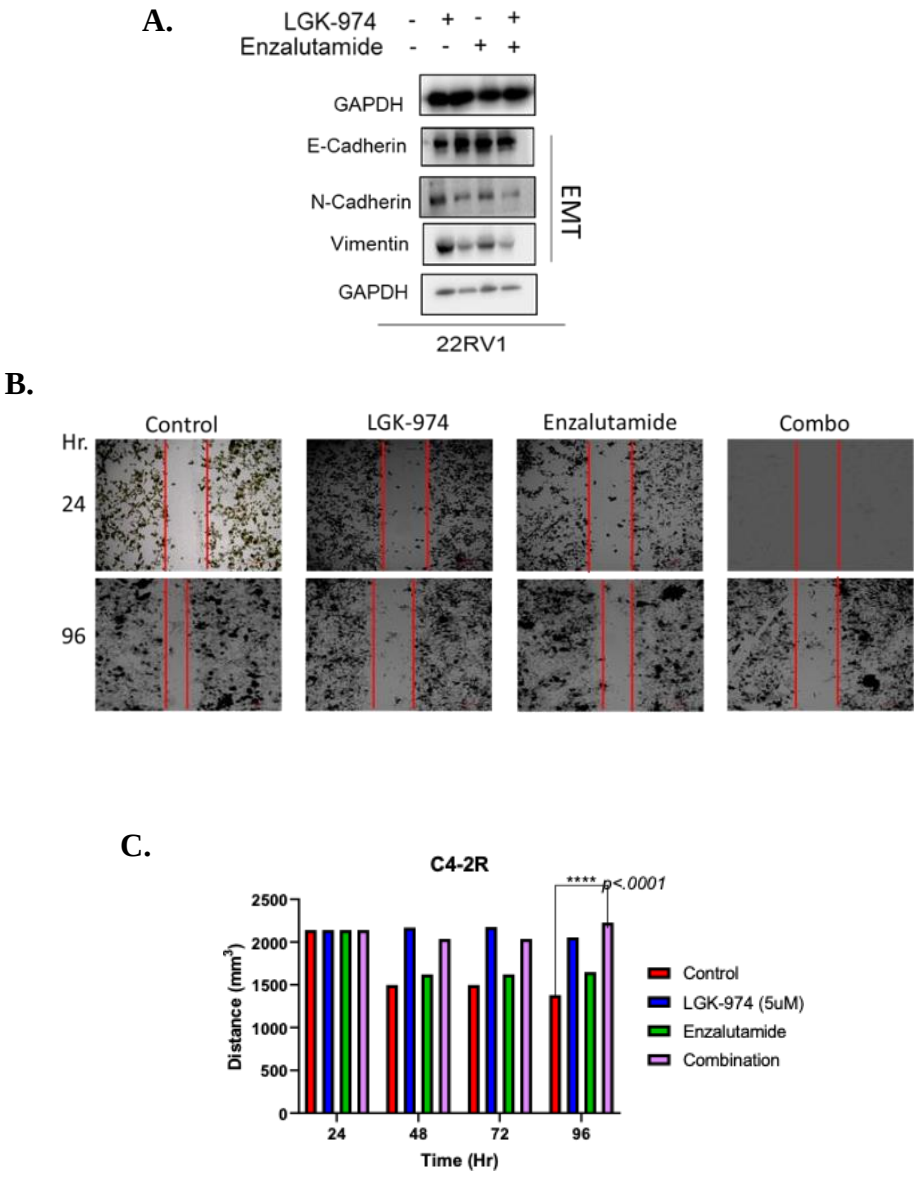
A.
LGK-974 - + - +
Enzalutamide - - + +
GAPDH
E-Cadherin
N-Cadherin
Vimentin
EMT
GAPDH
22RV1
B.
Control
LGK-974
Enzalutamide
Combo
Hr.
24
96
C.
C4-2R
**** p<.0001
Distance (mm3)
2500
2000
1500
1000
500
0
24
48
72
96
Time (Hr)
Control
LGK-974 (5uM)
Enzalutamide
Combination

Figure 3.4

Figure 3.4 Porcupine and AR Combination Treatment Reverses EMT and Prevents Migration/Invasion Capabilities

A) 22Rv1 cell were plated in a 6-well plated at 3 $x10^5$ and divided into four treatment groups: Control, LGK-974, Enz, and combination of the two inhibitors. 22Rv1 cells were subjected to inhibitors for 72 hrs before harvested for western blot. These samples were immunoblotted against classical EMT markers such as, E-Cadherin, N-Cadherin, and Vimentin. Western blot results show that combination therapy has a loss of mesenchymal markers and an increase in epithelial markers when compared to the other treatment groups. This indicates that the cells maybe be reverting EMT. B.) C4-2R cells were plated in a 6-well plated at a cell density of 1 x 10^6. After 24 hrs for the cells to adhere, a 1mL pipette tip was used to place a scratch down the center of each well. The scratch assay/wound healing assay was performed for 96 hrs and imaged/measured every 24 hrs, to show a significant decrease of migration and closure of combination therapy compared to control. C.) Quantification of wound healing/scratch assay, which was completed in triplicates (n=3) and statistics were ran at $p< 0.05$.

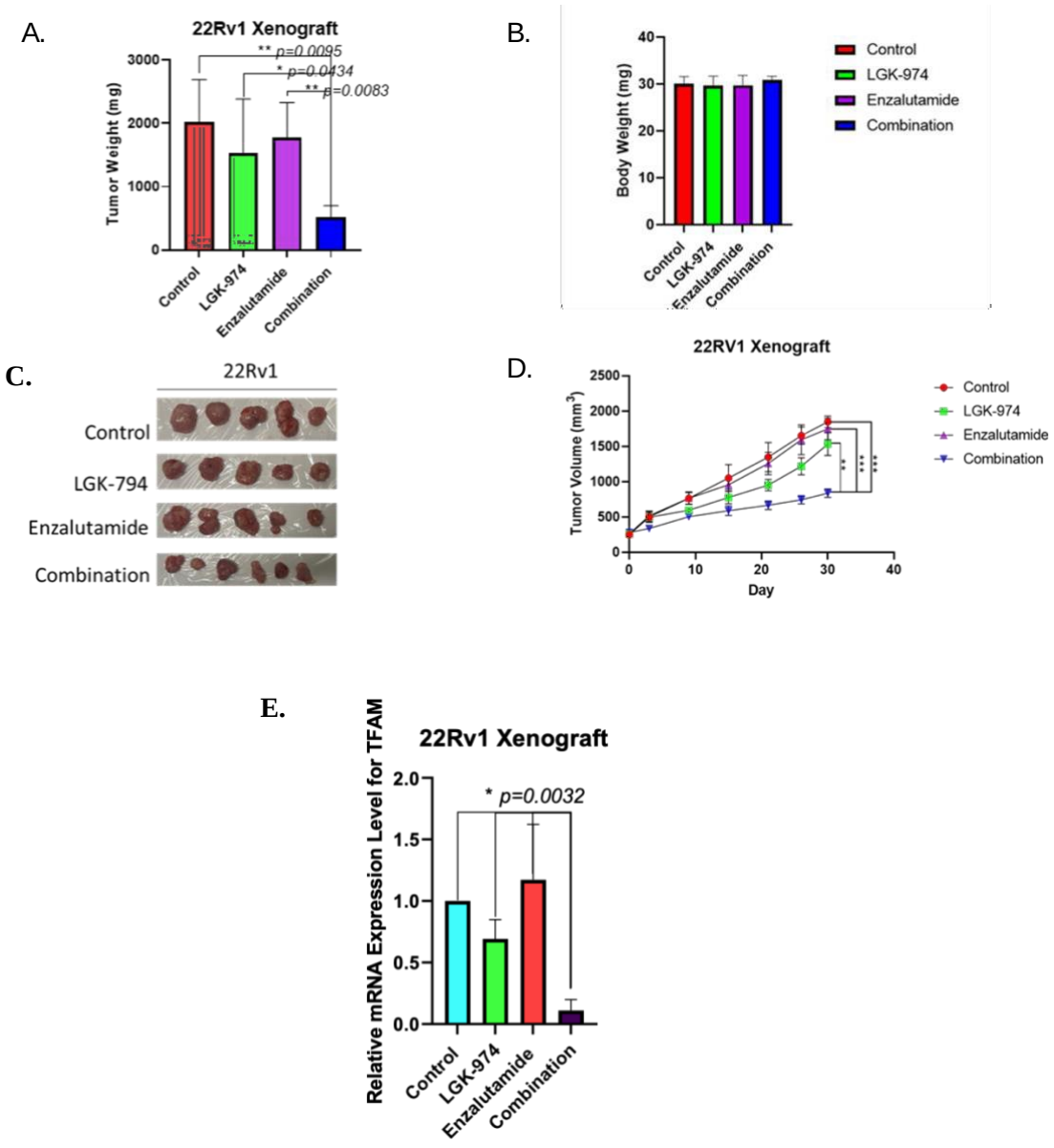
A.
22Rv1 Xenograft
** p=0.0095
* p=0.0434
** p=0.0083
Tumor Weight (mg)
3000
2000
1000
0
Control
LGK-974
Enzalutamide
Combination
B.
Body Weight (mg)
40
30
20
10
0
Control
LGK-974
Enzalutamide
Combination
C.
22Rv1
Control
LGK-794
Enzalutamide
Combination
D.
22RV1 Xenograft
Tumor Volume (mm3)
2500
2000
1500
1000
500
0
0
10
20
30
40
Day
Control
LGK-974
Enzalutamide
Combination
E.
22Rv1 Xenograft
* p=0.0032
Relative mRNA Expression Level for TFAM
2.0
1.5
1.0
0.5
0.0
Control
LGK-974
Enzalutamide
Combination

Figure 3.5

Figure 3.5 LGK-974 and Enz combination treatment leads to reduction of tumor proliferation and mitochondrial biogenesis.

A) 22Rv1 cells were mixed with Matrigel and 2 $x10^6$ of those cells were subcutaneously injected into the flank of the nude mice. Mice were then randomly assigned into four groups, control (n=5), LGK-974 (n=5), Enz (n=5), and combination (n=6). Mice was subjected to the following concentration of each inhibitor: Control=corn oil, LGK-974= 5mg/kg, Enz=20mg/kg, and combination= LGK-974 5mg/kg + Enz 20mg/kg. This treatment course was 5 days on and 2 days off for a duration of 4 weeks. This graph depicts the growth between inhibitor groups and showed a significant decrease in the combination treatment tumor growth rate compared to the other treatment groups. B) Tumor weight of the mice was then weighed and recorded, and combination treatment showed a significant decrease compared to other treatment groups. C) Body weight of the mice was documented, and the graph showed that there was no striking difference between treatment groups, indicating a lack of toxicity. D) mRNA was then extracted from the mouse tumors described above and used for RT-qPCR to determine mRNA levels of TFAM within the mouse tissues. Results showed that the combination treatment had a significantly decreased TFAM mRNA level compared to other treatment groups, indicating a loss of mitochondrial biogenesis. Experiments were completed in triplicate (n=3) and $p< 0.05$ were used.

A.

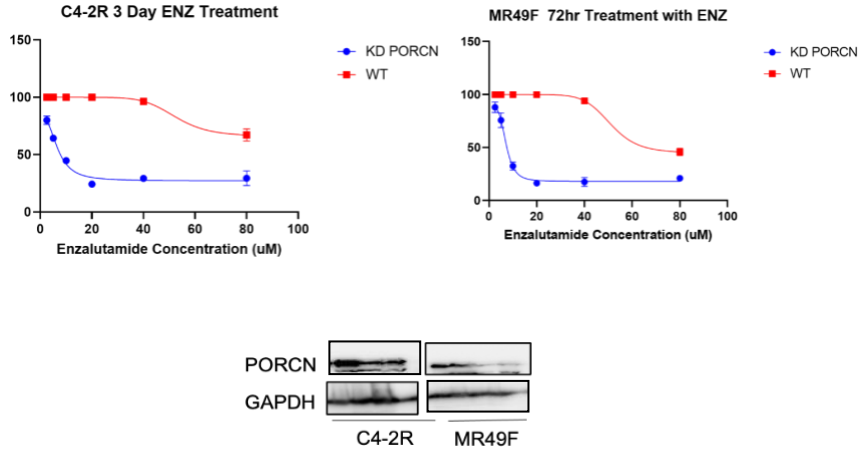

Supplementary Figure 3.6

Supplementary Figure 3.6 Loss of PORCN Leads to Enhance Efficacy and Enz

A) Enz-Resistant PCa cell lines, C4-2R and MR49F were depleted of PORCN using shRNA, and then the shPORCN and wildtype-PORCN cells were subjected to Enz treatment for a duration of 72 hrs. The cells were then administrated AquaBluer to measure cell survival. Western Blot was collected to visualize loss of PORCN expression in shPORCN cells. Results show that with a loss of PORCN, there is an enhancement if Enz efficacy in the Enz-resistant PCa cell lines when compared to the control. This indicated that PORCN plays vital role in the cell survival of Enz-resistant PCa cell lines and that loss of this component leads to a re-sensitivity of the traditional PCa treatment.

CHAPTER 4. MITOCHONDRIAL BIOGENSIS' INVOLVEMENT AND METABOLIC SWITCH IN DRUG RESISTANT PROSTATE CANCER

4.1 Introduction

According to the Warburg effect, cancer cells are able to increase their glucose uptake and reprogram their glucose metabolism to primarily fuel aerobic glycolysis [174]. Though aerobic glycolysis does not directly increase the production of ATP, it does allow for the conversion of glucose to be used as biomass, such as lipids or amino acids, to support cell growth [175]. Contrastingly to the Warburg's findings, many cells, particularly advanced prostate cancer cells, have a heavy dependence on mitochondrial function for existence [176]. Prostate cancer retains a unique metabolic profile that changes with the progression of the disease. Interestingly, normal prostate epithelial cells and localized disease have a high reliance on glycolysis for energy [177]. During this state, glucose is converted into citrate. The citrate that is secreted for the prostate tissues is theorized to act as a scavenger for free radicals and as a chelator for zinc and calcium [178]. As prostate cancer progresses and turns into a more aggressive phenotype, there is a lost ability to concentrate zinc and citrate [178]. Due to this event, prostate cancer goes from citrate-secreting to citrate-oxidizing and creates a change in metabolic pathway usage [178]. This leads to a reactivation event for mitochondrial oxidative phosphorylation that is associated with a rise of glucose metabolism and decrease in glycolysis [178]. It is thought that AR is able to reprogram metabolic pathways in order to support the metabolic needs of the cancer cell.

Mitochondria are typically called the cell powerhouse due to their abundant energy production, and their alternations affect function and signaling expression [179]. These

alternations within the mitochondrial genome are a common occurrence due to the lack of protective histones and DNA repair pathways, which allows an increase of vulnerability to DNA damage [180]. Mitochondria are also known as the structure that generates the most ATP from oxidative phosphorylation [179]. During oxidative phosphorylation, various electrons are transported to the electron transport chain. As they pass through the electron transport chain complexes I and IV, the protons are then pumped from the mitochondrial matrix to the intramembrane space via complexes I, III, and IV [178]. This increase in energy demand subsequently results in an elevation of mitochondrial biogenesis. Mitochondrial biogenesis is a process in which mitochondrial number increases to meet the energy demands, in this instance the cancer cell energy requirements. This upregulation can drive cancer cells to proliferate causing enhanced tumor growth [181]. This process can be mediated through various factors, but it is mainly regulated by transcriptional programs, such as proliferator-activated receptor gamma coactivator-1 alpha (PGC-1α) [179]. PGC-1α is a central regulator of mitochondrial biogenesis and its expression level is often correlated with the tumor dependence on mitochondrial oxidative phosphorylation [182]. Specifically in prostate cancer, PGC-1α has reported to interact with and activate AR, which causes the cancer cell to modify its metabolism by increasing mitochondrial biogenesis and glucose uptake [182]. Researchers also documented that inhibiting PGC-1α in AR-dependent cell lines resulted in G1 cell cycle arrest and suppressed tumor growth [182]. This leads to further validation that mitochondrial function plays a vital role in the survival and progression of prostate cancer models.

Due to the high reliance on oxidative phosphorylation to meet energy demand, there has been increasing interest in targeting the mitochondria of cancer cells to disrupt their

energy source. Unfortunately, cancer cells possess great metabolic flexibility that would allow them to upregulate other outlets, such as glycolysis, which could act as compensation to enhance cell survival in the case of mitochondrial metabolism inhibition [183]. This raises the idea that a therapy which can target both mitochondrial metabolism and glycolysis, could pose as an attractive approach to repressing advanced prostate cancer models.

4.2 Results

4.2.1 Increased Mitochondrial Biogenesis Induced by Enzalutamide-Resistance is Blocked by Porcupine and AR Inhibition

Traditionally, drug resistant prostate cancer has a metabolic switch from glycolysis to oxidative phosphorylation. Though this switch is well documented, the reasoning behind the shift is still undetermined. This shift is important to note because it shows the cell changing its methods to meet energy demand. Due to the difference in how the cell now responds to energy demand, there are other various aspects that also become affected and transformed. As mentioned above, c-Myc gene expression had a significant decrease when utilizing the combination approach. c-Myc has many individual functions, but one in particular is its involvement in mitochondrial biogenesis.

Mitochondrial biogenesis is known as a process that increases the cells mitochondrial numbers and in cancer models has been linked to driving tumor proliferation [179]. Due to this information and the switch in achieving energy demand, the question arose of whether mitochondria were the source of energy production. To answer this question, a MitoStress test was performed. The MitoStress test is used to measure

mitochondrial respiration and oxygen consumption, since intracellular adenosine triphosphate (ATP) is generated via mitochondria respiration. Utilizing the Seahorse XFe96 instrument, Enz-sensitive and –resistant PCa cells, C4-2 and C4-2R respectfully, were analyzed to determine if there was an increase in mitochondrial respiration. The Enz-resistant cell line, C4-2R, showed a significant increase in maximal respiration and spare respiratory capacity (Figure 4.1 A). Maximal respiration is the measure of maximum capacity that can be achieve by the electron transport chain and spare respiration is a measurement by the difference found between the maximal and basal respiration, reflecting the cell's ability to respond to changes in energetic demand and its fitness [184]. So, Enz-resistant cells having an increase in these two features indicates the gain of resistance could affect mitochondrial respiration (Figure 4.1 A). The other aspects to recognize are the basal oxygen consumption rate (OCR), which represents the energetic demand of cells under basal conditions, mitochondrial proton leak, which determines the mitochondrial health, non-mitochondrial oxygen consumption, which indicates oxygen consumption due to other cellular process, and ATP production, which were all increased in the Enz-resistant line (Figure 4.1 A) [185]. These data points further strength the idea of drug resistance affecting mitochondrial respiration. To investigate the mechanism of resistance, a RT-qPCR was performed to determine the mRNA level of mitochondrial biogenesis markers, such as TFAM, MYC, and PGC1-α in drug-resistant and sensitive PCa cells. As shown, C4-2R had a significantly increased mRNA level of mitochondrial biogenesis markers when compared to C4-2 (Figure 4.1 B). This could be an indication of tumorigenesis promotion. Next was to determine if the combination therapy could disrupt this upregulation. To elucidate this, C4-2R was subjected to a treatment scheme of control, LGK-974, Enz, and

combination for 72hrs and then harvested for RT-qPCR analysis. The relative mRNA expression level of TFAM (D), PGC1-α (C), and c-MYC (E) were measured, and showed that our combination therapy yielded a significantly decreased expression when compared to control and monotherapies (Figure 4.1 C-E). This loss of mitochondrial biogenesis markers could indicate an inability to promote tumorigenesis and lessen the reliance on mitochondrial respiration.

4.2.2 Enzalutamide Resistance Induces Glycolytic Reserve and Glucose Uptake

According to our OCR data, there is an upregulation of mitochondrial respiration within the Enz-resistant samples, but there needs to be a consideration of extracellular acidification rate (ECAR) activity within this model. To answer this question, the Glycolytic Stress Test was utilized. The purpose of the Glycolytic Stress Test was to understand the capacity of glycolysis pathway after glucose starvation of the cells [186]. To accomplish this, cells are driven towards glycolysis and their ability to increase glycolytic activity to meet metabolic and energy demand is recorded [186]. To begin this assay, the cells are incubated in glucose stress test medium, which lacks glucose and pyruvate, and the ECAR is measured to obtain baseline levels [186]. Then cells are then subjected to a saturation of glucose to obtain the rate of glycolysis under basal conditions [187]. The second injection that the cells receive is oligomycin, which is an ATP synthase inhibitor, that prevents mitochondrial ATP production and pushes energy production to glycolysis [187]. This allows for a measurement of maximum cellular glycolytic capacity. The final injection is 2-Deoxy-D-Glucose (2-DG), which acts as a glucose analogue and works in inhibiting glucose via competitively binding to glucose hexokinase [187]. The decrease in ECAR confirms that the ECAR values found in the assay are solely due to

glycolysis. The glycolytic reserve is calculated by the difference between glycolytic capacity and rate [187]. There is an additional measurement, referred to as non-glycolytic acidification, which is the value of ECAR before glucose introduction [187]. This is to assess the other processes that could be contributing to energy demand aside from glycolysis. To address the ECAR activity and reliance on glycolysis in Enz-resistant cells, the following experiments were completed. C4-2 and C4-2R cells were seeded in the Seahorse XFe 96 well plates and taken to our Redox facility for the performance of a Glycolytic Stress Test. The results collected showed there was no difference in the glycolysis measurement between the two cell lines (Figure 4.2 A). Since this is the measurement of ECAR after the saturation of glucose, this indicated that there was difference in the cells ability to convert glucose to pyruvate. When analyzing the measurement of glycolytic capacity, there is a slight elevation within the Enz-resistant cell line when compared to the sensitive line (Figure 4.2 A). Since this measurement indicates the ECAR rate after oligomycin induction, that even after ablating oxidative phosphorylation that cell is still able to rely on glycolysis for energy demand. It is important to note that the resistant cell can match the demand and increase its ability compared to the sensitive cell, which is interesting because traditionally Enz-resistance is known to cause a shift from glycolysis reliance to oxidative phosphorylation. This could be defined as a survival mechanism for the cancer cell, but further evaluation is needed. Lastly, the glycolytic reserve of the resistant cell line shows a significant increase, suggesting that the resistant cell has a higher ability to respond to energy demand and an increase in glycolytic function compared to the sensitive cell line (Figure 4.2 A). This data alludes to idea that the induction of drug resistance may convert the cell response to energy to oxidative

reliance, but the cell still maintains the ability to utilize glycolysis in energy crisis to maximize survival. This ability to switch between two energy-producing pathways, illustrates the resistant cells' ability to easily adapt to various environmental changes. This could potentially be a reason to why there is great difficulty in producing therapeutic targets to combat drug resistance.

The process of glycolysis is to convert glucose into pyruvate, which is then turned into lactate within the cytoplasm or $0_2/H_20$ in the mitochondria [188]. Due to this conversion, a measurement of lactate and glucose within the cancer cells needed to be evaluated. Also, as previously described, increased activation of c-Myc could lead to an increase in lactate secretion and glucose uptake. To address these concerns, the LactateGlo™ and GlucoseGlo™ Assay kits were used to determine the intracellular and extracellular concentrations of each product. For the following experiment the cell lines C4-2 and C4-2R were used. As shown, C4-2R had a significant increase in extracellular lactate production when compared to the sensitive cell, C4-2 (Figure 4.2 B). This finding could indicate that there is extracellular lactic acidosis occurring, which could result in the reprogramming of the stromal cells within the TME to ensure cancer cell survival under stressful or hostile conditions. This could potentially explain how the cancer cells begin to gain resistance against Enz and continue to proliferate. Also, this could indicate that lactate production is necessary for tumor progression. To determine the effect of our combination therapy on this situation, extracellular levels of lactate were documented after exposure to inhibitors. The data shows that the combination therapy was able to decrease the levels of lactate within the extracellular matrix, possibly suggesting an increase in cell's vulnerability by preventing the activation of c-Myc via the shutdown of Wnt signaling

(Figure 4.2 D). In contrast, the glucose intracellular levels within the resistant cell were significantly increased compared to the sensitive line (Figure 4.2 C). This result strengthens the validity of the outcomes found with the glycolytic stress test, in that the resistant cell maintains a higher glycolytic reserve due to the increased uptake of glucose within the cell. To understand if our inhibitor treatment would yield similar results to the lactate experiment, cells were subjected to inhibitor therapy and intracellular glucose levels were evaluated. As shown, the combination therapy was able to significantly decrease intracellular glucose uptake (Figure 4.2 E). These data points taken together suggest that the resistant cell lines possibly maintain a glycolytic energy reserve and implementing the combination therapy could deplete the cell of this reserve, pushing it into cell death.

4.2.3 Enzalutamide-Resistance Contributes to Mitochondrial Membrane Potential and Increase in ROS Production

Based on the OCR findings discussed above, there became a deep interest in understanding the role of mitochondria in an Enz-resistant model. Firstly, the amount of mitochondrial and their activity needed to be measured within the sensitive and resistant cell lines, in order to determine whether the mitochondrial function was linked to the gain of Enz resistance. In order to accomplish this task, ThermoFisher MitoTracker®Green was used in combination with flow cytometry to determine mitochondrial mass and activity at a cellular level. The MitoTracker®Green probes are specific fluorescent dyes that are mitochondrion-selective and cell-permeable [189]. These dyes can accumulate within the cell membrane [189]. MitoTracker®Green works by binding to free thiols groups of cysteine resides, belonging to mitochondrial proteins [189]. These dyes have also been known to be associated with increase cellular mitochondrial content and respiration. C4-2

and C4-2R cell lines were plated and stained with the MitoTracker®Green, and then collected for further analysis. Results showed that the resistant cell lines significantly harbored an increase in mitochondrial mass when compared to the sensitive cell lines (Figure 4.3 A). This is congruent with the OCR findings described previously. The increase in mitochondrial mass explains why there was a significant increase in spare respiratory capacity in the OCR data. Also, this correlated nicely with the increase in mitochondrial biogenesis factors previously found. Next was to determine whether the combination therapy of Enz and LGK-974 could affect the mitochondrial mass within the resistant cell line. C4-2R cell lines was subjected to treatment, stained with the MitoTracker®Green, and processed for flow cytometry. Results illustrated that with therapeutic addition, there was a significant loss of mitochondrial loss (Figure 4.3 B). Previously we showed that with the combination therapy there was a significant decrease in mRNA expression of TFAM, so it is feasible that if there is a halt in mitochondrial production, then there would be a decrease in mitochondrial mass.

Another aspect that needed to be explored was the mitochondrial membrane and its polarization state. Studies have shown that cancer cell mitochondria have a higher polarization rate of their membrane and one method to disrupt the cancer cell is to cause a depolarization of the mitochondrial membrane. The reason behind this is due to the mitochondria membrane being a double-layered structure that prevents foreign substances from entering. This makes it difficult to create mitochondria directed treatment, but if there was a depolarization of the membrane then this could result in substance to enter the mitochondria leading to cell death. To determine if the resistant cell line exhibited characteristics for hyperpolarized mitochondrial membrane potential, ThermoFisher's JC-

1 dye in combination with flow cytometry was used. Membrane potential is indicated by the emission of a green, fluorescent color (monomeric form of the probe) or there can be a shift towards a red fluorescent color that specifies an aggregate formation. In summary, the depolarization of the mitochondria membrane can be determined by the decrease of red to green ratio produced via the fluorescent intensity. C4-2 and C4-2R cells were plated and subjected to this stain. Results showed that the resistant cell line had a significantly high red to green ratio when compared to the sensitive line (Figure 4.3 C). This information suggests that the resistant cell line had an increase in aggregate formation, implying that the mitochondrial membrane was hyperpolarized. The next step was to verify that the combination of Enz and LGK-974 could cause a depolarization event within the membrane. C4-2R cells were subjected to inhibitor treatment, stained with JC-1 dye, and collect for analysis. As shown, the combination therapy was able to depolarize the mitochondrial membrane by reducing the red to green ratio, indicating a decrease in aggregate formation and increase in monomer abundance (Figure 4.3 D). This data taken together suggests that the mitochondrial function is an important component to Enz-resistant prostate cancer survival and that the depolarization of the mitochondrial membrane could potentially lead the malignancy to cell death.

Since mitochondria play a vital role in the regulation of Reactive Oxygen Species (ROS) production, so it was sought to determine whether the combination treatment affected ROS levels or activity. ROS levels were evaluated using ThermoFisher's CellROX™, which allows for flow cytometry instruments to detect the stain within living cells. This reagent is able to penetrate the cell but maintains a weak fluorescence until it is oxidized. C4-2R cells were plated and inhibitor treatments were given, then the cells were

collected for flow cytometry analysis. As recorded, the combination therapy was able to significantly increase the oxidative stress of the cell (Figure 4.3 E). This data collected suggests that the combination therapy was able to increase oxidative stress within the resistant cell and cause possible membrane damage. All the data points gathered in this section suggests that the Enz-resistant cancer cell has an increase in mitochondrial mass and hyperpolarized mitochondrial membrane, which potentially explains the difficulty in overcovering drug resistance and accounts for the metastatic and aggressive phenotype presented. It was also shown that with the addition of the combination treatment, there yielded a decrease in mitochondrial mass, depolarization of the mitochondrial membrane, and increasing oxidative stress levels within the cancer cell. These events taken together could indicate a potential mechanism to why this is significant decrease in cell survival with the combination approach.

4.3 Discussion

Mitochondria function and energy demand requirements play an important role in the health, proliferation, and survival of the drug resistant prostate cancer cell. In summary, we were able to show that cancer cells possessing a resistance to Enz, had an increase in mitochondrial biogenesis. This increase in biogenesis possibly was one of the factors that attributed to tumor progression and ability to evade Enz treatment. The loss of these components via the drug combination of LGK-794 and Enz resulted in the cell's inability to proliferate and provided a potential mechanism of why the cell is pushed into cellular death with the addition of these inhibitors. Next, we examined the cell ability to rely on glycolysis during an energy crisis. Traditionally, drug resistant prostate cancer is known to have a heavier dependence on oxidative phosphorylation for energy, but in this project, we

alluded to idea that in the absence of oxidative phosphorylation, the cell maintained a glucose reserve for survival. We showed in the Glycolytic Stress Test that the cell was still able to maintain similar responses to energy demand through glycolysis compared to the drug sensitive lines. It was also shown that the cell was up-taking glucose and exporting lactate into an extracellular space causing a possible acidic TME. Though the acidity of the TME needs to be further elucidated, the idea that in absence of oxidative phosphorylation, the cancer cell maintains the ability to meet energy demand via glycolysis is an interesting phenomenon. Also, in the presence of the inhibitor combination, LGK-974 and Enz, it was shown that the cell decreased its capacity to uptake glucose and there was a reduction in lactate within the extracellular component. This suggests that the combination therapy could deplete the cell of its potential to use glycolysis as secondary source of energy in a stressful situation. Lastly, there was an investigation on the amount of mitochondria present, and how the gain of Enz resistance influenced mitochondrial health and membrane potential. As shown and discussed above, the Enz-resistant cell lines maintained a higher amount of mitochondrial mass and illustrated a hyperpolarized mitochondrial membrane. This data implied that there could be a higher amount of mitochondrial activity occurring within the resistant models and this could potentially explain tumor progression and increase in OCR readings. Again, when imploring the combination treatment, there was a significant decrease in mitochondrial mass, a depolarization of the mitochondrial membrane, and an increase in ROS production. These findings taken together suggest that with the inclusion of LGK-974 and Enz, resistant cancer cells lose their source of energy by a depolarizing of the mitochondrial membrane, leading to the irreversible damage. This damage could be the reason that there is an increase in oxidative stress levels, which

triggers cell death pathway activation. Though the data collected is a glimpse into the possible mechanism to how Enz-resistant are able to maintain survival and provides a feasible approach to halting this progression, there are limitations that need to be addressed in future experiments.

Though the results presented in this section alluded to an interesting finding, further experiments could be done to increase the validity of the findings. To justify the ECAR results, C4-2R-PORCN-KD cells should be taken and tested to verify with the loss of PORCN, leads to a decrease in the cell's ability to meet energy demand. Previously, we did use the combination treatment and test the ECAR output, but an argument could be made that the ECAR value produced could be due to the health of the cell. This is why using the knockdown line would be more beneficial and it would eliminate the issue of off target effects. Another experiment that should be completed is determining which cell death pathway is occurring. Since mitochondria are closely associated with necrosis, it would be interesting to link the combination therapy with an induction of necrosis. This can be done through using treated cells for flow cytometry to detect for DNA-binding dye propidium iodide (PI) (necrosis), GFP-LC3 degradation (autophagy), or annexin V-FITC (apoptosis). This would provide a clearer picture of what is happening to the cell post treatment. It was described above that the resistant cell line had an increase in mitochondrial membrane potential, but this was in a whole cell lysate scenario. It would be interesting to isolate the mitochondria from the individual cell lines and drug treatment categories to visualize if there are similar phenotypes to the whole cell lysate. One drawback is that it is difficult to isolate and purify enough mitochondria with centrifugation. To address this concern, there is an isolation kit from ThermoFisher™ that

has been successful in producing a clean and viable final product. Regarding the CellROX results, since CellROX determines whole cell ROS and oxidative stress levels, MitoSOX should be used to determine mitochondria specificity. This will strengthen the importance of mitochondria regulation within this model. Also, to explain the increase in lactate extracellular concentrations and increase of glucose intracellular concentrations, it would be an appropriate approach to look at the expression level of glucose transporters. The mRNA expression levels of GLUT 1, 3, and 4, were determined via RT-qPCR. Results showed the Enz-sensitive PCa cell lines yielded a significantly higher mRNA expression when compared to the Enz-resistant PCa cell lines. This was a shocking result because it was expected that the Enz-resistant PCa cell line would contain a higher expression level to the GLUT transporters to explain the increase in lactate and glucose concentrations. Though it shows that the GLUT transporters are not the correct component that contributes to gain of resistance, there are other subjects that could be contributing, such as the monocarboxylate transporters (MCTs). Another method for understanding energy use within the Enz-resistant PCa cell lines, is to perform glucose tracing, to determine if the cell is converting glucose into lactate or other products. It would also be beneficial to utilize prostate cancer patient derived data banks of non-responder and responder samples to analysis whether certain mitochondrial markers are upregulated. With the completion of these experiments, a clearer picture can be illustrated for understanding drug resistance within prostate cancer patients.

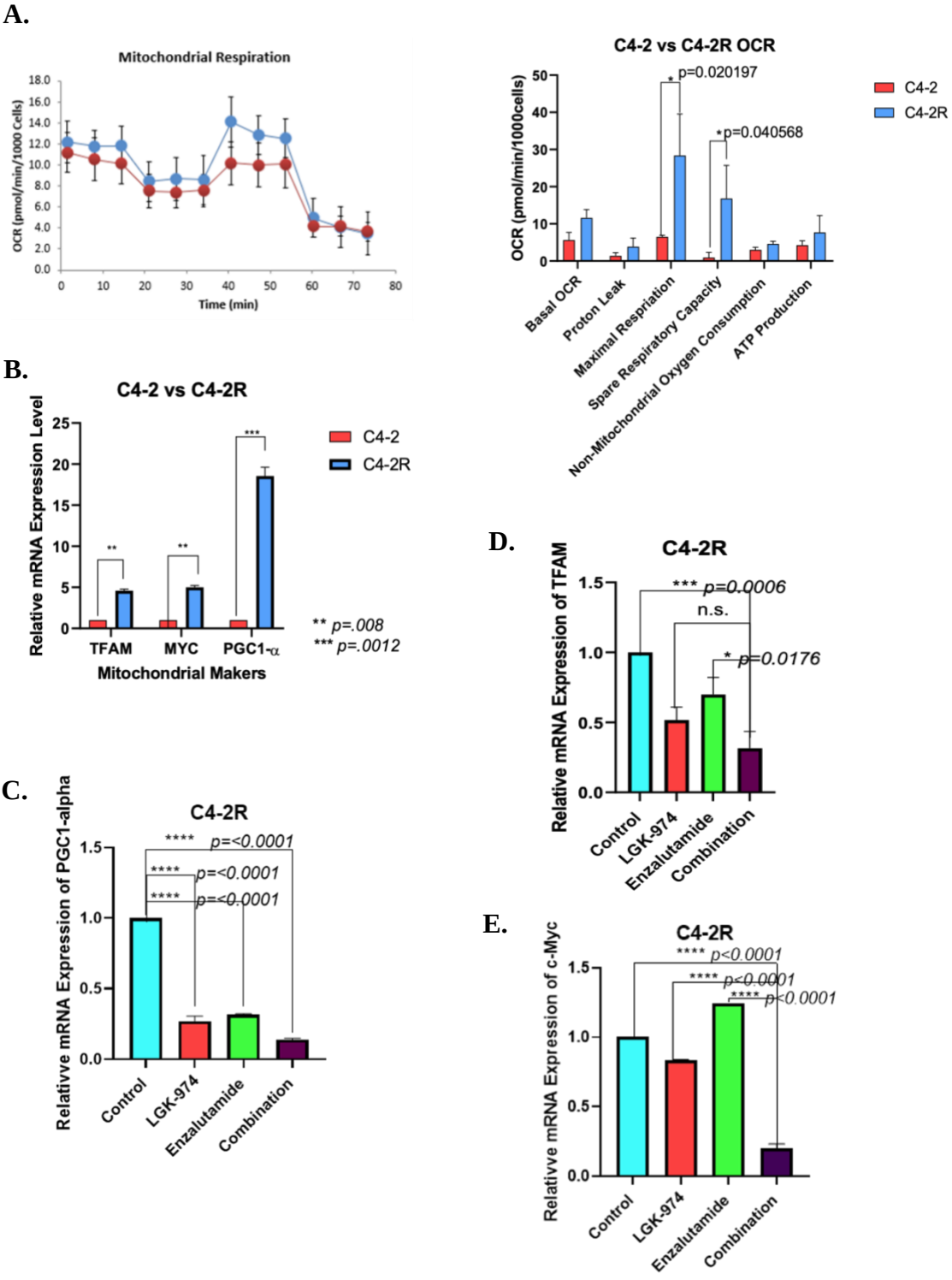
A.
Mitochondrial Respiration
OCR (pmol/min/1000 Cells)
Time (min)
C4-2 vs C4-2R OCR
OCR (pmol/min/1000cells)
p=0.020197
p=0.040568
C4-2
C4-2R
Basal OCR
Proton Leak
Maximal Respiration
Spare Respiratory Capacity
Non-Mitochondrial Oxygen Consumption
ATP Production
B.
C4-2 vs C4-2R
Relative mRNA Expression Level
TFAM
MYC
PGC1-α
Mitochondrial Makers
** p=.008
*** p=.0012
C.
C4-2R
Relative mRNA Expression of PGC1-alpha
**** p=<0.0001
Control
LGK-974
Enzalutamide
Combination
D.
C4-2R
Relative mRNA Expression of TFAM
*** p=0.0006
n.s.
* p=0.0176
E.
C4-2R
Relative mRNA Expression of c-Myc
**** p<0.0001

Figure 4.1

Figure 4.1 Increased Mitochondrial Biogenesis Induced by Enzalutamide-Resistance is Blocked by Porcupine and AR Inhibition

A) C4-2 and C4-2R cell lines were plated in Agilent Seahorse 96-well plates at a seeding density of 10,000 cells/well and given 24hrs to adhere. Cells mitochondrial oxygen consumption was measured utilizing the Agilent XFe instrument and showed the C4-2R had an increase in mitochondrial oxygen reliance compared to C4-2. This experiment was performed in triplicate (n=3) and statistics were done at $p < 0.05$. B.) C4-2 and C4-2R cell lines and had mRNA extracted and converted into cDNA. The cDNA was then used in RT-qPCR to determine the mitochondrial biogenesis markers expression levels between to two cell lines. The markers looked at were TFAM, MYC, and PGC1-α, and results showed a significant increase in Enz-resistant cell line. This experiment was performed in triplicate (n=3) and a $p< 0.05$. This indicated that the Enz-resistant cell lines have an upregulation of mitochondrial biogenesis. D) C4-2R cells were then treated with control, LGK-974, Enz, and a combination of inhibitors for 24 hrs. RNA was then extracted from the samples and converted into cDNA. The cDNA was then used for RT-qPCR to determine if there is a difference in expression of mitochondrial biogenesis marker when exposed to the combination treatment. Results showed that the combination treatment had a significant decrease of mRNA expression within the combination treatment compared to the other treatments. Experiments were done in triplicate (n=3) and statistics were ran at $p <0.05$.

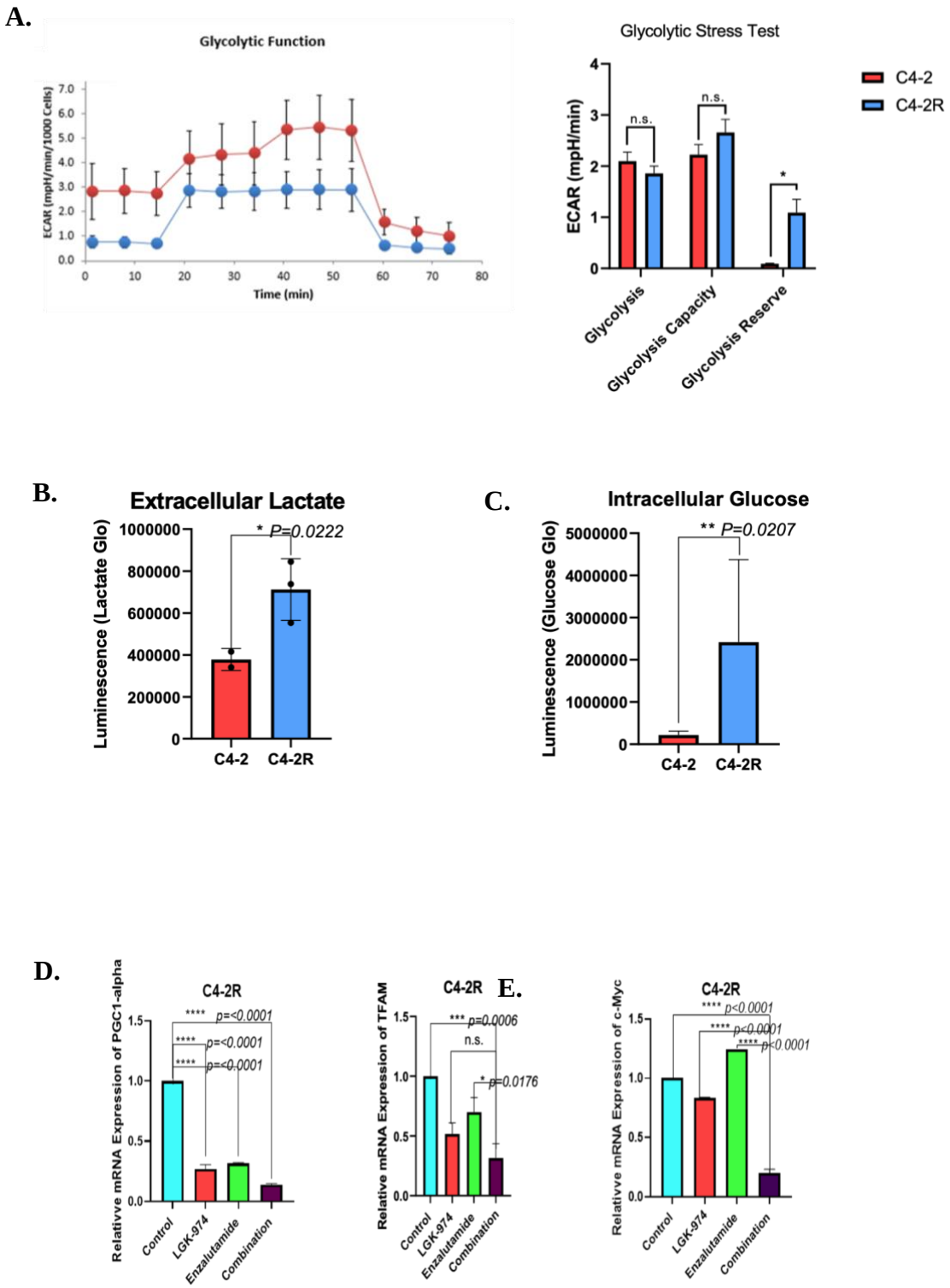
A.
Glycolytic Function
ECAR (mpH/min/1000 Cells)
Time (min)
Glycolytic Stress Test
ECAR (mpH/min)
n.s.
n.s.
*
Glycolysis
Glycolysis Capacity
Glycolysis Reserve
C4-2
C4-2R
B.
Extracellular Lactate
Luminescence (Lactate Glo)
* P=0.0222
C4-2
C4-2R
C.
Intracellular Glucose
Luminescence (Glucose Glo)
** P=0.0207
C4-2
C4-2R
D.
C4-2R
Relativve mRNA Expression of PGC1-alpha
**** p=<0.0001
**** p=<0.0001
**** p=<0.0001
Control
LGK-974
Enzalutamide
Combination
E.
C4-2R
Relative mRNA Expression of TFAM
*** p=0.0006
n.s.
* p=0.0176
Control
LGK-974
Enzalutamide
Combination
C4-2R
Relativve mRNA Expression of c-Myc
**** p<0.0001
**** p<0.0001
**** p<0.0001
Control
LGK-974
Enzalutamide
Combination

Figure 4.2

Figure 4.2 Enzalutamide Resistance Induces Glycolytic Reserve and Glucose Uptake A) C4-2 and C4-2R cells were seeded at 10,000 cells/well in an Agilent Seahorse 96-well plate and left to incubate for 24 hrs. The plate was then subjected to Glycolytic Stress Test and the Enz-resistant cell line showed a significant increase in glycolytic reserve. Experiments were done in triplicate (n=3) and statistics were ran at $p < 0.05$. For the next series of experiments, all cells were plates in 96-well plates at a seeding density of 2,000 cells/well. B) A LactateGlo kit was used to measure the amount of extracellular lactate found within the cell media. Results showed the C4-2R yielded a higher amount of excreted lactate within the cell media. Experiments were done in triplicate (n=3) and statistics were ran at $p < 0.05$. C) GlucoseGlo kit was used to determine the amount of intracellular glucose within the cell. C4-2R compared to C4-2 showed a significant increase in intracellular glucose. Experiments were done in triplicate (n=3) and statistics were ran at $p < 0.05$. D) C4-2R was subjected to inhibitor treatment for 24hr and then the extracellular lactate levels were analyzed and quantified using the LactateGlo assay. Results showed the combination treatment led to a significant decrease in released lactate. Experiments were done in triplicate (n=3) and statistics were ran at $p < 0.05$. E) C4-2R was subjected to inhibitors for 24 hrs and then the level of intracellular glucose was measured via GlucoseGlo kit and showed that the combination treatment significantly decreased the amount of glucose uptake. Experiments were done in triplicate (n=3) and statistics were ran at $p < 0.05$.

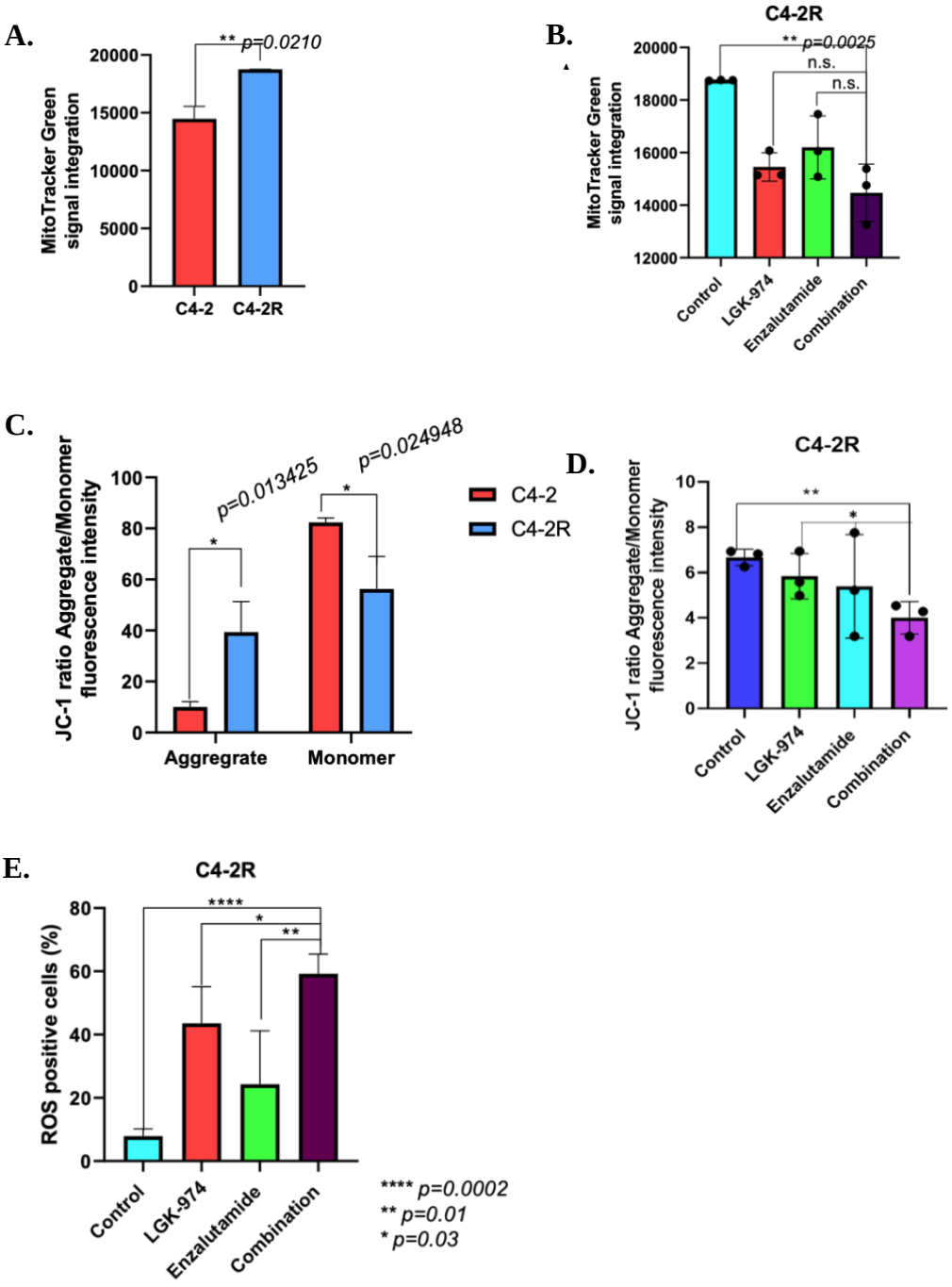
A.
** p=0.0210
MitoTracker Green signal integration
20000
15000
10000
5000
0
C4-2
C4-2R
B.
C4-2R
** p=0.0025
n.s.
n.s.
MitoTracker Green signal integration
20000
18000
16000
14000
12000
Control
LGK-974
Enzalutamide
Combination
C.
JC-1 ratio Aggregate/Monomer fluorescence intensity
p=0.013425
p=0.024948
*
*
100
80
60
40
20
0
Aggregrate
Monomer
C4-2
C4-2R
D.
C4-2R
JC-1 ratio Aggregate/Monomer fluorescence intensity
**
*
10
8
6
4
2
0
Control
LGK-974
Enzalutamide
Combination
E.
C4-2R
ROS positive cells (%)
****
*
**
80
60
40
20
0
Control
LGK-974
Enzalutamide
Combination
**** p=0.0002
** p=0.01
* p=0.03

Figure 4.3

Figure 4.3 Enzalutamide-Resistance Contributes to Mitochondrial Membrane Potential and Increase in ROS Production

A) C4-2 and C4-2R cells were plated in a 24 well cell culture plated at a seeding density of 1 x 10^5. Cells were then stained and collected based on the instructions were MitoTracker™ Green. This stain was used to show the level of mitochondrial mass via flow cytometry. Results showed C4-2R contained a higher mitochondrial mass when compared to C4-2. FCCP was used as an internal control and the experiments were done in triplicate with $p< 0.05$. B) C4-2R cell lines were subjected to treatment for 24hrs and then collected via the MitoTracker™ Green protocol and flow cytometry was used to analyze the amount of mitochondrial mass. Resulted showed that combination treatment significantly decreased the amount of mitochondrial mass. FCCP was used as an internal control and the experiments were done in triplicate with $p< 0.05$. C.) Utilizing the JC-1 protocol, we were able to analyze the amount of mitochondrial membrane polarization. C4-2R compared to C4-2 showed an increase in aggregate indicating that there was more polarized mitochondrial membrane potential. FCCP was used as an internal control and the experiments were done in triplicate with $p< 0.05$. D) C4-2R was then subjected to inhibitor treatment for 24hrs and collected via the JC-1 protocol and analyzed via flow cytometry. Results showed that the combination treatment was able to significantly decrease aggregate formation indicating a loss on the polarization of mitochondrial membranes. FCCP was used as an internal control and the experiments were done in triplicate with $p< 0.05$. E) C4-2R cells were plated into a 24 well plate and subjected to the treatment course for 24hrs and stained/collected via the CellROX protocol. Samples were then used for flow cytometry and to show that the combination treatment had an increase in oxidative stress.

FCCP was used as an internal control and the experiments were done in triplicate with $p < 0.05$.

A.

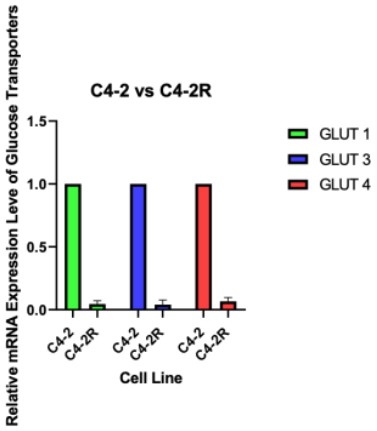

Supplementary Figure 4.4. Expression of GLUT Transporters in Enz-Resistant PCa Cell Lines.

A) Enz-sensitive (C4-2) and Enz-resistant (C4-2R) were plated and allowed 24 hrs to adhere to the cell culture plates. Cells were harvested for RNA isolation and used in RT-qPCR to determine levels of GLUT 1,3, and 4. Results showed that the Enz-sensitive lines had an increase in Glut 1,3, and 4 when compared to the Enz-resistant PCa cell lines. This indicates that GLUT transporters maybe not be the correct transporters that contribute to drug resistance and other glucose transporters should be considered, such as MCT 1-4.

CHAPTER 5: DISCUSSION

5.1 Future Directions

5.1.1 Up-Regulation of PORCN Leads to DRP-1 Activation and Metabolic Switch in Enz-Resistant Prostate Cancer

Based on the evidence collected thus far, the future studies of this work can fraction into various other directions. Since we have demonstrated that the loss of both Wnt signaling cascades increases the efficacy of Enz and alluded to a possible mechanism, future studies would be to further define the mechanism of action. Since we have indicated in our work that the upregulation of β-catenin signaling cascade results in an overexpression of mitochondrial biogenesis markers, such as MYC, PGC1-α, and TFAM, we need to further understand how the activation of these genes leads to the proliferation and survival of prostate cancer cells and causes a metabolic shift. The main focus of this project would be elucidating the mechanism in which PORCN activation results in advanced PCa cells developing a metabolic shift.

Enzalutamide therapy has been revolutionary in the treatment of prostate cancer patients that have advanced into mCRPC. This therapeutic has been shown to significantly reduce PSA levels, and tumor progression decline [190]. Unfortunately, the prolonged and continuous use of this AR-inhibitor results in disease progression via a gain of resistance to Enz treatment [191]. This gain of resistance leads to a metabolic rewiring that allows the cancer cell to utilize mitochondrial oxidative phosphorylation to promote survival [192]. Though this is a major phenotype of advanced stage prostate cancer, the mechanisms that initiates this switch have yet to be elucidated.

Dynamin-Related Protein-1 (DRP-1), is a GTPase that functions to regulate mitochondrial factors, such as acting as regulator of mitochondrial fission [193]. The process of mitochondrial fission and fusion is tightly regulated by the dynamin GTPase family, and the balance of this process is pertinent to the preservation of mitochondrial morphology and function [193]. Mitochondrial fission works to compartmentalization mitochondria during cell division, remove defective mitochondria, regulate Ca^{2+} homeostasis, release pro-apoptotic factors, and mediate G2/M cell cycle progression [194]. Mitochondrial fusion primarily works to prevent the accumulation of defective mitochondria and is required to stimulate oxidative phosphorylation for maximal ATP synthase to meet energy demand [195]. A dysfunction in this dynamic, has been correlated to cancerous phenotypes [194]. Specifically, increased expression of DRP-1 protein, has been linked to the promotion of various cancers such as CRC, lung, gastric, and breast [196]. It has been reported that mitochondrial fission mediated via DRP-1, stimulates invasion, migration, drug resistance, and tumor growth within cancer models, and an inhibition of DRP-1 has led to enhanced apoptotic events and reduce tumor burden [196]. DRP-1 harbors two phosphorylation sites, pDRP1-S616 and pDRP1-S637 [194]. The phosphorylation of the pDRP-1S637, via cAMP-dependent protein kinase residue, is an indication of the inactivation of DRP-1, and this inactivation leads to a lack of mitochondrial fission [197]. The direct phosphorylation of pDRP1-S616, via ERK 1/2 and MAPK, is analogous to DRP-1 activation and promotes mitochondrial fission [198]. Within cancer models, the activation of DRP-1 has also been known to cause an increase in mitochondrial biogenesis and mitophagy. Due to DRP-1's high implication in cancer progression and increase in mitochondrial biogenesis, a possible future direction is pDRP1-

S616 phosphorylation could be a key component of metabolic switch after AR inhibition, causing a reliance of mitochondrial oxidative phosphorylation [196]. Since the calcineurin pathway plays a pivotal role in non-canonical Wnt signaling and is a major regulator of the dephosphorylation of pDRP1-S637, there could be a connection between the activation of noncanonical Wnt signaling and DRP-1 activation. This presents the idea that the combination treatment of LGK-974 and Enz could potentially lead to silencing the activity of DRP-1 and prevent mitochondrial biogenesis.

To understand the role of DRP-1 within Enz-resistance models, the transcription level was determined. C4-2 and C4-2R were used in RT-qPCR and showed that C4-2R had an increase of mRNA level of DRP-1 (S. Figure 5.1 A). Since the hypothesis relies on the phosphorylation of pDRP1-S616, the next experiment would be to immunoblot against pDRP1-S616 and pDRP1-S637 in the C4-2 and C4-2R lines to determine protein expression (S. Figure 5.1 B). Hopefully, these results would show that C4-2R had an increase in pDRP1-S616 and decrease expression of pDRP1-S637, to indicate that loss of Wnt and AR signaling can result in an inactivation of DRP-1. One method to further elucidate our working model is understanding the metabolic response to AR inhibition. Some experiments that can be used to explain metabolic changes would be to use RNA-seq with Enz-sensitive and -resistant cell lines. This approach would be used to visualize the gene expression differences between glycolytic and oxidative phosphorylation genes. Ideally, we would like to see that the Enz-resistant cell line retains a higher gene enrichment in the oxidative phosphorylation pathway in comparison to Enz-sensitive cells, and the Enz-sensitive cells should have a higher level of glycolytic genes compared to Enz-resistant cells. This would indicate that Enz treatment may switch the cancer cell from

glycolytic reliance to oxidative phosphorylation dependency. Though this finding is not novel, it will establish the foundation for further experiments.

Future studies could include taking Enz-sensitive PCa cell lines, C4-2 and LNCaP, and overexpressing PORCN. After stably establishing PORCN-OE in C4-2, this line, and wildtype C4-2, would be subjected to Enz treatment. These cells would then be used in cell survival and proliferation experiments to show that the overexpression of PORCN leads to a decreased efficacy of Enz. If the overexpression of PORCN does not decrease Enz efficacy, then AR may still need to be challenged with inhibitors in future experiments. The C4-2-PORCN-OE cell line could then be used in a MitoStress Test to evaluate mitochondrial respiration. With the overexpression of PORCN, the expected outcome would be a higher OCR value compared to the wildtype sample. This would suggest that increased PORCN levels can switch cells from utilizing glycolysis to possessing a reliance on mitochondrial respiration. This cell line should also be used to determine the mRNA level of DRP-1, and the protein level of pDRP1-S637 and pDRP1-S616. Also, the expression level of the mitochondrial biogenesis markers, PGC1-α, TFAM, and Myc, should be determined to show that upregulation of PORCN leads to increased mitochondrial function. Along with these experiments, a Glycolysis Stress Test should be performed to see if the cells gain a metabolic switch from glycolysis to oxidative phosphorylation reliance. These results would hopefully show that overexpression of PORCN in Enz-sensitive lines, causes a reduction in glycolysis, increased reliance on mitochondrial oxidative phosphorylation, and an increase in levels of pDRP1-S616 activation, mimicking the metabolic switch seen in Enz-resistance. Another experiment to be performed would be to visualize the morphology of the mitochondria between C4-2 and

C4-2R, and C4-2 and C4-2-PORCN-OE. This can be done by staining the mitochondria for mitochondria-associated protein Tu Translation elongation factor (TUFM). Utilizing immunofluorescence, elongated mitochondria could be detected and quantified via calculating the mitochondrial aspect ratio. The mitochondrial aspect ratio is an equal ratio of the major axis to the minor axis of the object being measured. The expected outcome of this experiment would be a visualize mitochondrial elongation of C4-2R and C4-2-PORCN-OE. This would suggest that drug resistance and PORCN can cause mitochondrial morphology change. These findings would further elucidate the mechanism of drug resistance.

Since it has been hinted that AR may regulate DRP-1, encoded as *DNM1L* gene, expression, I would perform an immunoprecipitation-sequencing (CHIP-seq) using C4-2 and C4-2R cells to see if there is binding to the *DNM1L* locus. Also, organoids could be derived from LuCaP35CR patient derived xenografts (PDXs). LuCaP35CR is a PDX that was collected from a 66-year-old Caucasian male that presented with T4 PCa tumor and treated with diethylstilbestrol (DES) and trans-urethral radical prostatectomy (TURP) [199]. After this treatment course, the patient had a detection of bone and bladder metastasis, which was treated with bilateral orchiectomy and cytoprostatectomy, respectively [199]. One month later the left inquinal lymph node was removed and implanted in Balb/c nu/nu mice [199]. These tumors were then harvested and implanted SCID mice who were then subjected to castration [199]. This established the LuCaP35 CR model. Since this model is castration-resistant and not Enz-resistant, animals inoculated with this tumor will need to be subjected to 20 mg/kg Enz for two weeks. The organoids derived can then be used to detect pDRP1-S616 and pDRP1-S637 levels. I would also

immunoblot for Lactate Dehydrogenase A (LDHA) and Hexokinase 2 (HK2) as markers for glycolysis. It would be expected to see a downregulation of glycolysis genes after Enz inhibition.

5.1.2 Cancer Associated Fibroblasts Contributes to Prostate Cancer Enz Resistance via Secretion of Wnt Ligands and Metabolic Manipulation

Cancer Associated Fibroblasts (CAFs) are a prominent component of TME, and they have been documented to be extremely abundant in the prostate cancer TME [200]. Research has suggested that in prostate cancer, CAFs are highly involved in tumor progression and acting as a barrier to prevent drug delivery to cancer cells [201]. They have also been associated with contributing to the increasing aggressiveness of PCa through lactate shuttling via monocarboxylate transporter 1 (MCT1) [201]. Recently it has been observed in prostate cancer, that CAFs rely on aerobic glycolysis upon interaction with cancer cells [202]. This energy dependance is then reprogrammed to oxidative phosphorylation due to CAF-released lactate, which converts cancer cells to utilizing oxidative phosphorylation [201]. This action further progresses chemotherapy resistance and promotes metastatic burden [202]. Based on the information that we have gathered regarding the metabolic switch of Enz resistant prostate cancer; it would be interesting to see if CAFs promoted disease progression through Wnt ligand secretion and the transfer of mitochondria.

To investigate this idea, performing a secretion assay to determine if PCa CAFs secrete Wnt ligands would be the first step. This can be done by harvesting the cell culture media and going through a process of centrifugation and separation through isolation columns to

effectively separate Wnts from other cellular structures. These samples could be immunoblotted for Wnt3a and Wnt5a, specific for prostate cancer Wnt signaling activation, and Bovine Serum Albumin (BSA) as a loading control. The predicted outcome would be that the CAFs are able to secrete Wnt3a and Wnt5a. Next, PCa CAFs harboring PORCN-KD could be co-cultured with Enz-resistant cancer cells. These cells can then be used to measure migration and invasion. Hopefully, the results would show a loss in the cancer cell migration and invasion, indicating that PCa CAFs contribute to cancer cell disease progression.

To determine if CAFs play a part in the metabolic switch of the cancer cell, it would be interesting to use PCa CAFs with PORCN-KD and wildtype PORCN, and harvest their conditioned, serum-free media. This media can then be placed on Enz-resistant cells for about 72 hrs. These cells can then be used to determine the expression level of mitochondrial biogenesis markers and be used in a MitoStress Test. This can illustrate that a loss of PORCN in CAFs, leads to a reduction of mitochondrial biogenesis activation and reliance on mitochondrial respiration. It would be interesting to use the PORCN-KD CAFs conditioned media on the Enz-resistant cell lines, to determine if there is a loss of mitochondrial mass. This can be detected by using FACS or confocal analysis. The expected results would be to see a decrease in mitochondrial mass and activity with the cells that have been exposed to PORCN-KD CAF conditioned media. To determine whether there is a mitochondrial transfer from CAF cells to Enz-resistant PCa cells, CAFs mitochondria can be labeled with MitoTracker Green. The labeled CAFs can then be incubated with unlabeled C4-2R or MR49F cells. Confocal analysis of the co-culture can then be used to show that C4-2R or MR49F can uptake the mitochondria released from the

CAFs via the green staining. This would suggest that the cancer cell was able to acquire stromal mitochondria. As a control you can label the mitochondria in the cancer cell and show that it is not present in the unlabeled CAFs. This would confirm that this is a one directional transfer.

Additionally, to test this system within an *in vivo* model, the prostate reconstitution assay could be performed. In detail, Urogenital Sinus Mesenchymal (UGSM) cells could be isolated from 16 days old mouse embryos and then cultured harboring PORCN-KD. These cells can then be co-cultured with isolated prostate epithelial cells, to form a graft that can be placed under the renal capsule of a NSG mouse. After 2-3 months, the graft can be harvested and stained against various PCa and mitochondrial biogenesis markers. This can show that a loss of PORCN within a TME component can cause disruption of prostate structure. To determine if Enz-resistant PCa cells recruit mitochondria from CAFs in an *in vivo* setting, pre-castrated nude mice could be subcutaneously inoculated with unlabeled C4-2R together with MitoGTP-expressing CAFs. As a control, the C4-2R cells could also be labeled with Tom to ensure that the C4-2R mitochondria are not transferring to the CAFs. After 4 weeks or until tumors reached endpoints, tumors can be harvested and retrieved cells can be analyzed via FACS or confocal to determine the quantity of mitochondria from CAFs transferred to C4-2R. To further implement PORCN with this model, CAFs could be depleted of PORCN and labeled with MitoGTP, and co-inoculated with C4-2R. This would show that with a loss of PORCN within the CAFs, there would be a lack of mitochondria from the CAFs in C4-2R. This would suggest the PORCN plays a paramount role in CAF mitochondrial transfer.

With these data points completed, this could further confirm that PORCN plays an important role in a metabolic demand in the Enz-resistant PCa, that influences a metabolic switch and an increase reliance on oxidative phosphorylation.

A.

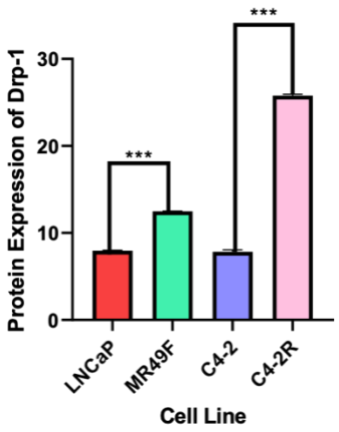

B.

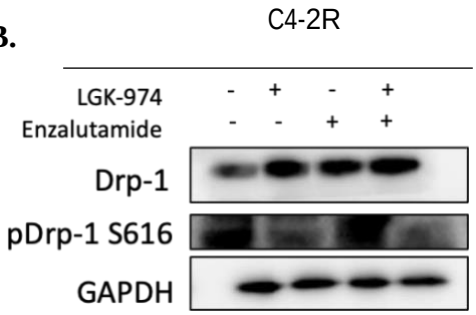

Supplementary Figure 5.1

Supplementary Figure 5.1 DRP-1 Expression Levels and Activation in Enz-Resistant PCa Cell Lines.

A)Enz-sensitive and -resistant cell lines were plated and then were harvested for RNA analysis. The isolated RNA was used in RT-qPCR to determine the transcription level of DRP-1 within each line. The experiment was done in triplicate (n=3) and statistical analysis was done to illustrate that the Enz-resistant PCa cell lines had a significantly higher mRNA expression level compared to the Enz-sensistive PCa cell lines, $p<0.05$. B) Enz-resistant cells, C4-2R, were treated for 72 hrs following this scheme: Control, LGK-974, Enz, Combination. After 72 hrs, the cells were then collected and immunoblotted for DRP-1, pDRP-1 S616, and GAPDH (loading control). As shown, there is a loss of pDRP-1 S616 in both the LGK-974 and combination group, indicating the the inhibitor treatment causes a loss of DRP-1 activation within the drug-resistant PCa cell lines. Through the pDRP-1 S637 should also be blotted to ensure loss of activation.

REFERENCES

1. Ng, L.F., et al., *WNT Signaling in Disease.* Cells, 2019. **8**(8).
2. Nusse, R. and H.E. Varmus, *Many tumors induced by the mouse mammary tumor virus contain a provirus integrated in the same region of the host genome.* Cell, 1982. **31**(1): p. 99-109.
3. Nusse, R., et al., *A new nomenclature for int-1 and related genes: the Wnt gene family.* Cell, 1991. **64**(2): p. 231.
4. Gruber, J., Z. Yee, and N.S. Tolwinski, *Developmental Drift and the Role of Wnt Signaling in Aging.* Cancers (Basel), 2016. **8**(8).
5. Kaur, P., et al., *Modeling the Role of Wnt Signaling in Human and Drosophila Stem Cells.* Genes (Basel), 2018. **9**(2).
6. Nusse, R., *Wnt signaling in disease and in development.* Cell Res, 2005. **15**(1): p. 28-32.
7. Komiya, Y. and R. Habas, *Wnt signal transduction pathways.* Organogenesis, 2008. **4**(2): p. 68-75.
8. He, X., et al., *LDL receptor-related proteins 5 and 6 in Wnt/beta-catenin signaling: arrows point the way.* Development, 2004. **131**(8): p. 1663-77.
9. Yu, F., et al., *Wnt/beta-catenin signaling in cancers and targeted therapies.* Signal Transduct Target Ther, 2021. **6**(1): p. 307.
10. Shipitsin, M., et al., *Molecular definition of breast tumor heterogeneity.* Cancer Cell, 2007. **11**(3): p. 259-73.
11. Green, J., R. Nusse, and R. van Amerongen, *The role of Ryk and Ror receptor tyrosine kinases in Wnt signal transduction.* Cold Spring Harb Perspect Biol, 2014. **6**(2).
12. Lu, W., et al., *Mammalian Ryk is a Wnt coreceptor required for stimulation of neurite outgrowth.* Cell, 2004. **119**(1): p. 97-108.
13. Menck, K., et al., *The WNT/ROR Pathway in Cancer: From Signaling to Therapeutic Intervention.* Cells, 2021. **10**(1).
14. Masiakowski, P. and R.D. Carroll, *A novel family of cell surface receptors with tyrosine kinase-like domain.* J Biol Chem, 1992. **267**(36): p. 26181-90.
15. Petrova, I.M., et al., *Wnt signaling through the Ror receptor in the nervous system.* Mol Neurobiol, 2014. **49**(1): p. 303-15.
16. de Lau, W.B., B. Snel, and H.C. Clevers, *The R-spondin protein family.* Genome Biol, 2012. **13**(3): p. 242.

17. Kazanskaya, O., et al., *R-Spondin2 is a secreted activator of Wnt/beta-catenin signaling and is required for Xenopus myogenesis.* Dev Cell, 2004. **7**(4): p. 525- 34.
18. Tocci, J.M., et al., *R-spondin-mediated WNT signaling potentiation in mammary and breast cancer development.* IUBMB Life, 2020. **72**(8): p. 1546-1559.
19. Zebisch, M., et al., *Structural and molecular basis of ZNRF3/RNF43 transmembrane ubiquitin ligase inhibition by the Wnt agonist R-spondin.* Nat Commun, 2013. **4**: p. 2787.
20. Hao, H.X., et al., *ZNRF3 promotes Wnt receptor turnover in an R-spondin- sensitive manner.* Nature, 2012. **485**(7397): p. 195-200.
21. Kuhl, M., et al., *The Wnt/Ca2+ pathway: a new vertebrate Wnt signaling pathway takes shape.* Trends Genet, 2000. **16**(7): p. 279-83.
22. McQuate, A., E. Latorre-Esteves, and A. Barria, *A Wnt/Calcium Signaling Cascade Regulates Neuronal Excitability and Trafficking of NMDARs.* Cell Rep, 2017. **21**(1): p. 60-69.
23. Fukami, K., *Structure, regulation, and function of phospholipase C isozymes.* J Biochem, 2002. **131**(3): p. 293-9.
24. Harlan, J.E., et al., *Pleckstrin homology domains bind to phosphatidylinositol-4,5- bisphosphate.* Nature, 1994. **371**(6493): p. 168-70.
25. Bill, C.A. and C.M. Vines, *Phospholipase C.* Adv Exp Med Biol, 2020. **1131**: p. 215-242.
26. Essen, L.O., et al., *Crystal structure of a mammalian phosphoinositide-specific phospholipase C delta.* Nature, 1996. **380**(6575): p. 595-602.
27. Ellis, M.V., S. U, and M. Katan, *Mutations within a highly conserved sequence present in the X region of phosphoinositide-specific phospholipase C-delta 1.* Biochem J, 1995. **307 (Pt 1)**(Pt 1): p. 69-75.
28. Streb, H., et al., *Release of Ca2+ from a nonmitochondrial intracellular store in pancreatic acinar cells by inositol-1,4,5-trisphosphate.* Nature, 1983. **306**(5938):
p. 67-9.
29. Sun, M.K. and D.L. Alkon, *Pharmacology of protein kinase C activators: cognition-enhancing and antidementic therapeutics.* Pharmacol Ther, 2010. **127**(1): p. 66-77.
30. Rosse, C., et al., *PKC and the control of localized signal dynamics.* Nat Rev Mol Cell Biol, 2010. **11**(2): p. 103-12.

31. Mochly-Rosen, D., K. Das, and K.V. Grimes, *Protein kinase C, an elusive therapeutic target?* Nat Rev Drug Discov, 2012. **11**(12): p. 937-57.
32. Cooke, M., et al., *Protein kinase C in cancer: The top five unanswered questions.* Mol Carcinog, 2017. **56**(6): p. 1531-1542.
33. Ono, Y., et al., *Phorbol ester binding to protein kinase C requires a cysteine-rich zinc-finger-like sequence.* Proc Natl Acad Sci U S A, 1989. **86**(13): p. 4868-71.
34. Murphy, N.P., et al., *Molecular subversion of Cdc42 signalling in cancer.* Biochem Soc Trans, 2021. **49**(3): p. 1425-1442.
35. Hodge, R.G. and A.J. Ridley, *Regulating Rho GTPases and their regulators.* Nat Rev Mol Cell Biol, 2016. **17**(8): p. 496-510.
36. Salat-Canela, C., et al., *Stress-dependent inhibition of polarized cell growth through unbalancing the GEF/GAP regulation of Cdc42.* Cell Rep, 2021. **37**(5): p. 109951.
37. Lisman, J., R. Yasuda, and S. Raghavachari, *Mechanisms of CaMKII action in long-term potentiation.* Nat Rev Neurosci, 2012. **13**(3): p. 169-82.
38. Schulman, H. and P. Greengard, *Ca2+-dependent protein phosphorylation system in membranes from various tissues, and its activation by "calcium-dependent regulator".* Proc Natl Acad Sci U S A, 1978. **75**(11): p. 5432-6.
39. Beckendorf, J., M.M.G. van den Hoogenhof, and J. Backs, *Physiological and unappreciated roles of CaMKII in the heart.* Basic Res Cardiol, 2018. **113**(4): p. 29.
40. Shibuya, H., et al., *Role of TAK1 and TAB1 in BMP signaling in early Xenopus development.* EMBO J, 1998. **17**(4): p. 1019-28.
41. Yamaguchi, K., et al., *Identification of a member of the MAPKKK family as a potential mediator of TGF-beta signal transduction.* Science, 1995. **270**(5244): p. 2008-11.
42. Bosman, M.C., et al., *The TAK1-NF-kappaB axis as therapeutic target for AML.* Blood, 2014. **124**(20): p. 3130-40.
43. Xu, Y.R. and C.Q. Lei, *TAK1-TABs Complex: A Central Signalosome in Inflammatory Responses.* Front Immunol, 2020. **11**: p. 608976.
44. Ishitani, T., et al., *The TAK1-NLK-MAPK-related pathway antagonizes signalling between beta-catenin and transcription factor TCF.* Nature, 1999. **399**(6738): p. 798-802.
45. Yamada, M., et al., *NARF, an nemo-like kinase (NLK)-*

associated ring finger protein regulates the ubiquitylation and degradation of T cell factor/lymphoid enhancer factor (TCF/LEF). J Biol Chem, 2006. **281**(30): p. 20749-20760.
46. Sharma, M., et al., *Dishevelled: A masterful conductor of complex Wnt signals.* Cell Signal, 2018. **47**: p. 52-64.
47. Schwarz-Romond, T., et al., *The DIX domain of Dishevelled confers Wnt signaling by dynamic polymerization.* Nat Struct Mol Biol, 2007. **14**(6): p. 484- 92.
48. Nguyen, L.K., B.N. Kholodenko, and A. von Kriegsheim, *Rac1 and RhoA: Networks, loops and bistability.* Small GTPases, 2018. **9**(4): p. 316-321.
49. Kotelevets, L. and E. Chastre, *Rac1 Signaling: From Intestinal Homeostasis to Colorectal Cancer Metastasis.* Cancers (Basel), 2020. **12**(3).
50. Mehta, P., et al., *LyGDI, a novel SHIP-interacting protein, is a negative regulator of FcgammaR-mediated phagocytosis.* PLoS One, 2011. **6**(6): p. e21175.
51. Mosaddeghzadeh, N. and M.R. Ahmadian, *The RHO Family GTPases: Mechanisms of Regulation and Signaling.* Cells, 2021. **10**(7).
52. Jacobs, M., et al., *The structure of dimeric ROCK I reveals the mechanism for ligand selectivity.* J Biol Chem, 2006. **281**(1): p. 260-8.
53. Julian, L. and M.F. Olson, *Rho-associated coiled-coil containing kinases (ROCK): structure, regulation, and functions.* Small GTPases, 2014. **5**: p. e29846.
54. Matsubara, M. and M.J. Bissell, *Inhibitors of Rho kinase (ROCK) signaling revert the malignant phenotype of breast cancer cells in 3D context.* Oncotarget, 2016. **7**(22): p. 31602-22.
55. ode, A.M. and Z. Dong, *The functional contrariety of JNK.* Mol Carcinog, 2007. **46**(8): p. 591-8.
56. Lin, B., et al., *Role of Protein Glycosylation in Host-Pathogen Interaction.* Cells, 2020. **9**(4).
57. Tokmakov, A.A., et al., *Multiple post-translational modifications affect heterologous protein synthesis.* J Biol Chem, 2012. **287**(32): p. 27106-16.
58. Hanson, S.R., et al., *The core trisaccharide of an N-linked glycoprotein intrinsically accelerates folding and enhances stability.* Proc Natl Acad Sci U S A, 2009. **106**(9): p. 3131-6.

59. Shental-Bechor, D. and Y. Levy, *Effect of glycosylation on protein folding: a close look at thermodynamic stabilization.* Proc Natl Acad Sci U S A, 2008. **105**(24): p. 8256-61.
60. Komekado, H., et al., *Glycosylation and palmitoylation of Wnt-3a are coupled to produce an active form of Wnt-3a.* Genes Cells, 2007. **12**(4): p. 521-34.
61. Kurayoshi, M., et al., *Post-translational palmitoylation and glycosylation of Wnt- 5a are necessary for its signalling.* Biochem J, 2007. **402**(3): p. 515-23.
62. Mehta, S., S. Hingole, and V. Chaudhary, *The Emerging Mechanisms of Wnt Secretion and Signaling in Development.* Front Cell Dev Biol, 2021. **9**: p. 714746.
63. Luo, X., et al., *Acylation of Anthocyanins and Their Applications in the Food Industry: Mechanisms and Recent Research Advances.* Foods, 2022. **11**(14).
64. Chang, S.C. and A.I. Magee, *Acyltransferases for secreted signalling proteins (Review).* Mol Membr Biol, 2009. **26**(1): p. 104-13.
65. Paton, C.M. and J.M. Ntambi, *Biochemical and physiological function of stearoyl-CoA desaturase.* Am J Physiol Endocrinol Metab, 2009. **297**(1): p. E28- 37.
66. Li, Y. and B. Qi, *Progress toward Understanding Protein S-acylation: Prospective in Plants.* Front Plant Sci, 2017. **8**: p. 346.
67. Mosimann, C., G. Hausmann, and K. Basler, *Parafibromin/Hyrax activates Wnt/Wg target gene transcription by direct association with beta-catenin/Armadillo.* Cell, 2006. **125**(2): p. 327-41.
68. Smotrys, J.E. and M.E. Linder, *Palmitoylation of intracellular signaling proteins: regulation and function.* Annu Rev Biochem, 2004. **73**: p. 559-87.
69. van den Heuvel, M., et al., *Mutations in the segment polarity genes wingless and porcupine impair secretion of the wingless protein.* EMBO J, 1993. **12**(13): p. 5293-302.
70. Hofmann, K., *A superfamily of membrane-bound O-acyltransferases with implications for wnt signaling.* Trends Biochem Sci, 2000. **25**(3): p. 111-2.
71. Rios-Esteves, J., B. Haugen, and M.D. Resh, *Identification of key residues and regions important for porcupine-mediated Wnt acylation.* J Biol Chem, 2014. **289**(24): p. 17009-19.
72. Caricasole, A., et al., *Induction of Dickkopf-1, a*

negative modulator of the Wnt pathway, is associated with neuronal degeneration in Alzheimer's brain. J Neurosci, 2004. **24**(26): p. 6021-7.
73. Tanaka, K., et al., *The evolutionarily conserved porcupine gene family is involved in the processing of the Wnt family.* Eur J Biochem, 2000. **267**(13): p. 4300-11.
74. Goltz, R.W., et al., *Focal dermal hypoplasia.* Arch Dermatol, 1962. **86**: p. 708-17.
75. Torres, V.I., J.A. Godoy, and N.C. Inestrosa, *Modulating Wnt signaling at the root: Porcupine and Wnt acylation.* Pharmacol Ther, 2019. **198**: p. 34-45.
76. Nie, X., et al., *Emerging Roles of Wnt Ligands in Human Colorectal Cancer.* Front Oncol, 2020. **10**: p. 1341.
77. Dela Cruz, C.S., L.T. Tanoue, and R.A. Matthay, *Lung cancer: epidemiology, etiology, and prevention.* Clin Chest Med, 2011. **32**(4): p. 605-44.
78. Rudin, C.M., et al., *Small-cell lung cancer.* Nat Rev Dis Primers, 2021. **7**(1): p. 3.
79. Zappa, C. and S.A. Mousa, *Non-small cell lung cancer: current treatment and future advances.* Transl Lung Cancer Res, 2016. **5**(3): p. 288-300.
80. Xue, W., et al., *WNT ligands in non-small cell lung cancer: from pathogenesis to clinical practice.* Discov Oncol, 2023. **14**(1): p. 136.
81. Mazieres, J., et al., *Wnt signaling in lung cancer.* Cancer Lett, 2005. **222**(1): p. 1- 10.
82. Lin, S., et al., *Roles of Wnt/beta-Catenin Signaling Pathway Regulatory Long Non-Coding RNAs in the Pathogenesis of Non-Small Cell Lung Cancer.* Cancer Manag Res, 2020. **12**: p. 4181-4191.
83. Nakano, T., et al., *Biological properties and gene expression associated with metastatic potential of human osteosarcoma.* Clin Exp Metastasis, 2003. **20**(7): p. 665-74.
84. Azamjah, N., Y. Soltan-Zadeh, and F. Zayeri, *Global Trend of Breast Cancer Mortality Rate: A 25-Year Study.* Asian Pac J Cancer Prev, 2019. **20**(7): p. 2015- 2020.
85. Xu, X., et al., *Wnt signaling in breast cancer: biological mechanisms, challenges and opportunities.* Mol Cancer, 2020. **19**(1): p. 165.
86. Makki, J., *Diversity of Breast Carcinoma: Histological Subtypes and Clinical Relevance.* Clin Med Insights Pathol, 2015. **8**: p. 23-31.
87. Dejmek, J., et al., *Expression and signaling activity of Wnt-5a/discoidin domain receptor-1 and Syk plays*

distinct but decisive roles in breast cancer patient survival. Clin Cancer Res, 2005. **11**(2 Pt 1): p. 520-8.
88. Roarty, K., et al., *Loss of TGF-beta or Wnt5a results in an increase in Wnt/beta- catenin activity and redirects mammary tumour phenotype.* Breast Cancer Res, 2009. **11**(2): p. R19.
89. Gujral, T.S., et al., *A noncanonical Frizzled2 pathway regulates epithelial- mesenchymal transition and metastasis.* Cell, 2014. **159**(4): p. 844-56.
90. Yun, X., et al., *Immunohistochemical study of beta-catenin and functionally related molecular markers in tongue squamous cell carcinoma and its correlation with cellular proliferation.* Oncol Lett, 2010. **1**(3): p. 437-443.
91. Rawla, P., T. Sunkara, and A. Barsouk, *Epidemiology of colorectal cancer: incidence, mortality, survival, and risk factors.* Prz Gastroenterol, 2019. **14**(2): p. 89-103.
92. Zhu, Y. and X. Li, *Advances of Wnt Signalling Pathway in Colorectal Cancer.* Cells, 2023. **12**(3).
93. Lu, J., M. Kornmann, and B. Traub, *Role of Epithelial to Mesenchymal Transition in Colorectal Cancer.* Int J Mol Sci, 2023. **24**(19).
94. Vermeulen, L., et al., *Wnt activity defines colon cancer stem cells and is regulated by the microenvironment.* Nat Cell Biol, 2010. **12**(5): p. 468-76.
95. Valkenburg, K.C., et al., *Wnt/beta-catenin Signaling in Normal and Cancer Stem Cells.* Cancers (Basel), 2011. **3**(2): p. 2050-79.
96. Ouko, L., et al., *Wnt11 signaling promotes proliferation, transformation, and migration of IEC6 intestinal epithelial cells.* J Biol Chem, 2004. **279**(25): p. 26707-15.
97. Tian, S., et al., *Secreted AGR2 promotes invasion of colorectal cancer cells via Wnt11-mediated non-canonical Wnt signaling.* Exp Cell Res, 2018. **364**(2): p. 198-207.
98. Nishioka, M., et al., *Possible involvement of Wnt11 in colorectal cancer progression.* Mol Carcinog, 2013. **52**(3): p. 207-17.
99. Rawla, P., *Epidemiology of Prostate Cancer.* World J Oncol, 2019. **10**(2): p. 63- 89.
100. Xu, X., et al., *Risk of prostate cancer in relatives of prostate cancer patients in Sweden: A nationwide cohort study.* PLoS Med, 2021. **18**(6): p. e1003616.
101. Adhyam, M. and A.K. Gupta, *A Review on the Clinical*

Utility of PSA in Cancer Prostate. Indian J Surg Oncol, 2012. **3**(2): p. 120-9.
102. Rebello, R.J., et al., *Prostate cancer.* Nat Rev Dis Primers, 2021. **7**(1): p. 9.
103. Koushyar, S., et al., *Exploring the Wnt Pathway as a Therapeutic Target for Prostate Cancer.* Biomolecules, 2022. **12**(2).
104. Wang, Q., et al., *A novel role for Wnt/Ca2+ signaling in actin cytoskeleton remodeling and cell motility in prostate cancer.* PLoS One, 2010. **5**(5): p. e10456.
105. Wang, Q., et al., *Hypomethylation of WNT5A, CRIP1 and S100P in prostate cancer.* Oncogene, 2007. **26**(45): p. 6560-5.
106. Chen, X., et al., *Inhibition of noncanonical Wnt pathway overcomes enzalutamide resistance in castration-resistant prostate cancer.* Prostate, 2020. **80**(3): p. 256- 266.
107. Lei, Z.N., et al., *Understanding and targeting resistance mechanisms in cancer.* MedComm (2020), 2023. **4**(3): p. e265.
108. Hankey, W., W.L. Frankel, and J. Groden, *Functions of the APC tumor suppressor protein dependent and independent of canonical WNT signaling: implications for therapeutic targeting.* Cancer Metastasis Rev, 2018. **37**(1): p. 159-172.
109. Groden, J., et al., *Identification and characterization of the familial adenomatous polyposis coli gene.* Cell, 1991. **66**(3): p. 589-600.
110. Nishisho, I., et al., *Mutations of chromosome 5q21 genes in FAP and colorectal cancer patients.* Science, 1991. **253**(5020): p. 665-9.
111. Rubinfeld, B., et al., *Binding of GSK3beta to the APC-beta-catenin complex and regulation of complex assembly.* Science, 1996. **272**(5264): p. 1023-6.
112. Korinek, V., et al., *Constitutive transcriptional activation by a beta-catenin-Tcf complex in APC-/- colon carcinoma.* Science, 1997. **275**(5307): p. 1784-7.
113. Morin, P.J., et al., *Activation of beta-catenin-Tcf signaling in colon cancer by mutations in beta-catenin or APC.* Science, 1997. **275**(5307): p. 1787-90.
114. Arques, O., et al., *Tankyrase Inhibition Blocks Wnt/beta-Catenin Pathway and Reverts Resistance to PI3K and AKT Inhibitors in the Treatment of Colorectal Cancer.* Clin Cancer Res, 2016. **22**(3): p. 644-56.
115. Hoimes, C.J. and W.K. Kelly, *Redefining hormone resistance in prostate cancer.* Ther Adv Med Oncol, 2010. **2**(2): p. 107-123.

116. Kishore, C. and X. Zi, *Wnt Signaling and Therapeutic Resistance in Castration- Resistant Prostate Cancer.* Curr Pharmacol Rep, 2023. **9**(5): p. 261-274.
117. Wang, G., et al., *Genetics and biology of prostate cancer.* Genes Dev, 2018. **32**(17-18): p. 1105-1140.
118. Miyamoto, D.T., et al., *RNA-Seq of single prostate CTCs implicates noncanonical Wnt signaling in antiandrogen resistance.* Science, 2015. **349**(6254): p. 1351-6.
119. Seo, W.I., et al., *Wnt signaling promotes androgen-independent prostate cancer cell proliferation through up-regulation of the hippo pathway effector YAP.* Biochem Biophys Res Commun, 2017. **486**(4): p. 1034-1039.
120. Scarborough, H.A., et al., *AZ1366: An Inhibitor of Tankyrase and the Canonical Wnt Pathway that Limits the Persistence of Non-Small Cell Lung Cancer Cells Following EGFR Inhibition.* Clin Cancer Res, 2017. **23**(6): p. 1531-1541.
121. Rathert, C., M.D. Wyrwich, and S.A. Boren, *Patient-centered care and outcomes: a systematic review of the literature.* Med Care Res Rev, 2013. **70**(4): p. 351-79.
122. Zhong, Z. and D.M. Virshup, *Wnt Signaling and Drug Resistance in Cancer.* Mol Pharmacol, 2020. **97**(2): p. 72-89.
123. Ruan, Y., et al., *Wnt Signaling in Leukemia and Its Bone Marrow Microenvironment.* Int J Mol Sci, 2020. **21**(17).
124. Koni, M., V. Pinnaro, and M.F. Brizzi, *The Wnt Signalling Pathway: A Tailored Target in Cancer.* Int J Mol Sci, 2020. **21**(20).
125. Zimmerli, D., et al., *Pharmacological interventions in the Wnt pathway: inhibition of Wnt secretion versus disrupting the protein-protein interfaces of nuclear factors.* Br J Pharmacol, 2017. **174**(24): p. 4600-4610.
126. Rao, D.M., et al., *Wnt family member 4 (WNT4) and WNT3A activate cell- autonomous Wnt signaling independent of porcupine O-acyltransferase or Wnt secretion.* J Biol Chem, 2019. **294**(52): p. 19950-19966.
127. Liu, J., et al., *Targeting Wnt-driven cancer through the inhibition of Porcupine by LGK974.* Proc Natl Acad Sci U S A, 2013. **110**(50): p. 20224-9.
128. Li, J., et al., *Porcupine Inhibitor LGK974 Downregulates the Wnt Signaling Pathway and Inhibits Clear Cell Renal Cell Carcinoma.* Biomed Res Int, 2020. **2020**: p. 2527643.

129. Zhang, Y. and X. Wang, *Targeting the Wnt/beta-catenin signaling pathway in cancer.* J Hematol Oncol, 2020. **13**(1): p. 165.
130. Ghosh, N., et al., *The Wnt signaling pathway: a potential therapeutic target against cancer.* Ann N Y Acad Sci, 2019. **1443**(1): p. 54-74.
131. Madan, B., et al., *Wnt addiction of genetically defined cancers reversed by PORCN inhibition.* Oncogene, 2016. **35**(17): p. 2197-207.
132. Pecina-Slaus, N., et al., *Wnt Signaling Inhibitors and Their Promising Role in Tumor Treatment.* Int J Mol Sci, 2023. **24**(7).
133. Doi, T., et al., *Safety, pharmacokinetics, and antitumour activity of trastuzumab deruxtecan (DS-8201), a HER2-targeting antibody-drug conjugate, in patients with advanced breast and gastric or gastro-oesophageal tumours: a phase 1 dose-escalation study.* Lancet Oncol, 2017. **18**(11): p. 1512-1522.
134. Li, C., et al., *The Delivery of a Wnt Pathway Inhibitor Toward CSCs Requires Stable Liposome Encapsulation and Delayed Drug Release in Tumor Tissues.* Mol Ther, 2019. **27**(9): p. 1558-1567.
135. Rim, E.Y., H. Clevers, and R. Nusse, *The Wnt Pathway: From Signaling Mechanisms to Synthetic Modulators.* Annu Rev Biochem, 2022. **91**: p. 571-598.
136. Fischer, M.M., et al., *WNT antagonists exhibit unique combinatorial antitumor activity with taxanes by potentiating mitotic cell death.* Sci Adv, 2017. **3**(6): p. e1700090.
137. Gurney, A., et al., *Wnt pathway inhibition via the targeting of Frizzled receptors results in decreased growth and tumorigenicity of human tumors.* Proc Natl Acad Sci U S A, 2012. **109**(29): p. 11717-22.
138. Tam, B.Y., et al., *The CLK inhibitor SM08502 induces anti-tumor activity and reduces Wnt pathway gene expression in gastrointestinal cancer models.* Cancer Lett, 2020. **473**: p. 186-197.
139. Diamond, J.R., et al., *Phase Ib clinical trial of the anti-frizzled antibody vantictumab (OMP-18R5) plus paclitaxel in patients with locally advanced or metastatic HER2-negative breast cancer.* Breast Cancer Res Treat, 2020. **184**(1): p. 53-62.
140. Davis, S.L., et al., *A phase 1b dose escalation study of Wnt pathway inhibitor vantictumab in combination with nab-paclitaxel and gemcitabine in patients with previously*

untreated metastatic pancreatic cancer. Invest New Drugs, 2020. **38**(3): p. 821-830.
141. Wang, Z., et al., *Salinomycin nanocrystals for colorectal cancer treatment through inhibition of Wnt/beta-catenin signaling.* Nanoscale, 2020. **12**(38): p. 19931-19938.
142. Wang, J., et al., *Niclosamide-induced Wnt signaling inhibition in colorectal cancer is mediated by autophagy.* Biochem J, 2019. **476**(3): p. 535-546.
143. Jurgeit, A., et al., *Niclosamide is a proton carrier and targets acidic endosomes with broad antiviral effects.* PLoS Pathog, 2012. **8**(10): p. e1002976.
144. Arend, R.C., et al., *Niclosamide and its analogs are potent inhibitors of Wnt/beta- catenin, mTOR and STAT3 signaling in ovarian cancer.* Oncotarget, 2016. **7**(52): p. 86803-86815.
145. Venerando, A., et al., *Pyrvinium pamoate does not activate protein kinase CK1, but promotes Akt/PKB down-regulation and GSK3 activation.* Biochem J, 2013. **452**(1): p. 131-7.
146. Xu, L., et al., *WNT pathway inhibitor pyrvinium pamoate inhibits the self-renewal and metastasis of breast cancer stem cells.* Int J Oncol, 2016. **48**(3): p. 1175-86.
147. Fan, J., R.R. Reid, and T.C. He, *Pyrvinium doubles against WNT-driven cancer*. J Biol Chem, 2022. **298**(10): p. 102479.
148. Zhang, C., et al., *Targeting of Wnt/beta-Catenin by Anthelmintic Drug Pyrvinium Enhances Sensitivity of Ovarian Cancer Cells to Chemotherapy.* Med Sci Monit, 2017. **23**: p. 266-275.
149. Hecht, A., et al., *The p300/CBP acetyltransferases function as transcriptional coactivators of beta-catenin in vertebrates.* EMBO J, 2000. **19**(8): p. 1839-50.
150. He, W., et al., *Wnt/beta-catenin signaling promotes renal interstitial fibrosis.* J Am Soc Nephrol, 2009. **20**(4): p. 765-76.
151. Chehelgerdi, M., et al., *Progressing nanotechnology to improve targeted cancer treatment: overcoming hurdles in its clinical implementation.* Mol Cancer, 2023. **22**(1): p. 169.
152. Vernooij, R.W., et al., *Radical prostatectomy versus deferred treatment for localised prostate cancer.* Cochrane Database Syst Rev, 2020. **6**(6): p. CD006590.
153. Chandrasekar, T., et al., *Mechanisms of resistance in castration-resistant prostate cancer (CRPC).* Transl

Androl Urol, 2015. **4**(3): p. 365-80.
154. Fujita, K. and N. Nonomura, *Role of Androgen Receptor in Prostate Cancer: A Review.* World J Mens Health, 2019. **37**(3): p. 288-295.
155. Beilin, J., et al., *Effect of the androgen receptor CAG repeat polymorphism on transcriptional activity: specificity in prostate and non-prostate cell lines.* J Mol Endocrinol, 2000. **25**(1): p. 85-96.
156. Giovannucci, E., et al., *The CAG repeat within the androgen receptor gene and its relationship to prostate cancer.* Proc Natl Acad Sci U S A, 1997. **94**(7): p. 3320- 3.
157. Turcu, A., et al., *Adrenal androgens and androgen precursors-definition, synthesis, regulation and physiologic actions.* Compr Physiol, 2014. **4**(4): p. 1369-81.
158. Simons, P., et al., *Sex hormone-binding globulin: biomarker and hepatokine?*
Trends Endocrinol Metab, 2021. **32**(8): p. 544-553.
159. Davey, R.A. and M. Grossmann, *Androgen Receptor Structure, Function and Biology: From Bench to Bedside.* Clin Biochem Rev, 2016. **37**(1): p. 3-15.
160. Bevan, C.L., et al., *The AF1 and AF2 domains of the androgen receptor interact with distinct regions of SRC1.* Mol Cell Biol, 1999. **19**(12): p. 8383-92.
161. Semenas, J., N. Dizeyi, and J.L. Persson, *Enzalutamide as a second generation antiandrogen for treatment of advanced prostate cancer.* Drug Des Devel Ther, 2013. **7**: p. 875-81.
162. Moreira, R.B., et al., *Differential side effects profile in patients with mCRPC treated with abiraterone or enzalutamide: a meta-analysis of randomized controlled trials.* Oncotarget, 2017. **8**(48): p. 84572-84578.
163. Le, T.K., et al., *Castration-Resistant Prostate Cancer: From Uncovered Resistance Mechanisms to Current Treatments.* Cancers (Basel), 2023. **15**(20).
164. Tisseverasinghe, S., et al., *Advances in PARP Inhibitors for Prostate Cancer.*
Cancers (Basel), 2023. **15**(6).
165. Ragupathi, A., et al., *Targeting the BRCA1/2 deficient cancer with PARP inhibitors: Clinical outcomes and mechanistic insights.* Front Cell Dev Biol, 2023. **11**: p. 1133472.
166. Madan, R.A. and J.L. Gulley, *Sipuleucel-T: harbinger of a new age of therapeutics for prostate cancer.* Expert Rev Vaccines, 2011. **10**(2): p. 141-50.

167. Frantellizzi, V., et al., *Analysis of Unusual Adverse Effects After Radium-223 Dichloride Administration.* Curr Radiopharm, 2020. **13**(2): p. 159-163.
168. Hennrich, U. and M. Eder, *[(177)Lu]Lu-PSMA-617 (Pluvicto(TM)): The First FDA-Approved Radiotherapeutical for Treatment of Prostate Cancer*. Pharmaceuticals (Basel), 2022. **15**(10).
169. Keam, S.J., *Lutetium Lu 177 Vipivotide Tetraxetan: First Approval.* Mol Diagn Ther, 2022. **26**(4): p. 467-475.
170. Bianchi, L., et al., *PSMA-PET Guided Treatment in Prostate Cancer Patients with Oligorecurrent Progression after Previous Salvage Treatment.* Cancers (Basel), 2023. **15**(7).
171. Li, Y., et al., *Recent Estimates and Predictions of 5-Year Survival in Patients with Gastric Cancer: A Model-Based Period Analysis.* Cancer Control, 2022. **29**: p. 10732748221099227.
172. Zhang, Z., et al., *Inhibition of the Wnt/beta-Catenin Pathway Overcomes Resistance to Enzalutamide in Castration-Resistant Prostate Cancer.* Cancer Res, 2018. **78**(12): p. 3147-3162.
173. Kalluri, R. and R.A. Weinberg, *The basics of epithelial-mesenchymal transition.* J Clin Invest, 2009. **119**(6): p. 1420-8.
174. Liberti, M.V. and J.W. Locasale, *The Warburg Effect: How Does it Benefit Cancer Cells?* Trends Biochem Sci, 2016. **41**(3): p. 211-218.
175. Vander Heiden, M.G., L.C. Cantley, and C.B. Thompson, *Understanding the Warburg effect: the metabolic requirements of cell proliferation.* Science, 2009. **324**(5930): p. 1029-33.
176. Burns, J.S. and G. Manda, *Metabolic Pathways of the Warburg Effect in Health and Disease: Perspectives of Choice, Chain or Chance.* Int J Mol Sci, 2017. **18**(12).
177. Lin, C., et al., *Prostate Cancer Energetics and Biosynthesis.* Adv Exp Med Biol, 2019. **1210**: p. 185-237.
178. Mamouni, K., G. Kallifatidis, and B.L. Lokeshwar, *Targeting Mitochondrial Metabolism in Prostate Cancer with Triterpenoids.* Int J Mol Sci, 2021. **22**(5).
179. Rossmann, M.P., et al., *Mitochondrial function in development and disease.* Dis Model Mech, 2021. **14**(6).
180. Druzhyna, N.M., G.L. Wilson, and S.P. LeDoux, *Mitochondrial DNA repair in aging and disease.* Mech Ageing Dev, 2008. **129**(7-8): p. 383-90.

181. Martinez-Outschoorn, U.E., et al., *Mitochondrial biogenesis drives tumor cell proliferation.* Am J Pathol, 2011. **178**(5): p. 1949-52.
182. Abu Shelbayeh, O., et al., *PGC-1alpha Is a Master Regulator of Mitochondrial Lifecycle and ROS Stress Response.* Antioxidants (Basel), 2023. **12**(5).
183. Fendt, S.M., C. Frezza, and A. Erez, *Targeting Metabolic Plasticity and Flexibility Dynamics for Cancer Therapy.* Cancer Discov, 2020. **10**(12): p. 1797- 1807.
184. Kim, Y.S., et al., *The Effects of Mitochondrial Transplantation on Sepsis Depend on the Type of Cell from Which They Are Isolated.* Int J Mol Sci, 2023. **24**(12).
185. Hill, B.G., et al., *Integration of cellular bioenergetics with mitochondrial quality control and autophagy.* Biol Chem, 2012. **393**(12): p. 1485-1512.
186. Staricha, K., et al., *Effect of high glucose condition on glucose metabolism in primary astrocytes.* Brain Res, 2020. **1732**: p. 146702.
187. TeSlaa, T. and M.A. Teitell, *Techniques to monitor glycolysis.* Methods Enzymol, 2014. **542**: p. 91-114.
188. Li, X., et al., *Lactate metabolism in human health and disease.* Signal Transduct Target Ther, 2022. **7**(1): p. 305.
189. Clutton, G., et al., *A Reproducible, Objective Method Using MitoTracker(R) Fluorescent Dyes to Assess Mitochondrial Mass in T Cells by Flow Cytometry.* Cytometry A, 2019. **95**(4): p. 450-456.
190. Armstrong, A.J., et al., *ARCHES: A Randomized, Phase III Study of Androgen Deprivation Therapy With Enzalutamide or Placebo in Men With Metastatic Hormone-Sensitive Prostate Cancer.* J Clin Oncol, 2019. **37**(32): p. 2974-2986.
191. Wang, Y., et al., *Mechanisms of enzalutamide resistance in castration-resistant prostate cancer and therapeutic strategies to overcome it.* Br J Pharmacol, 2021. **178**(2): p. 239-261.
192. Basu, H.S., et al., *Prostate cancer cells survive anti-androgen and mitochondrial metabolic inhibitors by modulating glycolysis and mitochondrial metabolic activities.* Prostate, 2021. **81**(12): p. 799-811.
193. Hu, C., Y. Huang, and L. Li, *Drp1-Dependent Mitochondrial Fission Plays Critical Roles in Physiological and Pathological Progresses in Mammals.* Int J Mol Sci, 2017. **18**(1).
194. Deng, Y., et al., *Mitochondrial Dynamin-Related Protein*

Drp1: a New Player in Cardio-oncology. Curr Oncol Rep, 2022. **24**(12): p. 1751-1763.
195. Chiu, Y.H., et al., *Molecular Machinery and Pathophysiology of Mitochondrial Dynamics.* Front Cell Dev Biol, 2021. **9**: p. 743892.
196. Adhikary, A., et al., *DRP1: At the Crossroads of Dysregulated Mitochondrial Dynamics and Altered Cell Signaling in Cancer Cells.* ACS Omega, 2023. **8**(48): p. 45208-45223.
197. Yu, R., et al., *The phosphorylation status of Ser-637 in dynamin-related protein 1 (Drp1) does not determine Drp1 recruitment to mitochondria.* J Biol Chem, 2019. **294**(46): p. 17262-17277.
198. Kashatus, J.A., et al., *Erk2 phosphorylation of Drp1 promotes mitochondrial fission and MAPK-driven tumor growth.* Mol Cell, 2015. **57**(3): p. 537-51.
199. Corey, E., et al., *LuCaP 35: a new model of prostate cancer progression to androgen independence.* Prostate, 2003. **55**(4): p. 239-46.
200. Bonollo, F., et al., *The Role of Cancer-Associated Fibroblasts in Prostate Cancer Tumorigenesis.* Cancers (Basel), 2020. **12**(7).
201. Bedeschi, M., et al., *Cancer-Associated Fibroblast: Role in Prostate Cancer Progression to Metastatic Disease and Therapeutic Resistance.* Cells, 2023. **12**(5).
202. Chetta, P., R. Sriram, and G. Zadra, *Lactate as Key Metabolite in Prostate Cancer Progression: What Are the Clinical Implications?* Cancers (Basel), 2023. **15**(13).

VITA

KATELYN JONES

Education

University of Kentucky, 08/2020- expected 08/2024

Doctor of Philosophy, Toxicology and Cancer Biology

Graduate Research Assistant in Dr. Xiaoqi Liu's Lab

Longwood University, 08/2014-05/2019

Bachelor of Science, Biology

Minor in Chemistry

Awards and Honors

NCI T32 Training Grant (T32 CA 165990), University of Kentucky 2022-2024

NIEHS T32 Training Grant, University of Kentucky 2020-2021

Best Poster Presentation Award, University of Kentucky 2021

Brother of the Year, Longwood University 2018

Publications

1. Liu J, Zhao Y, He D, **Jones KM**, Tang S, Allison DB, Zhang Y, Chen J, Zhang Q, Wang X, Li C, Wang C, Li L, Liu X. A kinome-wide CRISPR screen identifies CK1α as a target to overcome enzalutamide resistance of prostate cancer. Cell Rep Med. 2023 Apr 18;4(4):101015. doi: 10.1016/j.xcrm.2023.101015. PMID: 37075701.127

2. **Jones K**, Zhang Y, Kong Y, Farah E, Wang R, Li C, Wang X, Zhang Z, Wang J, Mao F, Liu X, Liu J. Epigenetics in prostate cancer treatment. J Transl Genet Genom. 2021;5:341-

356. doi: 10.20517/jtgg.2021.19. Epub 2021 Aug 27. PMID: 35372800; PMCID: PMC8974353.

3.Mao F, Kong Y, Liu J, Rao X, Li C, Donahue K, Zhang Y, **Jones K**, Zhang Q, Xu W, Liu X. Diptoindonesin G antagonizes AR signaling and enhances the efficacy of antiandrogen therapy in prostate cancer. Prostate. 2022 Jun;82(8):917-932. doi: 10.1002/pros.24336. Epub 2022 Mar 24. PMID: 35322879; PMCID: PMC9035130.